

**UNIVERSITY OF TURIN**

**PhD School in Life and Health Sciences**  
*Molecular Medicine*



*Different Strategies to Increase Doxorubicin Efficacy in Drug  
Resistant Cancer Cells Based on Physical, Natural and  
Pharmacological Approaches*

**Gamal Eldein Fathy Abd-Ellatef Abd-Elrahman**

# UNIVERSITY OF TURIN

PhD School in Life and Health Sciences  
*Molecular Medicine*

*XXXI Cycle*  
*Academic Years: 2015-2019*



***Different Strategies to Increase Doxorubicin Efficacy in Drug Resistant Cancer Cells Based on Physical, Natural and Pharmacological Approaches***

Tutor: Prof. Chiara Riganti

Co-tutors: Prof. Mohamed Assem. S. Marie  
Prof. Sohair Ramadan Fahmy  
Prof. Abdel-Hamid Zaki Abdel-Hamid

Candidate: Gamal Eldein Fathy Abd-Ellatef Abd-Elrahman

Coordinator: Prof. Francesco Novelli

# CONTENTS

<b>ABSTRACT</b> .....	4
<b>1. INTRODUCTION</b> .....	8
<b>1.1 Multidrug resistance</b> .....	9
1.1.1 Mechanisms of multidrug resistance .....	9
<b>1.2 ABC transporters</b> .....	11
<b>1.3 Melanoma and resistance related to ABC transporters</b> ....	13
<b>1.4 Breast cancer and resistance related to ABC transporters</b>	14
<b>1.5 Mechanisms of doxorubicin resistance</b> .....	17
<b>1.6 Strategy to overcome resistance</b> .....	18
1.6.1 Photodynamic therapy: overview of its possible use as a tool to overcome drug resistance .....	19
1.6.2 Natural products: overview of their use as chemosensitizers .	22
1.6.2.1 Glabratephrin as a bioactive natural compound .....	22
1.6.2.2 Curcumin as a natural P-gp inhibitor .....	23
1.6.2.2.1 Curcumin-loaded solid lipid nanoparticles .....	23
<b>2. Aims</b> .....	26
<b>3. MATERIALS AND METHODS</b> .....	28
<b>3.1 Chemicals</b> .....	29
<b>3.2 Cell lines</b> .....	29
<b>3.3 Photo-excitable/NO-releasing doxorubicins synthesis and         characterization</b> .....	30
<b>3.4 Plant materials and natural pure compounds</b> .....	32
3.4.1 Extraction and isolation of Glabratephrin .....	35
<b>3.5 Solid lipid nanoparticles (SLN) preparation</b> .....	36
<b>3.6 Nitrite release</b> .....	36
<b>3.7 Cytotoxicity</b> .....	37
<b>3.8 Cell viability</b> .....	37
<b>3.9 Immunoblotting</b> .....	38
<b>3.10 ATPase activity</b> .....	39
<b>3.11 Intracellular doxorubicin accumulation</b> .....	39

3.12 Quantitative real time-PCR (qRT-PCR) .....	40
3.13 Flow cytometry analysis .....	41
3.14 Rhodamine 123 efflux .....	42
3.15 Overexpression of wild-type and mutated P-gp .....	42
3.16 ROS measurement .....	43
3.17 $\alpha$ NF-kB and HIF-1 $\alpha$ activity .....	43
3.18 Chromatin Immunoprecipitation (ChIP) assays .....	43
3.19 Docking studies .....	44
3.20 <i>In vivo</i> tumor growth .....	45
3.21 Statistical analysis .....	46
<b>4. RESULTS</b> .....	<b>48</b>
4.1 Aim 1: Use of photoexcitable/NO-releasing doxorubicins (PNODOXOs) to reverse drug resistance in human melanoma .....	49
4.1.1 Stability of PNODOXOs .....	49
4.1.2 Spectroscopic and photochemical properties .....	50
4.1.2.1 NO-photorelease of PNODOXOs .....	50
4.1.3 Biological assays .....	51
4.2 Aim 2: Using natural products to overcome doxorubicin resistance in human and murine TNBC cells .....	56
4.2.1 A screening on natural pure compounds to overcome doxorubicin resistance .....	56
4.2.1.1 Doxorubicin accumulation and viability in MDA-MB-231 cells, resistant counterpart MDA-MB-231/DX cells and JC cells .....	56
4.2.2 Mechanisms of the chemosensitizing effects of Glabratephrin .....	62
4.2.2.1 Molecular docking studies of glabratephrin on P-gp .....	65
4.2.3 Efficacy of Glabratephrin against drug-resistant JC tumors .....	69
4.3 Aim 3: The use of curcumin-loaded SLN as a nanotechnological approach to inhibit P-gp .....	71
4.3.1 Curcumin-loaded SLN effect against drug-resistant cancer cells <i>in vitro</i> .....	71
4.3.2 Curcumin-loaded SLN is effective against drug-resistant JC tumors <i>in vivo</i> .....	83
<b>5. DISCUSSION</b> .....	<b>88</b>
<b>6. CONCLUSION AND FUTURE PERSPECTIVES</b> .....	<b>102</b>
<b>7. LIST OF FIGURES</b> .....	<b>107</b>

<b>8. LIST OF TABLES .....</b>	<b>111</b>
<b>9. LIST OF SCHEMES .....</b>	<b>113</b>
<b>10. LIST OF ABBREVIATIONS .....</b>	<b>115</b>
<b>11. REFERENCES .....</b>	<b>118</b>
<b>12. LIST OF PUBLICATIONS .....</b>	<b>141</b>
<b>13. ACKNOWLEDGEMENTS.....</b>	<b>143</b>
<b>14. PhD ACTIVITIES .....</b>	<b>145</b>
<b>15. ARABIC SUMMARY .....</b>	<b>149</b>
<b>16. ARABIC ABSTRACT .....</b>	<b>152</b>

# **ABSTRACT**

The resistance of cancer cells to a broad variety of anticancer drugs is known as multidrug resistance (MDR), which is a critical hindrance to the success of cancer chemotherapy and leads to tumor progression. It affects patients with hematological and solid tumors including breast, ovarian, lung, skin, and gastrointestinal tract cancers. The main responsible for MDR phenotype are ATP Binding Cassette (ABC) transporters, plasma-membrane associated transporters that efflux multiple drugs – unrelated for structure and activity – outside the cells, limiting their intracellular accumulation and cytotoxicity. The main ABC transporter related to MDR is P-glycoprotein (P-gp). Until now, different small molecules inhibitors of P-gp have been tested: although effective *in vitro*, they failed in preclinical models for their high toxicity and poor specificity.

In my thesis, I investigated three alternative approaches to inhibit P-gp in an effective and safe way: i) the use of photodynamic tools, i.e. molecules able to release a chemotherapeutic drug – doxorubicin – and a P-gp inhibitor – nitric oxide (NO) – only if irradiated with proper wavelengths within tumor cells; ii) the use of natural products, with poor toxicity on non-transformed cells and high selectivity for P-gp overexpressing cells; iii) the use of a nanotechnological approaches, based on the co-administration of doxorubicin and a natural chemosensitizing product – curcumin – loaded in biocompatible solid lipid nanoparticles (SLN).

In the first part of the Thesis, I validated a new class of photoexcitable/NO releasing doxorubicins (PNODOXOs), in which an appropriate NO-donor is linked through a photosensitive bridge to doxorubicin. The objective was to photo-generate NO at doses not toxic but

able to nitrate ABC transporters on critical tyrosines for their activity, reducing doxorubicin efflux. To this aim, I used human melanoma M14 cells that constitutively express multiple ABC transporters. With the proper wavelength, power and irradiance, PNODOXOs released NO that nitrates P-gp and other ABC transporters, increasing the cytotoxicity of doxorubicin. These results may pave the way to the future use NO-photodons characterized by a broad-spectrum inhibition of ABC transporters. This feature may result in the increased retention and cytotoxicity of several other chemotherapeutic drugs besides doxorubicin. Moreover, this strategy is based on a light-induced release of NO: by reaching a tight spatial- and temporal-controlled release of NO only within the tumor cells, it maximizes the benefit against resistant irradiated tumors, limiting the side effects on non-transformed tissues.

In the second and third part of the Thesis, I focused on the reversion of resistance to doxorubicin mediated by P-gp in triple negative breast cancer cells, where doxorubicin is the first therapeutic option but it is poorly effective because of the presence of P-gp. For my studies, I used three different cell lines: 1) MDA-MB-231, human triple-negative breast cancer cells poorly expressing P-gp; 2) MDA-MB-231/DX (generated by a stepwise selection of MDA-MB-231 in a medium containing doxorubicin) that show a moderate P-gp expression; 3) the murine JC cells highly expressing P-gp.

First, I screened twelve natural pure compounds, which have been selected according to their different biological activities. I found that Glabratephrin (Glab), a prenylated flavonoid from *Tephrosia purpurea*, induced a selective and preferential cytotoxicity against P-gp-expressing cells, reversed doxorubicin resistance *in vitro* and in JC tumors *in vivo*, without systemic toxicity. Mechanistically Glabratephrin inhibited the



catalytic ATPase activity of P-gp, reducing the  $V_{max}$  and increasing the  $K_m$  of doxorubicin efflux. This event was due to the direct interaction of Glabratephrin with P-gp. Experiments with mutants P-gp allowed to identify the domain centred around Glycine 185 as the putative binding site of Glabratephrin. Indeed, the compound lost its efficacy in Glycine->Valine 185 mutated P-gp. Reversing doxorubicin resistance with the association of Glabratephrin could decrease the dose necessary to eradicate resistant cancer cells, therefore diminishing the toxicity of the drug.

Third, I continued the studies on natural products as MDR revertants, focusing on curcumin, a known inhibitor of P-gp that is affected by low stability, solubility and bioavailability. To overcome these limitations, I validated the efficacy of curcumin loaded in biocompatible SLN, with or without chitosan coating, able to increase the stability, the hydrophilicity and the cellular uptake of curcumin. Both curcumin-loaded SLN were five to ten-fold more effective than free curcumin in increasing intracellular retention and toxicity of doxorubicin in MDA-MB-231-P-gp expressing cells and JC cells. The chemosensitizing effects were due to the decrease of intracellular reactive oxygen species and to the consequent inhibition of the Akt/IKK $\alpha$ - $\beta$ /NF- $\kappa$ B axis. In particular curcumin-loaded SLN reduced the binding of the p65/p50 NF- $\kappa$ B to the promoter of P-gp gene. The reduced transcriptional activity decreased P-gp mRNA and protein. Curcumin-loaded SLN also effectively rescued the sensitivity to doxorubicin against drug-resistant JC tumors, without signs of systemic toxicity.

Overall, my research activity used several innovative approaches, based on the combination of physics, medicinal chemistry, nanotechnology, biochemistry and pharmacology. Such multidisciplinary may represent a significant advancement in overcoming MDR related to ABC transporters.

# **1. INTRODUCTION**

## 1.1 Multidrug Resistance

The resistance of cancer cells to a broad variety of anticancer drugs is known as multidrug resistance (MDR) that produces chemotherapy failure and tumor progression (Chen *et al.*, 2016). MDR is characterized by a cross-resistance to structurally and functionally unrelated compounds (Chen *et al.*, 2016). Intrinsic drug resistance is a natural resistance of tumor cells to specific agents before the exposure to the agents. In acquired drug resistance tumor cells that are initially sensitive to drugs become resistant due to mutations and various adaptive responses during treatment (Holohan *et al.*, 2013).

### 1.1.1 Mechanisms of multidrug resistance

MDR major mechanisms are grouped into several categories, e.g. decreasing drug influx, increasing drug efflux via adenosine triphosphate-binding cassette (ABC) transporters, activating DNA repair mechanisms, modifying drug targets and detoxification enzymes, inhibiting apoptosis pathways, altering cell cycle checkpoint and cell cycle arrest (Chen *et al.*, 2016; Kumar and Jaitak, 2019).

The low influx and/or the high efflux of anticancer drugs from tumor cells result in the lower intracellular accumulation of drugs that could not efficiently kill tumor cells (Cheng *et al.*, 2019). One of the most studied mechanisms is the overexpression of several energy dependent drug efflux pumps that belonged to the ABC family of transporters (as detailed in paragraph 1.2). These proteins have broad and overlapping substrate specificity and activate the elimination of various hydrophobic compounds (Holohan *et al.*, 2013). Tumor cells become resistant to a variety of anticancer drugs as a consequence of the overexpression or increased activity of these integral membrane proteins (Chen *et al.*, 2016).

Resistance mechanisms related to modified drug activation and inactivation are specific for each class of drugs. For example, prodrugs (many antimetabolites and some alkylating agents) must be activated to their cytotoxic forms within tumor or other tissues as liver. It is known that resistance toward pyrimidine and purine analogs is linked to their inactivation by elevated deaminases (Moscow, *et al.*, 2003). It has been reported that, in breast cancer, the increased activity of cytochrome P450 is associated with increasing docetaxel inactivation and drug resistance (Mansoori *et al.*, 2017).

Three important events can mediate and facilitate cell death: necrosis, apoptosis, and autophagy. The increased resistance to chemotherapy in tumor cells is associated with the up-regulation of anti-apoptotic genes and down-regulation of pre-apoptotic genes (Mansoori *et al.*, 2017).

Modulation or mutation of a drug target expression can reduce the efficacy of the drug leading to resistance (Jones *et al.*, 2009). For example, mutations in topoisomerase II in cancer cells alter its inhibition by doxorubicin (Housman *et al.*, 2014). Similarly, mutations in ABL Proto-Oncogene 2 (ABL2) kinase cause the resistance to imatinib (Mansoori *et al.*, 2017).

DNA is a target molecule for many chemotherapeutic agents. One of the resistance mechanisms to chemotherapeutic drugs is the DNA repair systems (Salehan and Morse, 2013). Repair of DNA lesions takes place through number of DNA repair pathways including mismatch repair, nucleotide excision repair, and homology-directed repair (Brown *et al.*, 2017). An increased activity of these enzymes after the formation of DNA

adducts by platinum limits cell death upon the exposure to this drug (Freimund *et al.*, 2018).

## 1.2 ABC transporters

ABC transporters, consist of 48 members which are phylogenetically classified into seven subfamilies based on their sequence similarities from ABC-A to ABC-G (Ween *et al.*, 2015). Among the ABC transporters which were identified in humans, most of those which there are several located on the cancer cells plasma membrane that significantly reduce the intracellular concentration of drugs, drug conjugates and metabolites (Holland, 2011; Wu *et al.*, 2011). These proteins are considered the main responsible for the development of MDR (Vadlapatla *et al.*, 2013). In addition to the role of ABC transporters as protective pumps from exogenous compounds and xenobiotics, they have physiological roles in the export of peptides, fatty acids, cholesterol and sterols, in the detoxification, defence against oxidative stress, and antigen presentation (Bodó *et al.*, 2003; Shair *et al.*, 2018).

Structurally, all ABC transporters have two nucleotide-binding domains (NBDs) and two transmembrane domains (TMDs) (Rice *et al.*, 2014). ATP is hydrolysed by NBD via an ATPase activity (Dean, 2009). Changes in TMD conformation could be induced by binding of two ATPs at the dimer interface, that leading to the dimerization and configuration of a sandwich-like NBD. When a substrate binds to the TMD, it could induce a decrease in the activation energy for NBD dimerization. The bound ATP is hydrolyzed to ADP and Pi, which separates the NBDs, then the substrate is released extracellularly and the stable conformational state of the NBD is restored, making the protein ready for binding and transporting another substrate (Figure 1) (Chen *et al.*, 2016).

At least 20 ABC transporters are capable of effluxing anticancer drugs. Multiple substrates can be transported by ABC transporters at once (Ween *et al.*, 2015). The major ABC transporters involved in the development of MDR are P-glycoprotein (P-gp/ABCB1/MDR1), MDR Related Proteins (MRPs/ABCCs), and Breast Cancer Resistance Protein (BCRP/ABCG2/MXR) (Shapira *et al.*, 2011). In most tumors, MDR is not only mediated by overexpression of one ABC transporter, but by expression of several transporters. For example, the co-expression of P-gp and BCRP transporters at the blood–brain barrier prevent effective chemotherapy of brain tumors (Agarwal, S., 2011).

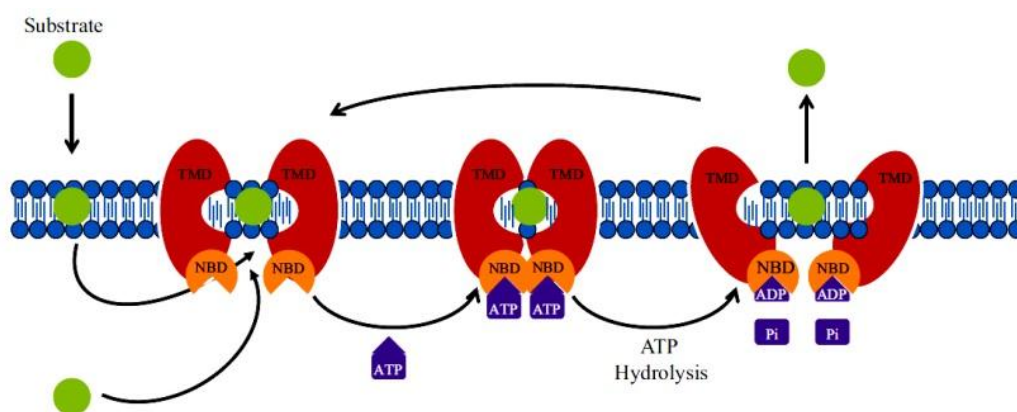


**Figure 1. Schematic representation of the function of ABC transporters.** ABC transporters are energy-dependent pumps, exhibiting a conformational change upon substrate binding and ATP hydrolysis that drives the substrate transport process (Chen *et al.*, 2016).

The ABCB subfamily consists of ABCB1, ABCB4, ABCB5 and ABCB11 which are full length transporters, and ABCB2/B3 and ABCB6-10 which are heterodimeric and homodimeric half transporters (Szöllősi *et al.*, 2018).

P-gp (ABCB1) was the first ABC member discovered with a strong linkage to drug resistance. Many studies have shown that overexpression of P-gp is induced by chemotherapy in various types of cancer (Wang, 2014).

Physiologically, P-gp is expressed in all tissues and mediates drug resistance in breast, gastric, liver, pancreas, colon, and kidney cancers, as well as in leukemias (Wang *et al.*, 2015).

### **1.3 Melanoma and resistance related to ABC transporters**

Skin cancers have a very high incidence among Caucasian people (Chandra Pal *et al.*, 2016). According to cellular origin, skin cancers are divided into two major groups: melanomas (derived from melanocytic cells) and non-melanoma (derived from epithelial cells) skin cancers (Khavari, 2006). Melanoma can be occurred in the skin, eye and ear (Toia *et al.*, 2015; Oellers *et al.*, 2018; Renzi *et al.*, 2019), and is one of the most aggressive forms of skin cancer with a high frequency of metastasis and a poor prognosis in the metastatic stage. According to the World Health Organization, worldwide about 132,000 new cases of melanoma are diagnosed each year (Hakkim *et al.*, 2019).

Chemotherapy is one of the therapeutic treatment options available to treat melanoma but in most cases it leads to severe side effects (Wu *et al.*, 2019), associated with treatment failure as a consequence of MDR (Sakil *et al.*, 2017). Melanoma is a highly chemoresistant because of the overexpression of multiple ABC transporters such as ABCA9, ABCB1, ABCB5, ABCB8, ABCC1, ABCC2, ABCD1, ABCG2 (Chen *et al.*, 2009). Doxorubicin is one of the leading chemotherapeutic drugs in melanoma treatment, but its efficacy is limited by drug resistance. Notwithstanding the use of new immune-therapeutic strategies in melanoma treatment, since also immune-therapy is affected by heavy side-effects and resistance rate of 30% patients, there is a renewed interest in improving the efficacy of chemotherapeutic approaches in melanoma.

## 1.4 Breast cancer and resistance related to ABC transporters

Worldwide, breast cancer is one of the most frequently diagnosed cancers and is the leading cause of cancer death in women. It is estimated that the global cancer burden to have risen to 18.1 million new cases and 9.6 million deaths in 2018 (Bray *et al.*, 2018), showing the highest oncological incidence in women (Hosni *et al.*, 2019).

In Egypt, breast cancer is the most frequent tumor, constituting about 38.6% of female cancer cases recorded by National cancer registry program of Egypt in 2010. Breast cancer female cases represented 32.04 % of cancers in Egypt, according to the National Population-Based Registry Program of Egypt 2008– 2011 (Ibrahim *et al.*, 2014). It is more prominent among young premenopausal Egyptian women, when it is characterized by poor prognosis and low survival rate (Omar *et al.*, 2003).

Based on molecular profile, breast cancer can be divided into subtypes including:

- 1) Luminal breast cancers, which can be subdivided into luminal A and B subtypes: they are heterogeneous in terms of mutation spectrum, gene expression, copy number changes and patient outcomes (Koboldt *et al.*, 2012);
- 2) Human epidermal growth factor receptor-2 (HER2) subtype;
- 3) Normal breast-like and basal-like triple negative breast cancer (TNBC) (Tajbakhsh *et al.*, 2019).

TNBC is an aggressive and invasive subtype and accounts for 10–20% of all breast cancers (Stuart, *et al.*, 2010). TNBC represent 28.5% of breast cancer patients in Egypt (El-Hawary *et al.*, 2012). It is characterized by the



lack of estrogen receptor (ER), progesterone receptor (PR), and HER2 (Neophytou, *et al.*, 2018). TNBC have a high frequency of TP53 mutations combined with loss of retinoblastoma1 (RB1) oncosuppressor (Perou, 2011). Seven subtypes of TNBC were identified through the analysis of differential expression of a set of genes and include a mesenchymal, a mesenchymal-stem cell-like, two basal-like, a luminal androgen receptor/luminal-like, an immunomodulatory, an unclassified type, with different prognosis (Neophytou, *et al.*, 2018).

Chemotherapy is the main treatment option for patients with TNBC. In spite of the rather aggressive clinical behavior of TNBC, after neo-adjuvant chemotherapy, about 30 to 40% of patients achieve a complete response with no histological evidence of disease at the time of surgery (Lehmann *et al.*, 2016). However, the emergence of drug resistance in many cases reduces the efficacy of the current neoadjuvant and adjuvant chemotherapy (Wu *et al.*, 2014; Willers *et al.*, 2019).

P-gp and ABCG2 are the main ABC transporters expressed in TNBC. P-gp, a 170 kDa plasma membrane drug efflux transporter encoded by the MDR1 gene (Juliano and Ling, 1976), is located on chromosome 7 (q21.12). It consists of two ATP binding cassettes and two homologous regions containing two hydrophobic TMDs of six  $\alpha$ -helices, and two NBDs located on the cytoplasmic side (Higgins *et al.*, 1997; Ren *et al.*, 2016). The drug binding activity results in the activation of one of the TMD of P-gp and in the subsequent hydrolysis of ATP, leading to a major conformational change, which causes drug efflux (Figure 1) (Saraswathy and Gong, 2013).

P-gp limits the chemotherapeutic drug intracellular accumulation and the drugs cytotoxicity in various cancers (Housman *et al.*, 2014), including

TNBC (Iris C Salaroglio *et al.*, 2018). The protein has one of the broadest spectrum of substrates, including anthracyclines (doxorubicin, daunorubicin and epirubicin), Vinca alkaloids (vinblastine and vincristine), epipodophyllotoxins (etoposide, teniposide), taxanes (paclitaxel, docetaxel), colchicine and some of the most recent anticancer targeted-therapies such as lapatinib, imatinib, dasatinib, sorafenib, erlotinib, gefitinib and gemtuzumab (Gottesman, *et al.*, 2002; Brózik *et al.*, 2011; Jiang *et al.*, 2014).

P-gp inhibition has been carried out using different class of pharmacological inhibitors, including competitive, non-competitive or allosteric blockers of drug-binding site(s), inhibitors of ATP hydrolysis, agents disrupting the integrity of cell membrane lipids (Figure 2) (Bansal *et al.*, 2009; Akhtar *et al.*, 2011), but these approaches all failed for the poor specificity and the high toxicity due to the inhibition of physiological functions of P-gp in non-transformed tissues.

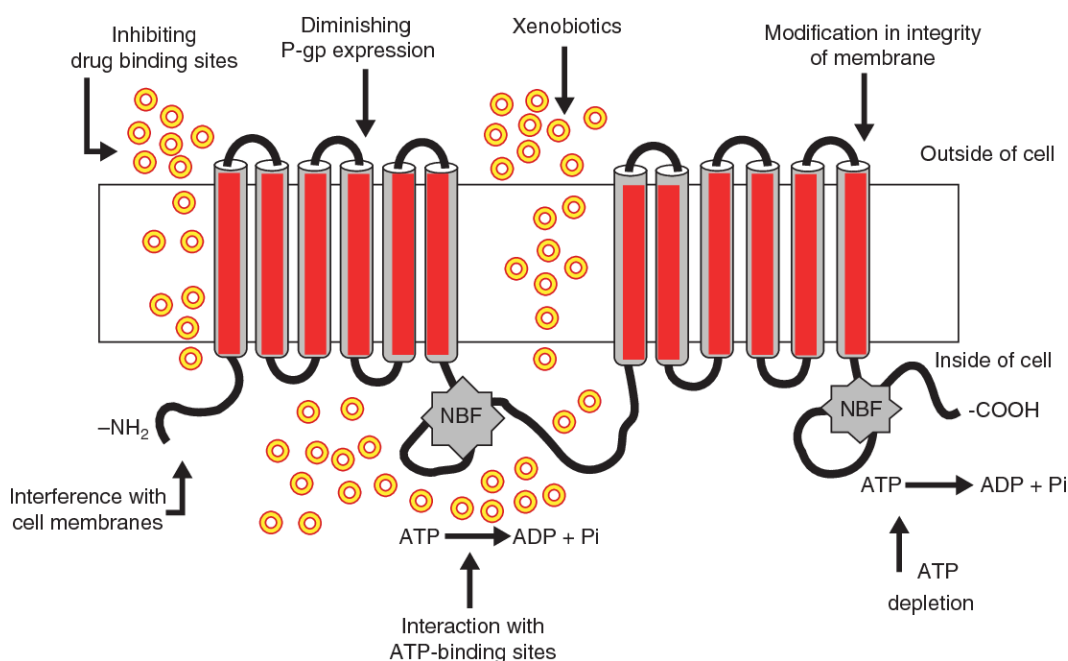


**Figure 2. Inhibitory mechanisms of P-glycoprotein** (Bansal *et al.*, 2009; Akhtar *et al.*, 2011).

BCRP is thought to function as homodimers or heterodimers (Mo and Zhang, 2012). It also transports anthracyclines, in particular mitoxantrone, and is similar to P-gp and MRP according to toxic-kinetic and pharmacokinetic properties (Jani *et al.*, 2014).

### **1.5 Mechanisms of doxorubicin resistance**

Doxorubicin (Adriamycin<sup>®</sup>) (Figure 3) is an antibiotic isolated from the cultural broth of bacteria belonging to *Streptomyces spp.* It is constituted by an aglycon (an anthracyclonic moiety) linked to an amino sugar (daunosamine). It is a class I anthracycline, widely used in therapy for the treatment of a variety of tumours including solid tumours, soft tissues sarcomas, osteosarcomas and many hematological malignancies (Minotti, 2004). Several molecular mechanisms which could underlie its anti-tumoral activity have been proposed, including: inducing DNA damage, increasing reactive oxygen species (ROS) and reactive nitrogen species (RNS) such as nitric oxide (NO), impairing mitochondrial metabolism, inducing endoplasmic reticulum (ER) stress and immunogenic cell death (Riganti, Gazzano, *et al.*, 2015; Riganti, Kopecka, *et al.*, 2015; Salaroglio, *et al.*, 2018).

The clinical use of doxorubicin is hampered by its cardiotoxicity and easy development of resistance. Among the several mechanisms proposed to explain the resistance, the overexpression of ABC transporters on cell surface such as P-gp, MRPs, BCRP and lung resistance protein (LRP) is one of the most critical factor (Wang, *et al.*, 2019). As a result, doxorubicin accumulates less within the cell, decreasing DNA damage and apoptosis, mitochondrial damage, ER stress and immunogenic cell death (Cox and Weinman, 2015; Gazzano, *et al.*, 2018; Salaroglio *et al.*, 2018). Besides P-gp and BCRP that mediates doxorubicin efflux, ABCB8 determines

doxorubicin resistance in melanoma cells by protecting the genome of the mitochondria (Tacar, *et al.*, 2013).

Since doxorubicin inhibits topoisomerase II (Tacar, *et al.*, 2013), also mutations or increased expression of this enzyme determines resistance to the drug (Lovitt, *et al.*, 2018). Moreover, an increase in anti-apoptotic pathway is also a critical mechanism of doxorubicin resistance (Xu *et al.*, 2018).

## **1.6 Strategy to overcome drug resistance**

To overcome clinical MDR a number of strategies have been proposed. Several pharmacological ABC transporters modulators have been tested in clinical trials. They are classified as first, second and third generation modulators, on the basis of their affinity and specificity for ABC transporters (Kathawala *et al.*, 2015; Li *et al.*, 2016). Most inhibitors have been directed towards P-gp.

P-gp substrates are capable of binding to P-gp specifically or non-specifically (Orelle *et al.*, 2008). The first generation modulators, such as verapamil and cyclosporine, despite their promising results in preclinical trials, showed major toxicities in clinical trials because of the inhibition of both P-gp and their physiological targets (such as Ca<sup>++</sup> channels, immune modulator proteins), producing unexpected drug-drug interactions and side-effects. The majority of second generation inhibitors are analogs of the first generation compounds, lacking of the original pharmacological activity. However, they were modulators of cytochrome p450 activities, determining the alteration in the metabolism of chemotherapeutic drugs, catabolites, xenobiotics and other co-administered drugs (Kumar and Jaitak, 2019). The third generation drugs, including Tariquidar and Elacridar, were developed to overcome the limitations of both first and second generations, being

more specific and potent on P-gp or BCRP, with minimal impact on cytochrome p450 system and drug pharmacokinetics (Hyafil *et al.*, 1993; Dantzig *et al.*, 1999; Mistry *et al.*, 2001). Although some of these inhibitors have succeeded to enhance the efficacy of anticancer drugs in preclinical studies and in some clinical trials, most of these inhibitors showed high toxicity (Thomas and Coley, 2003). The latest frontiers in ABC transporters inhibition is the co-administration of the antineoplastic agents with ABC transporters inhibitors (Szakács *et al.*, 2006; Zinzi *et al.*, 2014). To overcome pharmacokinetic and pharmacodynamic limitations, the co-encapsulation in liposomes of biocompatible nanoparticles have been experimented (Hu and Zhang, 2012), but these studies are still at preclinical levels.

Hence, alternative strategies inhibiting P-gp in order to improve chemotherapy efficacy is still an unmet need.

### **1.6.1 Photodynamic therapy: overview of its possible use as a tool to overcome drug resistance**

Photodynamic therapy (PDT) include a range of approaches that generate ROS and RNS within the target tissues, after energy-specific activation of photodynamic compounds (i.e. visible and near-infrared absorbing molecules or photosensitizers) upon irradiations with a specific wavelength, able to release ROS/RNS-generating moieties from the donor compound (Obaid *et al.*, 2016). PDT causes minimal toxicity to normal tissues in comparison with chemotherapy and radiotherapy, since the generation of ROS/RNS is a light-triggered process occurring only in irradiated tissues (specifically in tumors) and photosensitizers usually are not toxic if not irradiated (i.e. in non-transformed tissues) (Li *et al.*, 2013).

NO, a potent RNS is an endogenous messenger produced by the nitric oxide synthase (NOS) enzyme, which can exist in three isoforms: neuronal nNOS, endothelial eNOS, and inducible iNOS. The first two are constitutive and induce formation of little amount of NO (pM or nM concentrations), while the third one is an inducible isoform which produces high levels of NO ( $\mu$ M concentrations). At low concentrations NO displays cytoprotective and second-messenger effects, at high concentration toxic effects (Wink and Mitchell, 1998). At micromolar concentration it triggers antitumoral effects through the oxidative damage of DNA, inactivation of DNA-repairing systems, the reduction of nucleotide synthesis, the interference with tricarboxylic acid cycle and the mitochondrial respiratory chain, the generation – together with the ROS superoxide, of the strong pro oxidant species peroxynitrite (ONOO<sup>-</sup>) (Huerta *et al.*, 2008). NO-donors are products able to release NO, and consequently they can be used as NO-prodrugs (Sharma *et al.*, 2013).

Previous works from our group have shown that classical NO-donors such as *S*-nitrosopenicillamine, sodium nitroprusside and *S*-nitrosoglutathione, are able to reduce the efflux of doxorubicin in human cancer cells. The mechanism is not the typical activation of the soluble guanylate cyclase, but the nitration of critical tyrosine residues of P-gp and MRP transporters (Riganti *et al.*, 2005; De Boo *et al.*, 2009). Also furoxan derivatives (1,2,5-oxadiazole 2-oxides), which are known to release NO under the action of thiol co-factors, can inhibit in a similar manner P-gp and MRP1 (Fruttero *et al.*, 2010). On these bases, new doxorubicin derivatives, in which moieties containing nitrooxy or furoxan NO-donor groups were linked through an ester bridge at C-14 of the antibiotic, were developed. Some of these NO-releasing doxorubicins were able to overcome resistance by inhibiting ABC transporters via tyrosine nitration,

and increasing the intracellular retention of doxorubicin (Chegaev *et al.*, 2011; Riganti *et al.*, 2013; Gazzano *et al.*, 2016).

A particular kind of NO-donors is represented by the NO-photodonors (NOPDs), namely products able to release NO under the action of specific wavelengths. This strategy allows a precise control of timing, location and dosage of the NO-released. A NOPD must satisfy precise requisites for biological application; in particular it must be excited by the visible light. Its side photoproducts should not be toxic and or absorb visible light. Examples of such products are NO/nitrite complexes of transition metals combined with appropriate chromophores (Ford, 2008, 2013; Fry and Mascharak, 2011). These complex structures, however, are not suitable for chemical manipulations, in contrast to structurally simple NOPDs, e.g. substituted nitrobenzenes which undergo to a nitro-nitrite rearrangement followed by release of NO and formation of the related phenols under blue light (Suzuki *et al.*, 2005; Kitamura *et al.*, 2016). Structural modification of these products can be carried out by simple synthetic procedures. A typical examples of such NOPDs is 4-nitro-3-(trifluoromethyl)aniline (Figure 3) (Caruso *et al.*, 2007; Callari and Sortino, 2008; Conoci *et al.*, 2013). These NOPDs have never been exploited as possible MDR-overcoming strategies exploiting a photodynamic approach.

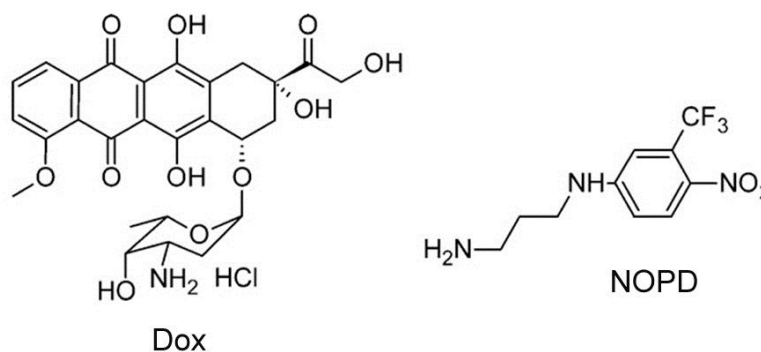


**Figure 3. Molecular structure of doxorubicin (Dox) and Nitric Oxide Photodonor (NOPD).**

## 1.6.2 Natural products: overview of their use as chemosensitizers

A variety of phytochemicals, including alkaloids, lipophilic terpenoids, steroids and triterpenes inhibit P-gp, MRP1 and BCRP in a competitive manner (Wink *et al.*, 2012). Several natural compounds such as quercetin, catechins, morin and capsaicin have been reported as selective P-gp inhibitors (Zhang and Morris, 2003; Nabekura *et al.*, 2005). Flavonoids and terpenoids are chemical compounds which are commonly present in several plants and have a wide range of pharmacological effects, enhancing or reducing the efficacy of other drugs through modulation of P-gp expression (Yu *et al.*, 2016). *Stemona* alkaloids increase the efficacy of anticancer drugs by reducing drug efflux via P-gp (Umsumarng *et al.*, 2017). Capsaicin reverses drug resistance *in vivo* by improving doxorubicin pharmacokinetic, reducing P-gp efflux (Kim *et al.*, 2018). *Zuccagnia punctata* (monotypic species widely distributed in western Argentina) and two of its components - 3,7-dihydroxyflavone and 20,40 dihydroxychalcone - have been reported to modulate both the expression and activity of P-gp (Yu *et al.*, 2016).

In this Thesis, I will focus mainly on two natural products: glabratephrin and curcumin.

### 1.6.2.1 Glabratephrin as a bioactive natural compound

Glabratephrin is a prenylated flavonoid from *Tephrosia purpurea* (Ammar *et al.*, 2013). *T. purpurea* was reported to contain rotenoids, flavones, isoflavones, flavanones, flavanols, chalcones (Pelter *et al.*, 1981). Prenylated flavonoids are the major compounds of this plant. Since their first isolation, glabratephrin (Vleggaar *et al.*, 1978), and recently, isoglabratephrin (Hegazy *et al.*, 2009) are the only examples in nature of prenylated flavonoids with 4-hydroxy-2,7-dioxaspiro[4.4]nonan-1-one-3,3-



dimethyl ring system. This prenylated flavonoid with its rare carbon framework is the major constituent in *T. purpurea* (Mohamed *et al.*, 2008).

It was found that glabratephrin has antifungal activity against four phytopathogenic fungi (*Helminthosporium spp.*, *Pestalotiopsis spp.*, *Alternaria alternata* and *Colletotrichum acutatum*) (Afzal *et al.*, 2014). Different fractions of the *T. purpurea* extract have hepatoprotective (Paharia and Pandurangan, 2013), anti-inflammatory (Gulecha *et al.*, 2011), anti-ulcer (Deshpande *et al.*, 2003), anti-diabetic (Pavana *et al.*, 2008) and antioxidant activities in rats (Saraf *et al.*, 2006).

### **1.6.2.2 Curcumin as a natural P-gp inhibitor**

Curcumin is a secondary metabolite isolated from the turmeric of *Curcuma longa L.* which have several biological activities, including inhibiting P-gp function and expression (Lopes-Rodrigues *et al.*, 2016). Turmeric or natural curcuminoids have been reported to have antioxidant (Llano *et al.*, 2019), anti-inflammatory (Menon and Sudheer, 2007), anticancer (López-Lázaro, 2008; Guerrero *et al.*, 2018) and antimicrobial activities (Zorofchian Moghadamtousi *et al.*, 2014). *Curcuma longa* safety has been studied in various animal models such as rats, guinea pigs and monkeys (Shankar *et al.*, 1980; Qureshi *et al.*, 1992), indicating that it is not toxic even at high doses in laboratory animals (Limtrakul *et al.*, 2004, 2005).

#### **1.6.2.2.1 Curcumin-loaded solid lipid nanoparticles**

Since curcumin is a highly lipophilic drug, nanotechnologists produced different formulations encapsulating curcumin, in order to enhance its solubility, stability, specificity, tolerability, cellular uptake/internalization efficacy and therapeutic index (Yallapu *et al.*, 2012,

2013) (Figure 4) (Yallapu *et al.*, 2015). Among the latest nanocarriers used for curcumin delivery there are solid lipid nanoparticles (SLNs), i.e. solid nanoparticles ranging from 300 to 600 nm formed by long chain saturated or unsaturated fatty acids that dispose themselves as in lipid micelles. SLNs advantageous properties are biocompatibility, small particle size, chemical and mechanical stability and easy functionalization that may enhance the delivery of bioactive lipophilic molecules (Guri *et al.*, 2013; Nakhband *et al.*, 2018; Rehman *et al.*, 2018). The lipid core within SLNs can protect the encapsulated lipophilic drugs from chemical degradation and enhance their physical stability. Moreover, SLNs have been reported to ameliorate the half-time of the drugs in the systemic circulation, modulate release kinetics, and increase therapeutic efficacy of anticancer drugs (Baek *et al.*, 2018; Wang *et al.*, 2018).

In my thesis, I used curcumin-loaded SLN with or without chitosan. Chitosan is a common coating agent in nanoparticulate drug delivery system. It is nontoxic, biocompatible and biodegradable and has been proven to control the release of drugs. It is soluble in aqueous media, avoiding the use of organic solvents during SLNs preparation, and, once added to the synthesized SLNs, it does not require further purification of nanoparticles (Agnihotri *et al.*, 2004).

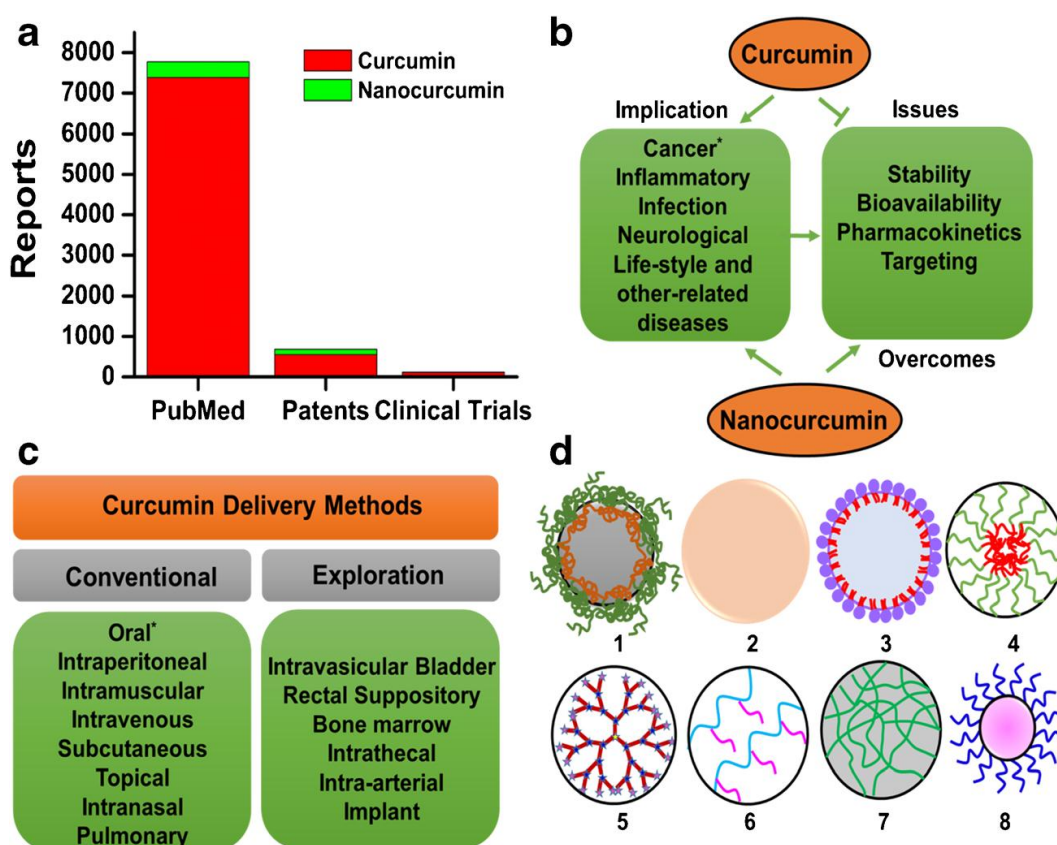


**Figure 4. Schematic transition from curcumin to curcumin nanoformulations.** A literature graphical representation using PubMed, patents (through online search engines) and websites of clinical trials (search conducted in April 2015). **b.** Implication of curcumin and nanocurcumin (curcumin nanoformulations) in different diseases (asterisk shows a widespread study). **c.** Delivery methods of curcumin and curcumin nanoformulations (asterisk represents the route which is commonly used to deliver curcumin). **d.** Types of nanocarriers commonly used to deliver curcumin efficiently. 1–8: polymer nanoparticles, solid nanoparticles, liposome/lipid nanoparticles, micelles, dendrimers, polymer conjugates, nanogels, and metal/metal oxide nanoparticles, respectively (Yallapu *et al.*, 2015).

## **2. AIMS**

The general aim of this thesis is to overcome doxorubicin resistance through using different strategies to increase doxorubicin efficacy in drug resistant cancer cells based on physical, natural and nanotechnological approaches.

In particular:

- 1- In the first part, I applied a physical PDT-based approach, using light-activated/NO-releasing doxorubicin, to overcome doxorubicin resistance in human melanoma (M14) cells.
- 2- In the second and third part, I used natural products to overcome doxorubicin resistance in human (MDA-MB-231 and their resistant counterpart MDA-MB-231/DX) and murine (JC) TNBC doxorubicin resistant cell lines. In particular, I studied the chemosensitizing efficacy and the biochemical mechanisms underlying chemosensitization of:
  - a. Glabratephrin as new natural compound inhibiting P-gp;
  - b. Curcumin-loaded SLN as new nanotechnological formulations of a natural product, able to inhibit P-gp.

### **3. MATERIALS AND METHODS**

### **3.1 Chemicals**

The plastic ware for cell cultures was obtained from Falcon (Becton Dickinson, Franklin Lakes, NJ). The electrophoresis reagents were obtained from Bio-Rad Laboratories (Hercules, CA). The protein content of cell lysates was assessed with the BCA kit from Sigma Chemicals Co. (St. Louis, MO). Unless specified otherwise, all reagents were purchased from Sigma Chemicals Co. Deionized water was obtained by a MilliQ system (Millipore, MO, USA).

### **3.2 Cell lines**

M14 melanoma cells, human breast cancer MCF7 cells, human TNBC MDA-MB-231, murine mammary cancer JC cells syngeneic with Balb/C mice, and rat cardiomyocytes H9c2 were purchased from ATCC (Manassas, VA). MDA-MB-231/DX were generated by culturing parental MDA-MB-231 cells in complete medium, adding Dox at increasing concentrations every 5 passages (p0: 10 nM Dox; p5: 25 nM; p10: 50 nM; p15: 100 nM; p20: 250 nM; p25: 500 nM; p30: 1000 nM). For all the reported experiments, MDA-MB-231/DX 500 nM was used. Human fibroblasts were a kind gift of Prof. Franco Novelli, Department of Molecular Biotechnology and Health Sciences, University of Torino, Italy.

Cells were maintained in RPMI-1640 (MCF-7, MDA-MB-231, JC cells) or in DMEM (H9c2, fibroblasts) media supplemented with 10% v/v fetal bovine serum, 1% v/v penicillin-streptomycin, 1% v/v L-glutamine. In photo-irradiation experiments, cells were exposed to a 400 nm wave length, 10W violet led for 20 minutes, using an irradiance of 7 mW/cm<sup>2</sup>, in PBS at room temperature. Non-irradiated cells were maintained in PBS in a dark room for 20 minutes at room temperature. After this period time, PBS was

changed with fresh medium and cells were left for 24 h in the incubator before the experimental procedures described below.

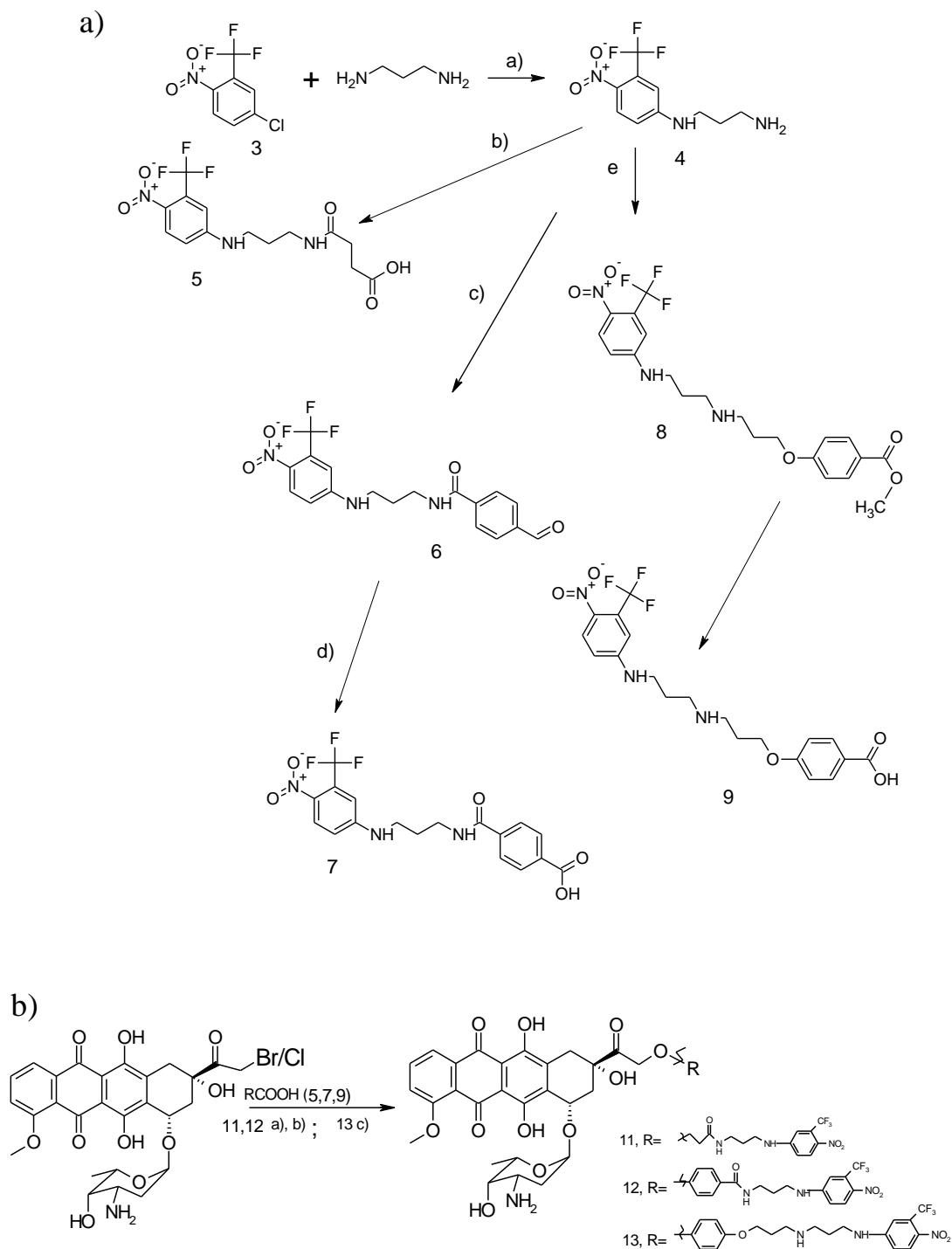
### 3.3 Photo-excitable/NO-releasing doxorubicins synthesis and characterization

The synthesis of **PNODOXOs** (Photodonor NO covalently linked to doxorubicin through a suitable bridge) was performed at the Department of Drug Science and Technology, University of Turin, as reported in (Chegaev *et al.*, 2017). The preparation of the acids used to synthesize the target PNODOXOs 11-13, is reported in Scheme 1a. A solution of 4-chloro-1-nitro-2-(trifluoro methyl)benzene (3) in 1,3-diaminopropane heated at 140°C afforded the diamine propane derivative 4. This product treated with succinic anhydride in CH<sub>2</sub>Cl<sub>2</sub> solution in the presence of Et<sub>3</sub>N gave the acid 5. The acid 7 was obtained by oxidation in with an aqueous solution of Na ClO<sub>2</sub> of the related aldehyde 6 dissolved in *t*-butanol. The aldehyde 6 resulted from the action of 4-formylbenzoyl chloride on 4 in CH<sub>2</sub>Cl<sub>2</sub> solution, in the presence of Et<sub>3</sub>N. Finally the acid 9 was prepared by hydrolysis of the corresponding methyl ester 8, in turn obtained by reacting 4 and methyl 4-(3-bromopropoxy)benzoate in MeCN in the presence of K<sub>2</sub>CO<sub>3</sub>.

Preparation of PNODOXOs 11-13 is outlined in Scheme 1b. Reaction of 14 bromo/chloro daunomicin hydrobromide 10 with the acids 5, 7, 9 was performed at room temperature in dry DMF in the presence of KF. The resulting products were purified by flash chromatography, successively suspended in dry THF and treated with 1 equiv. of HCl in dry dioxane to give the corresponding hydrochlorides. In the case of the preparation of 13 the oily product obtained by flash chromatography was only additionally purified by RP-flash chromatography (eluent gradient



from 4/6 to 2/8 MeCN/0.005M HCl). The final purity of the products was evaluated by RP-HPLC techniques.



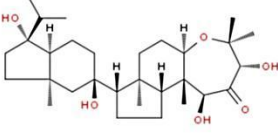
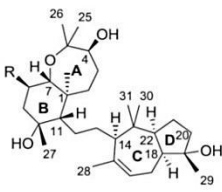
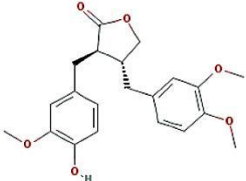
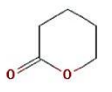
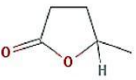
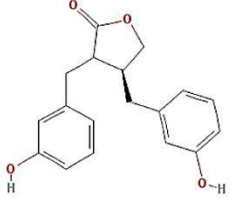
Scheme 1. a) KF, DMF, room temperature; b) THF, HCl in dry dioxane.

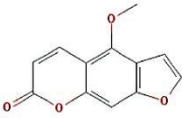
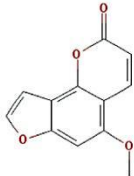
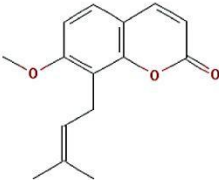
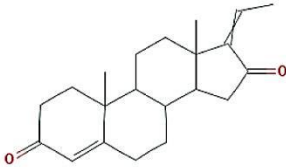
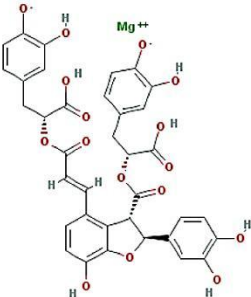
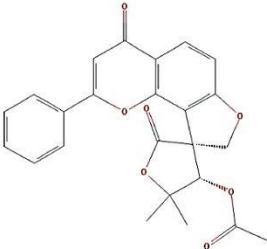
Stability and NO release from compound 11-13 were performed at the Department of Drug Science and Technology, University of Turin, as detailed in the Results section

### 3.4 Plant materials and natural pure compounds

Pure compounds were provided by Prof. Meselhy R. Meselhy from Department of Pharmacognosy, Faculty of Pharmacy, Cairo University, Egypt; Prof. Ahmed A. El-Beih from Chemistry of Natural and Microbial Products Department at National Research Centre (NRC), Egypt and Dr. Ahmed H. El-Desoky from Pharmacognosy Department at NRC, Egypt. The chosen compounds included: the triterpenes **neviotine A** and **sipholenol N** that were isolated from the Red Sea marine sponge *Siphonochalina siphonella* (El-Beih *et al.*, 2018); **Arctigenin** that was isolated from seeds of *Arctium lappa L.* (Jin *et al.*, 2007); **Delta-Valerolactone**, **Gamma-Valerolactone** and **Enterolactone** that are bacterial metabolites from Arctigenin (Jin *et al.*, 2007; Jin and Hattori, 2010); the furanocoumarins **Bergapten** and **Iso-Bergapten**, extracted from medicinal plant *Angelica pubescens* (Xiao and Liu, 2005); **Osthol**, extracted from *Tagetes L. Spp.* (López *et al.*, 2011); **Guggulsterone** that was isolated from the oleogum resin of *Commiphora wightii* (Arnott.) (Meselhy, 2003); **Magnesium lithospermate B**, extracted from *Cordia spinescens* (Boraginaceae species) (Lim *et al.*, 1997); **Glabratephrin**, a prenylated flavonoid from *T. purpurea* (Khalafallah *et al.*, 2009; Maldini *et al.*, 2011; Ammar *et al.*, 2013)(Table 1).

**Table 1. Tested natural pure compounds.**

N.	Compound name	Natural source	M.Wt. g/mol	Chemical structure
1	Neviotine A (Nev)	Red Sea marine sponge <i>Siphonochalina siphonella</i>	506.7	
2	Sipholenol N (Sip)		492	
3	Arctigenin (Arc)	Seeds of <i>Arctium lappa</i> L.	372.4	
4	Delta-Valerolactone (D-Val)	Bacterial metabolites from Arctigenin	100	
5	Gamma-Valerolactone (G-Val)		100	
6	Enterolactone (Ent)		298.3	

7	Bergapten (Ber)	<i>Angelica pubescens</i>	216.1	
8	Iso Bergapten (Iso-B)		216.1	
9	Osthol (Osh)	<i>Tagetes L. Sp.</i>	244.2	
10	Guggulsterone (Gug)	Oleogum resin of <i>Commiphora wightii</i> (Arnott.)	312.4	
11	Magnesium lithospermate B (MLB)	<i>Cordia spinescens</i> (Boraginaceae)	740.9	
12	Glabratephrin (Glab)	<i>Tephrosia purpurea</i>	420.4	

The aerial parts of *Tephrosia purpurea* were collected in February 2010, in Gabal Elba, Egypt. A voucher specimen has been deposited in the herbarium of National Research Centre, Cairo, Egypt. The plant was air dried in shade, reduced to 36 mesh powder using cutter mill and kept in tight closed containers till extraction.

### 3.4.1 Extraction and isolation of Glabratephrin

Air-dried aerial plant powder (1200 g) of *T. purpurea* was extracted with CH<sub>2</sub>Cl<sub>2</sub>–methanol (MeOH) (1:1) (3 L) by maceration at room temperature. Solvent was stripped off under vacuum at 40°C. The residue (70 g) was subjected to silica gel column chromatography and eluted with *n*-hexane, ethyl acetate (EtOAc) and MeOH in increasing order of polarity up to 100% EtOAc, then washed with MeOH. Similar fractions were combined to yield 9 main fractions. Fraction 7, eluted with *n*-hexane-EtOAc (4:6), was subjected to silica gel column chromatography, eluted with *n*-hexane-EtOAc (2:1) to yield 12 subfractions. Subfraction 11 was purified by Sephadex LH-20 column chromatography to yield compound 1 (94 mg), which was identified by <sup>1</sup>H-NMR analysis and was found to be glabratephrin (Figure 5).

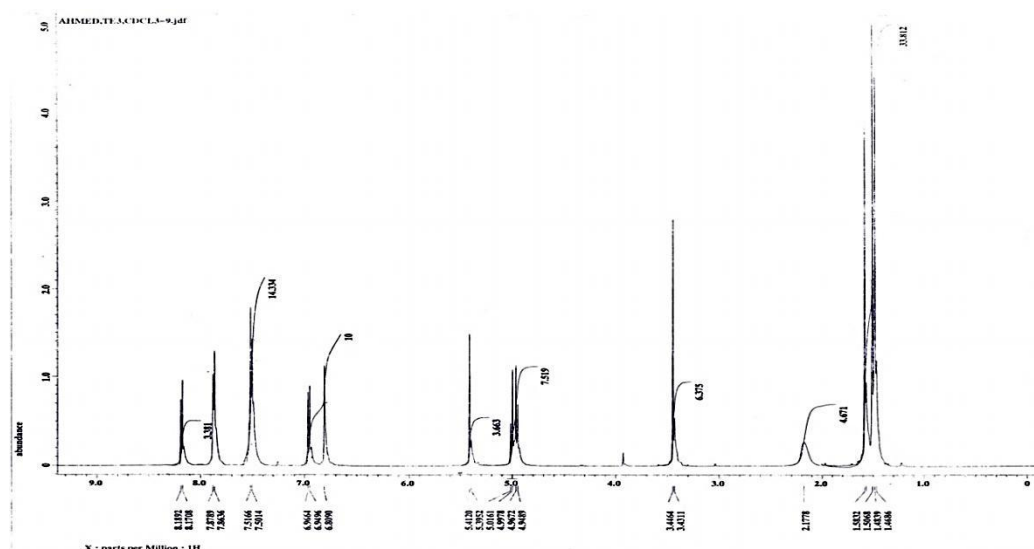


Figure 5. <sup>1</sup>H-NMR analysis of compound 1 (glabratephrin).

### 3.5 Solid lipid nanoparticles (SLN) preparation

SLNs, loaded with curcumin, with and without chitosan, were prepared at the Department of Drug Science and Technology, University of Turin, using the "cold dilution of microemulsion" method (Chirio *et al.*, 2018). This preparation method is based on the preparation of an Oil/Water microemulsion ( $\mu$ E), diluted by an aqueous solution at room temperature, to obtain nanoparticles precipitation as lipid solid matrices.

A saturated solution of trilaurin, dissolved in 1 mL of ethylacetate, was diluted in 5 mL deionized water to precipitate SLN, that were then collected and diluted in 5 mL of 2% w/w aqueous solution of Pluronic Pluronic® F68, as detailed in (Chirio *et al.*, 2019). 11 mg curcumin, dissolved in 1 mL 1,2 propanediol, was added to the 1 mL of SLN that were subsequently diluted in Pluronic® F68, as reported above. Curcumin-loaded SLN were subjected to gel filtration, to remove solvents and unencapsulated drugs. The mean diameter of the SLNs was  $215.3 \pm 5.4$  nm, with a polydispersity index of 0.222 and a  $\zeta$ -potential of  $-18.96 \pm 2.88$ . The encapsulation efficiency was  $70 \pm 2.1$  % (Chirio *et al.*, 2019). An aqueous solution of 15 mg chitosan in 10 ml were added to 100  $\mu$ l of SLN loaded with curcumin, incubated under stirring conditions for 4 h, precipitated by centrifugation at 25,000 x g for 10 min. The association of chitosan with the SLN was verified by UV-vis spectrophotometry, as detailed (Chirio *et al.*, 2011).

### 3.6 Nitrite release

The amount of nitrite, the stable derivative of NO, from PNODOXs or from cells treated with PNODOXOs, was measured spectrophotometrically by adding 0.15 ml of supernatants to 0.15 ml of Griess reagent (Riganti *et al.*, 2008), in a 96-well plate. After a 10 min

incubation at 37 °C in the dark, absorbance was measured at 540 nm with a HT Synergy 96-well micro-plate reader (Bio-Tek Instruments, Winooski, VT). For each experiment, a blank was prepared in the absence of cells, and its absorbance was subtracted from that measured in the presence of cells. Nitrite concentration was expressed as nmoles nitrite/mg cell proteins.

### **3.7 Cytotoxicity**

The release of lactate dehydrogenase (LDH) in the extracellular medium, considered an index of DOX cytotoxicity (Chegaev *et al.*, 2017), was measured spectrophotometrically (Riganti *et al.*, 2008). 50 µl of medium were centrifuged at 12,000 x g for 15 min, and diluted in 0.2 ml of 82.3 mM triethanolamine phosphate hydrochloride (TRAP, pH 7.6). Cells were washed with PBS, detached with trypsin/EDTA, and sonicated on ice (1 X 10 s, amplitude 40%; Hielscher UP200S ultrasound sonicator, GmbH, Teltow, Germany). LDH activity was measured in 200 µL of medium and by adding 5mM NADH and 20 mM pyruvic acid, measuring the change in absorbance at 340 nm with a HT Synergy 96-well micro-plate reader (Perkin Elmer, Shelton, CT). The reaction kinetics was linear. The results were expressed as µmoles NAD<sup>+</sup>/min/mg cell proteins.

### **3.8 Cell viability**

Cell viability was evaluated by measuring the percentage of cells stained with crystal violet (Riganti, Kopecka, *et al.*, 2015; Kopecka *et al.*, 2018) as indicated in the Results section. The quantitation of crystal violet staining was performed by reading the absorbance of each well at 540 nm (HT Synergy 96-well micro-plate reader). The mean absorbance of untreated cells was considered 100%; the absorbance units of the other experimental conditions were expressed as percentage of viable cells vs.

untreated cells. To calculate the IC<sub>50</sub> i.e. the concentration of each natural compound that decreased the cell viability by 50%, cells were seeded in quadruplicate in 96-well plates, treated at scalar concentrations (from 10<sup>-9</sup> M to 10<sup>-2</sup> M) of each compounds for 72 h and stained with crystal violet. IC<sub>50</sub> was calculated with the GraphPad Prism (v 6.01) software. The Combination Index (CI) was calculated by measuring the viability in cells incubated with scalar concentrations (from 10<sup>-10</sup> M to 10<sup>-3</sup> M) of doxorubicin and glabratephrin, using the CalcuSyn software ([www.biosoft.com/w/calculusyn.htm](http://www.biosoft.com/w/calculusyn.htm)).

### **3.9 Immunoblotting**

Cells were rinsed with ice-cold lysis buffer (50 mM, Tris, 10 mM EDTA, 1% v/v Triton-X100), supplemented with the protease inhibitor cocktail set III (80 µM aprotinin, 5 mM bestatin, 1.5 mM leupeptin, 1 mM pepstatin; Calbiochem, San Diego, CA), 2 mM phenylmethylsulfonyl fluoride and 1 mM Na<sub>3</sub>VO<sub>4</sub>, then sonicated and centrifuged at 13,000 × g for 10 min at 4 °C. 20 µg protein extracts were subjected to SDS-PAGE and probed with the antibodies for: anti-P-gp/ABCB1 (C219, Calbiochem), anti-MRP1 (Abcam, Cambridge, UK), anti-MRP2 (Abcam), anti-MRP3 (Santa Cruz Biotechnology Inc., Santa Cruz, CA), anti-MRP4 (Abcam), anti-MRP5 (Santa Cruz Biotechnology Inc.), anti-BCRP (Santa Cruz Biotechnology Inc.), anti-phosphoSer473 Akt (Cell Signalling Technology, Danvers, MA), anti-Akt (Cell Signalling Technology), anti-phosphoSer176/180 IKKα/β (Cell Signalling Technology), anti- IKKα/β (Cell Signalling Technology), anti- IκBα (Santa Cruz Biotechnology Inc), followed by a peroxidase-conjugated secondary antibody (Bio-Rad Laboratories). The membranes were washed with Tris-buffered saline-Tween 0.1% v/v solution, and the proteins were detected by enhanced chemiluminescence (Bio-Rad Laboratories). To check the equal control



loading in lysates, samples were probed with an anti-actin (Sigma Chemicals Co.) or with an anti- $\beta$ -tubulin (Santa Cruz Biotechnology Inc.) antibody. To analyse the presence of nitrated proteins, cell extracts were subjected to immunoprecipitation using a rabbit polyclonal anti-nitrotyrosine antibody (Millipore, Billerica, MA). Immunoprecipitated proteins were separated by SDS-PAGE and probed with the respective antibodies against ABC transporters, as indicated above.

### 3.10 ATPase activity

1 mg whole cell lysate was immunoprecipitated with antibodies for P-gp, MRP1, MRP3, MRP4, MRP5, BCRP, using the PureProteome protein A and protein G Magnetic Beads (Millipore). The ATPase activity of each immunopurified transporter was measured spectrophotometrically (Kopecka *et al.*, 2014). 20  $\mu$ g of each immunoprecipitated total protein were incubated for 30 min at 37°C with 50  $\mu$ l of the reaction mix (25 mM Tris/HCl, 3 mM ATP, 50 mM KCl, 2.5 mM MgSO<sub>4</sub>, 3 mM dithiothreitol, 0.5 mM EGTA, 2 mM ouabain, 3 mM NaN<sub>3</sub>; pH 7.0). The reaction was stopped by adding 0.2 ml ice-cold stopping buffer (0.2% w/v ammonium molybdate, 1.3% v/v H<sub>2</sub>SO<sub>4</sub>, 0.9% w/v SDS, 2.3% w/v trichloroacetic acid, 1% w/v ascorbic acid). After 30-min incubation at room temperature, the absorbance of the phosphate hydrolyzed from ATP was measured at 620 nm, using a Packard EL340 microplate reader (Bio-Tek Instruments). The absorbance was converted into nmol hydrolyzed phosphate (Pi)/min/mg proteins, according to the titration curve previously prepared.

### 3.11 Intracellular doxorubicin accumulation and efflux

$5 \times 10^5$  cells were incubated as reported in the Results section, then washed twice with PBS, detached with scraper and centrifuged at 13.000 x g for 5 min at 4°C. Cell pellets were resuspended in 400  $\mu$ l of a 1:1 mixture

of ethanol/0.3 N HCl and sonicated. The amount of intracellular doxorubicin was detected using a HT Synergy 96-well micro-plate reader. Excitation and emission wavelengths were 475 and 553 nm, respectively. A blank was prepared in the absence of cells in each set of experiments and its fluorescence was subtracted from that measured in each sample. Fluorescence was converted in nmoles doxorubicin/mg cell proteins using a calibration curve.

For doxorubicin efflux,  $5 \times 10^5$  cells were incubated for 10 min with increasing (0-50  $\mu$ M) concentrations of doxorubicin, with or without glabratephrin, then washed and analyzed for the intracellular concentration of doxorubicin. A second series of dishes, after the incubation under the same experimental conditions, were left for further 10 min at 37°C, then washed and tested for the intracellular drug content. The difference of doxorubicin concentration between the two series, expressed as nmol doxorubicin extruded/min/mg total cell proteins were plotted versus the initial drugs concentration. Values were fitted to Michaelis-Menten equation to calculate Vmax and Km, using the Enzfitter software (Biosoft Corporation, Cambridge, United Kingdom).

### 3.12 Quantitative real time-PCR (qRT-PCR)

Total RNA was extracted by phenol/chloroform method. 1  $\mu$ g RNA was reverse-transcribed using the iScript Reverse Transcription Supermix kit (Bio-Rad Laboratories), according to the manufacturer's instruction. 25 ng cDNA were amplified with 10  $\mu$ L IQ<sup>TM</sup> SYBR Green Supermix (Bio-Rad Laboratories). Primers were designed with the qPrimer Depot software (<http://primerdepot.nci.nih.gov/>): *P-gp/ABCB1/MDR1* (human): 5'-TGCTGGAGCGGTTCTACG-3', 5'-ATAGGCAATGTTCTCAGCAATG-3'; *MRP1/ABCC1* (human): 5'-CATTCAGCTCGTCTTGTCCTG-3'; 5'-

GGATTAGGGTCGTGGATGGTT-3’; *BCRP/ABCG2* (human): 5’-GTTTCAGCCGTGGAAC-3’; 5’-CTGCCTTTGGCTTCAAT-3’; *S14* (human): 5’-CGAGGCTGATGACCTGTTCT-3’, 5’-GCCCTCTCCCACTCTCTCTT-3’. RT-PCR was carried out with a iQ<sup>TM</sup>5 cyclor (Bio-Rad Laboratories). Cycling conditions were: 30 s at 95°C, followed by 40 cycles of denaturation (15 s at 95°C), annealing/extension (30 s at 60°C). The same cDNA preparation was used to quantify the genes of interest and the housekeeping gene *S14*, used to normalize gene expression. The relative quantitation of each sample was performed using the Gene Expression Quantitation software (Bio-Rad Laboratories). Results were expressed in arbitrary units. For each gene, the expression in untreated cells was considered “1”.

### 3.13 Flow cytometry analysis

Cells were harvested, washed twice in PBS, detached with cell dissociation solution (Sigma Chemical Co.) and re-suspended in culture medium containing 5% v/v fetal bovine serum. Samples were washed with 0.25% w/v PBS-bovine serum albumin (BSA), incubated with the primary antibody for anti-ABCB1/P-gp antibody (clone C219, Abcam) for 45 min at 4 °C. After twice washing with PBS-BSA 1% w/v, cells were incubated with a secondary fluorescein isothiocyanate (FITC)-conjugated antibody (Sigma Chemical Co.) for 30 min at 4 °C. After washing twice with PBS-BSA 1% w/v and fixing in paraformaldehyde 2 % w/v for 5 min at room temperature, samples were analyzed by Guava® easyCyte flow cytometer (Millipore), using the InCyte software (Millipore). Control experiments included incubation of cells with non-immune isotypic antibody, followed by the secondary antibody.

### 3.14 Rhodamine 123 efflux

Rhodamine 123 accumulation, which is inversely related to its efflux, was used as a second index of P-gp activity (Riganti *et al.*, 2011). Cells were washed with fresh PBS, detached and re-suspended in 1 ml of medium containing 5% v/v fetal bovine serum. The samples were maintained at 37°C for 20 min in the presence of 1 µg/ml rhodamine 123. After this incubation time, cells were washed and re-suspended in 0.5 ml of PBS. The intracellular rhodamine 123 content was detected fluorimetrically, using a HT Synergy 96-well micro-plate reader. The results were expressed as nmoles/mg total proteins.

### 3.15 Overexpression of wild-type and mutated P-gp

The pHa vector containing the complete *mdr1* cDNA, encoding for P-gp, was purchased from Addgene (Cambridge, MA) and subcloned into pCDNA3 vector as described (Doublier *et al.*, 2008). By sequencing the *mdr1* gene present in the pCDNA3 vector, we verified that it contained the wild-type sequence of P-gp (data not shown). pCDNA3 vector containing the wild-type *mdr1* cDNA, was subjected to PCR-based mutagenesis using the QuikChange kit (Stratagene, La Jolla, CA), following the manufacturer's instructions to generate the mutated constructs Gly185Val, Ser400Asn, Gly412Ala, Ser893Ala, Ser893Thr. The mutations were confirmed by DNA sequencing (data not shown). In transfection experiments,  $5 \times 10^4$  cells were seeded in fetal bovine serum-free medium and treated with 6 µl of jetPEI transfection reagent (Polyplus-transfection SA BIOPARC, Illkirch, France) and 3 µg DNA empty-pCDNA3 (mock cells), wild-type *mdr1*-pCDNA3 (wild-type P-gp) or mutated *mdr1*-pCDNA3 (mutated P-gp). After 6 h, cells were washed and grown in

complete medium for 48 h before the experiments indicated in the Results section.

### **3.16 ROS measurement**

$1 \times 10^5$  cells were re-suspended in 0.5 ml PBS, incubated for 30 min at 37°C with 5  $\mu$ M of the fluorescent probe 5-(and-6)-chloromethyl-2',7'-dichlorodihydro-fluorescein diacetate-acetoxymethyl ester (DCFDA-AM), centrifuged at 13,000 x g at 37°C and re-suspended in 0.5 ml PBS. The fluorescence of each sample, considered an index of ROS levels, was read at 492 nm ( $\lambda$  excitation) and 517 nm ( $\lambda$  emission), using a HT Synergy 96-well micro-plate reader. The results were expressed as nmoles/mg cell proteins.

### **3.17 $\alpha$ NF-kB and HIF-1 $\alpha$ activity**

Nuclea were isolated with the Nuclear Extraction kit (Active Motif, Rixensart, Belgium), as per manufacturer's instructions. NF-kB activity was measured on 10  $\mu$ g of nuclear proteins by using the TRansAM Flexi NF-kB activation kit (Active Motif), using the mix of antibodies provided by the kit (p50, p65, Rel-A, c-Rel, p52) or each antibody separately. HIF-1 $\alpha$  activity was measured using the HIF Activation Kit (Active Motif), as per manufacturer's instructions. The absorbance at 450 nm was measured with a Packard EL340 microplate reader (Bio-Tek Instruments). For each set of experiments, a blank was prepared with bis-distilled water, and its absorbance was subtracted from that obtained in the presence of nuclear extracts. Results were expressed as mU/mg nuclear proteins.

### **3.18 Chromatin Immunoprecipitation (ChIP) assays**

Chromatin immunoprecipitation (ChIP) experiments were performed using the Magna ChIP A/G Chromatin Immunoprecipitation kit (Millipore)

as per manufacturer's instructions. Samples were immunoprecipitated with 5 µg of ChIP grade anti-p50 (Abcam) or anti-p65 (Abcam) antibody, or with no antibody, as a blank. The immunoprecipitated DNA was then washed and eluted twice with 100 µl of elution buffer (0.1 M NaHCO<sub>3</sub>, 0.1% v/v sodium dodecyl sulfate), the crosslinking was reversed by incubating the samples at 65°C for 6 h, then samples were incubated with proteinase K (Sigma Chemicals Co.) for 1 h at 55°C. The DNA was eluted using the GenElute Mammalian Genomic DNA Miniprep kit (Sigma Chemicals Co.) and analyzed by qRT-PCR, as detailed above. The primer sequences of P-gp/ABCB1/MDR1 promoter, designed with Primer3 software (<http://frodo.wi.mit.edu/primer3>), were:

5'-CGATCCGCCTAAGAACAAG-3';

5'-AGCACAAATTGAAGGAAGGAG-3'. The following primers were used to amplify the sequence of P-gp/ABCB1/MDR1 promoter by qRT-PCR, from 20 ng of non-immuno-precipitated genomic DNA:

5'-GACCAAGCTCTCCTTGCATC-3';

5'-AGGGAAGTCTGGCAGCTGTA-3'. The results were expressed as ratio between the expression in immuno-precipitated samples and the expression in genomic samples. The relative expression of this ratio in untreated samples was considered as "1". As negative internal controls, immuno-precipitated samples were subjected to qRT-PCR with the following primers matching 10,000 bp upstream of the promoter:

5'-GTGGTGCCTGAGGAAGAGAG-3';

5'-GCAACAAGTAGGCACAAGCA-3'. In this condition, no qRT-PCR product was detected (data not shown).

### **3.19 Docking studies**

The docking studies were performed with the Molecular Operating Environment (MOE) software.

### 3.20 *In vivo* tumor growth

$1 \times 10^7$  JC cells were mixed with 100  $\mu$ l Matrigel and orthotopically implanted in 6 week-old female immunocompetent Balb/C mice (Charles River Laboratories Italia, Calco), housed (5 per cage) under 12 h light/dark cycle, with food and drinking provided *ad libitum*. Tumor growth was measured daily by caliper, according to the equation  $(L \times W^2)/2$ , where L=tumor length and W=tumor width. When tumor reached the volume of 50 mm<sup>3</sup>, mice (n= 8/group) were randomized. In a first experimental set, animals were treated on day 1, 7, 14 after randomization as it follows: 1) vehicle group (ctrl), treated with 200  $\mu$ l saline solution intravenously (i.v.); 2) glabratephrin group, treated with a 200  $\mu$ l water/10% DMSO solution i.v., containing 5  $\mu$ M glabratephrin; 3) doxorubicin group, treated with 5 mg/kg doxorubicin, dissolved in 200  $\mu$ l water i.v.; 4) glabratephrin + doxorubicin group, treated with 100  $\mu$ l of saline solution i.v. containing 5  $\mu$ M glabratephrin + 100  $\mu$ l water solution containing 5 mg/kg doxorubicin.

In a second experimental group, animals were treated on day 1, 7, 14 after randomization as it follows: 1) vehicle group (ctrl), treated with 200  $\mu$ L saline solution intravenously (i.v.); 2) curcumin group, treated with 5 mg/kg curcumin, dissolved in 200  $\mu$ l water/10% DMSO solution i.v.; 3) doxorubicin group, treated with 5 mg/kg doxorubicin, dissolved in 200  $\mu$ l water i.v.; 4) curcumin + doxorubicin group, treated with 100  $\mu$ l of water/10% DMSO solution containing with 5 mg/kg curcumin + 100  $\mu$ l water solution containing 5 mg/kg doxorubicin; 5) chitosan coated-SLN carrying curcumin group, treated i.v. with 200  $\mu$ l of saline solution containing 5 mg/kg curcumin; 6) chitosan coated-SLN carrying curcumin + doxorubicin group, treated i.v. with 100  $\mu$ l of saline solution. containing 5 mg/kg curcumin + 100  $\mu$ l water solution containing 5 mg/kg doxorubicin; 7) uncoated-SLN carrying curcumin group, treated i.v. with 100  $\mu$ l of

saline solution containing 5 mg/kg curcumin; 8) uncoated-SLN carrying curcumin + doxorubicin group, treated i.v with 200  $\mu$ l of saline solution containing 5 mg/kg curcumin + 100  $\mu$ l water solution containing 5 mg/kg doxorubicin.

Tumor volumes were monitored daily. Animals were euthanized at day 21 after randomization with zolazepam (0.2 ml/kg) and xylazine (16 mg/kg). lactate dehydrogenase (LDH), aspartate aminotransferase (AST), alanine aminotransferase (ALT), alkaline phosphatase (AP), creatinine, creatine phosphokinase (CPK) and CPK-MB, cardiac troponin I (cTnI) and T (cTnT) were measured on blood samples collected immediately after euthanasia, using commercially available kits from Beckman Coulter Inc. (Beckman Coulter, Miami, FL). The Animal care and experimental procedures were approved by the Bio-Ethical Committee of the Italian Ministry of Health (#122/2015-PR).

### **3.21 Statistical analysis**

All data in the text and figures are provided as means  $\pm$  SD. The results were analysed by a one-way analysis of variance (ANOVA) and Tukey's test, using GraphPad Prism (v 6.01) software and Statistical Package for Social Science (SPSS) software (IBM SPSS Statistics v.19).  $p < 0.05$  was considered significant.



## **4. RESULTS**

## 4.1 Aim 1: Use of photoexcitable/NO-releasing doxorubicins (PNODOXOs) to reverse drug resistance in human melanoma

### 4.1.1 Stability of PNODOXOs

The stability of the PNODOXOs 11, 12 and 13 (Scheme 1, section Materials and Methods) was evaluated by HPLC in phosphate buffer (PBS) pH 7.4., in Dulbecco Modified Eagle Medium (DMEM) and in human serum. All compounds were hydrolysed with pseudo-first kinetics. The observed pseudo-first-order rate constants ( $k_{obs}$ ) for the hydrolysis were calculated by fitting the remaining PNODOXOs against the time with one-phase exponential decay equation (Graf Pad, Prism software v6).

$$\text{Equation 1: } t_{1/2} = 0.693 / k_{obs}$$

The corresponding half-lives ( $t_{1/2}$ ), calculated from equation 1, were reported in Table 2.

**Table 2.** The stability of the target products 11-13 was evaluated by HPLC.

Compd	Stability $t_{1/2}$ (h)		
	PBS	DMEM	Human serum
11	2.0	1.8	0.75 (45 min)
12	Nd	> 24 84% conc. at 24 h	12.1
13	> 24 90% conc. at 24 h	> 24 85% conc. at 24 h	> 24 60% conc. at 24 h

Nd: non detectable

As expected the two aromatic esters 12, 13, were more stable than the aliphatic ester 11. HPLC analysis showed that doxorubicin and the acids 5, 7, 9 (Scheme 1) were the main degradation products. This is in keeping with the higher stability to hydrolysis in the compounds 12, 13 of the amide function as to the ester one.

#### 4.1.2 Spectroscopic and photochemical properties

##### 4.1.2.1 NO-photorelease of PNODOXOs

The capacity of 11-13 and of the reference compound 4, a strong photoexcitable NO donor (NOPD) with the same structure of the NO releasing moiety of compound 12, to release NO over 30 min, under irradiation with a violet led with wavelength 400 nm and 10W power was evaluated at 100  $\mu\text{M}$  concentration in PBS (pH 7.4), using an irradiance of 7  $\text{mW}/\text{cm}^2$ . NO released was detected as nitrite, its main degradation product in aerobic aqueous solution, by Griess reaction. The results are summarized in Figure 6. Upon irradiation, PNODOXOs 11, 12 were NO-donor as potent as the reference 4, while 13 displayed a significantly lower release. In these conditions, all compounds released NO time-dependently, while they did not release NO in the dark (data not shown).

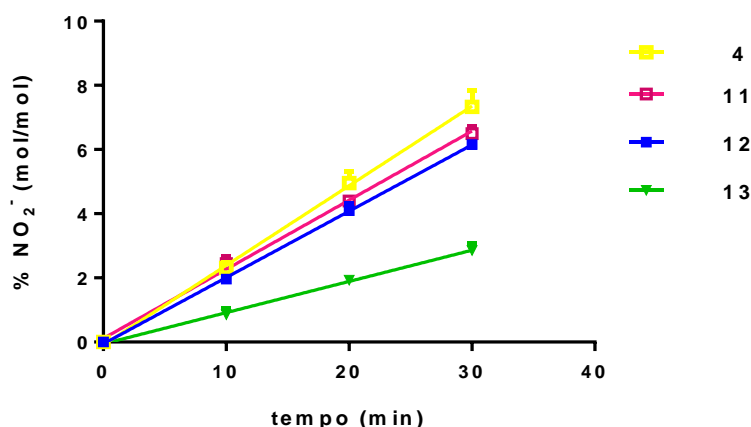


**Figure 6.** NO release by compounds 4, 11, 12 and 13 upon irradiation in PBS. Results were expressed as mmoles NO released/mmoles of each compound. The graph is representative of one out of three similar experiments.

### 4.1.3 Biological assays

The release of NO from compound 4 and two PNODOXOs 12 and 13 - i.e. a strong and poor NO-releasing PNODOXs - were tested in human melanoma M14 cells, which express several ABC transporters (Figure 7). Dox did not elicit any increase of nitrites independently from cell irradiation, except when co-incubated with compound 4 (Figure 8). In line with the NO release in acellular systems, compound 4 and 12 significantly increased nitrite levels in irradiated cells, whereas the less potent PNODOXO 13 did not. As expected, none of the compounds increased nitrite in not-irradiated cells (Figure 8).

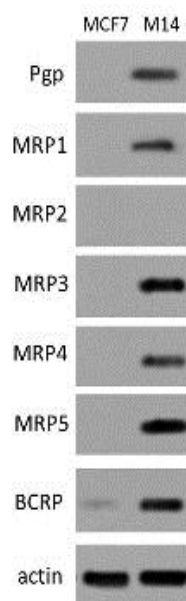


**Figure 7. ABC transporters expression in melanoma cells.** The expression of P-gp, MRP1, MRP2, MRP3, MRP4, MRP5, BCRP was measured in human melanoma M14 whole cell lysates by immunoblotting. Actin was used as control of equal protein loading. Human MCF7 cells were included as cell line with low/undetectable levels of most transporters. The figure is representative of one out of three similar experiments.

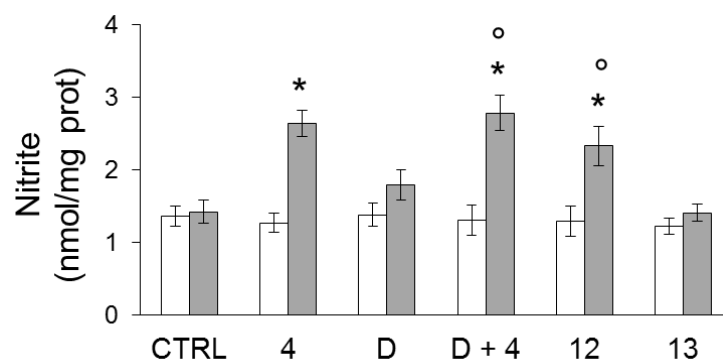


**Figure 8. Nitrites amount in melanoma cells treated with NOPD and PNODOXOs.**

M14 cells were maintained for 20 minutes at room temperature in PBS, in a dark room (white columns) or were subjected to irradiation (grey columns) with 400 nm, 10W violet led ( $7 \text{ mW/cm}^2$ ), in the absence (CTRL) or presence of  $5 \mu\text{M}$  compound 4 (NOPD), Dox (D), Dox + compound 4 (D + 4), compound 12 or 13 (PNODOXOs). After 24 h in complete medium, cells were subjected to the following assays. Nitrite levels were measured by the Griess methods. Measurements were performed in triplicate and data are presented as means  $\pm$ SD ( $n = 3$ ); vs. untreated cells (CTRL): \*  $p < 0.005$ ; vs. Dox-treated cells (D): °  $p < 0.005$ .

As mentioned earlier, NO inhibits the drug efflux activity of ABC transporters by nitrating critical tyrosines (Riganti *et al.*, 2005; De Boo *et al.*, 2009; Fruttero *et al.*, 2010; Chegaev *et al.*, 2011; Riganti *et al.*, 2013; Gazzano *et al.*, 2016). In line with these findings, P-gp, MRP1, MRP4 and BCRP were nitrated on tyrosines when exposed to compound 4 (alone or co-incubated with Dox) and compound 12, the strongest PNODOXO, upon irradiation (Figure 9A). When nitrated, these pumps had a reduced catalytic ATPase activity (Figure 9B), suggesting that cells treated with PNODOXO 12 can accumulate more of drug upon irradiation.

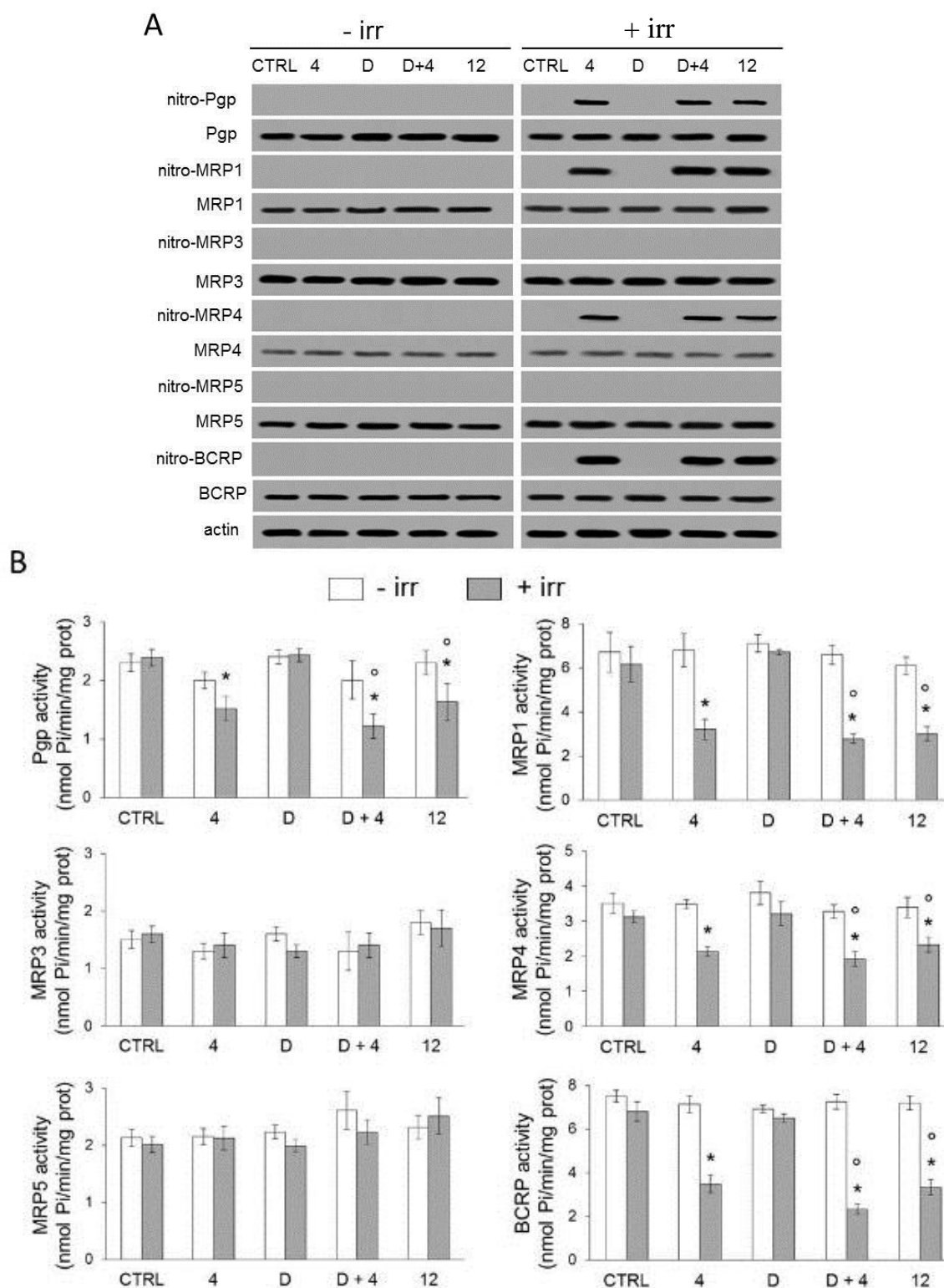


**Figure 9. Nitration and ATPase activity of ABC transporters by NOPD and PNODOXOs.** (A) Immunoblot detection of nitrated ABC transporters in M14 melanoma cells maintained for 20 min at room temperature in PBS in a dark room (-irr) or irradiated (+ irr;  $\lambda_{exc} = 400 \text{ nm}$ ,  $7 \text{ mW/cm}^2$ ), in the absence CTRL or presence of  $5 \mu\text{M}$  compound 4 (NOPD), Dox (D), Dox + compound 4, compound 12 PNODOXO). (B) ATPase activity. Data are presented as means  $\pm$  SD ( $n = 3$ ); vs untreated cells (CTRL), \* $p < 0.02$ ; vs Dox-treated cells,  $^{\circ}p < 0.002$ .

Although not all the transporters present in M14 cells were nitrated, we evaluated if the reduced activity of nitrated drug efflux transporters was sufficient to induce Dox-mediated damages. The anti-tumor efficacy of Dox and PNODOXOs by measuring the extracellular release of LDH, an index of cell damage and necrosis (Riganti *et al.*, 2005). As expected, Dox alone did not induce any cell damage in M14 cells. The co-incubation of Dox and compound 4, however, significantly induced cytotoxicity upon irradiation, overcoming Dox-resistance. A similar effect was exerted by the stronger PNODOXO 12, while no toxicity was elicited by the weaker PNODOXO 13 (Figure 10).

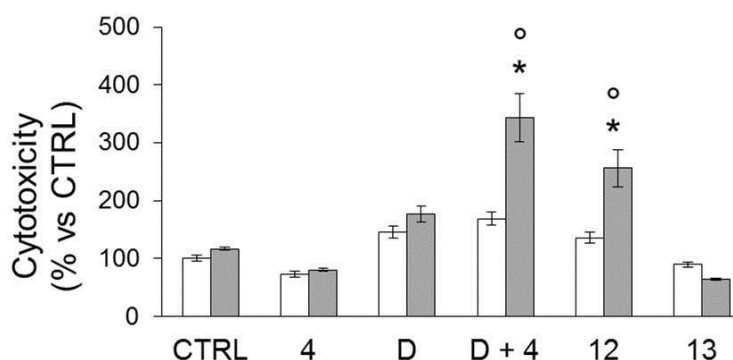


**Figure 10. Cytotoxicity of NOPD and PNODOXOs.** Cytotoxicity observed in melanoma M14 cells maintained for 20 min at room temperature in PBS in the dark (white columns) or irradiated (grey columns;  $\lambda_{exc} = 400$  nm, 7 mW/cm<sup>2</sup>), in the absence (CTRL) or in the presence of 5  $\mu$ M 5  $\mu$ M compound 4 (NOPD), Dox (D), Dox + compound 4, compound 12 and compound 13 (PNODOXOs). Measurements were performed in triplicate and data are presented as means  $\pm$  SD (n = 3); vs untreated cells (CTRL), \*p < 0.001; vs Dox-treated cells, °p < 0.001 significantly induced cytotoxicity upon irradiation, overcoming Dox-resistance.

The absence of toxicity of 4 and 13 was confirmed also in not-transformed cells, such as fibroblasts and cardiomyocytes (Figure 11), a well-known target of Dox (Granados-Principal *et al.*, 2010). As expected, Dox was toxic in both cell populations. Interestingly the co-incubation with

4 did not increase further the Dox's cytotoxicity. Curiously, compound 12, which was cytotoxic against melanoma cells, was less toxic than parental Dox on non-transformed cells, such as fibroblasts and cardiomyocytes (Figure 11 A-B).

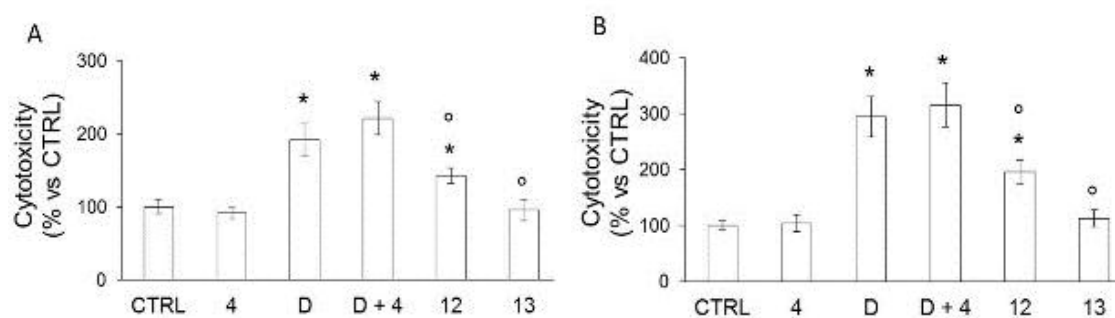


**Figure 11. Cytotoxicity on human fibroblasts and rat H9c2 cardiomyocytes.** Cytotoxicity observed human fibroblasts (A) and rat H9c2 cardiomyocytes (B) maintained for 20 min at room temperature in PBS in the absence (CTRL) or in the presence of 5  $\mu$ M compound 4 (NOPD), Dox (D), Dox + compound 4, compound 12 and compound 13 (PNODOXOs). Measurements were performed in triplicate and data are presented as means  $\pm$  SD ( $n = 3$ ); vs untreated cells (CTRL), \* $p < 0.001$ ; vs Dox-treated cells, ° $p < 0.001$ .



---

## **4.2 Aim 2: Using natural products to overcome doxorubicin resistance in human and murine TNBC cells**

### **4.2.1 A screening on natural pure compounds to overcome doxorubicin resistance**

We performed a screening of the twelve natural pure compounds, selected on the basis of their different biological activities on cell proliferation, cell death and redox properties reported in literature, and indicated in Table 1 (Materials and Methods section): neviotine A (Nev) and sipholenol N (Sip); Arctigenin (Arc); Delta-Valerolactone (D-Val), Gamma-Valerolactone (G-Val) and Enterolactone (Ent); Furanocoumarins; Bergapten (Ber) and Iso Bergapten (Iso-B); Osthol (Osh); Guggulsterone (Gug); Magnesium lithospermate B (MLB) and Glabratephrin (Glab).

#### **4.2.1.1 Doxorubicin accumulation and viability in MDA-MB-231 cells, resistant counterpart MDA-MB-231/DX cells and JC cells**

First, from MDA-MB-231 breast cancer cells, we generated the MDA-MB-231/DX subline by culturing parental cells in medium with increasing concentrations of doxorubicin, as detailed in the Material and Methods section. Murine mammary JC cells were used as a model of constitutively-expressing P-gp cells (Lee *et al.*, 2003). Starting from passage number 10, MDA-MB-231/DX sub line increased P-gp protein and mRNA, reaching a plateau level of protein and mRNA (Figure 12A-B) starting from passage 20, corresponding to culture conditions with 250 nM doxorubicin-containing medium.

The increase of P-gp was not accompanied by any increase in MRP1 or BCRP (Figure 12A), other two transporters involved in Dox efflux (Gottesman *et al.*, 2002). However, the increase in P-gp expression was accompanied by a progressive increase in the transcriptional activity of

Hypoxia Inducible Factor 1 $\alpha$  (HIF-1 $\alpha$ ), a transcription factor activated by doxorubicin (Kopecka *et al.*, 2015) and an inducer of P-gp gene transcription (Comerford *et al.*, 2002) (Figure 12C).

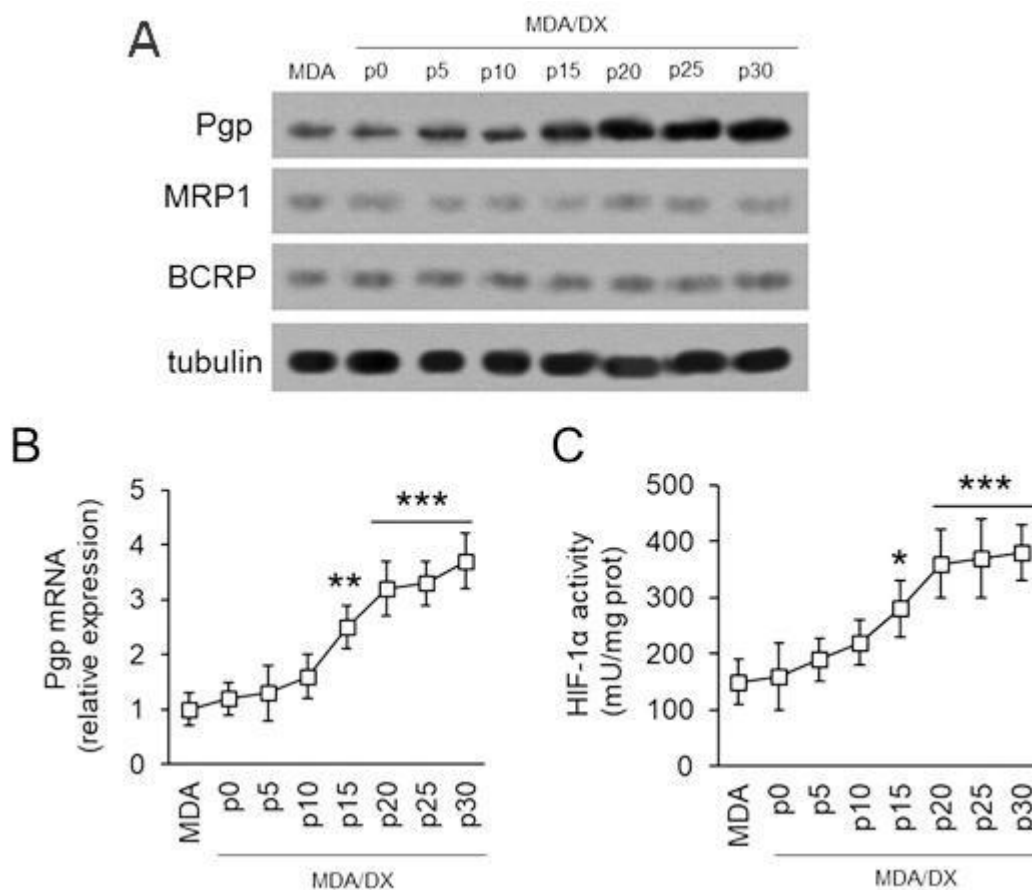


**Figure 12. MDA-MB-231/DX subline generation.**

(A) MDA-MB-231 cells were cultured in medium with increasing concentration of doxorubicin, as indicated in Materials and Methods section, generating the resistant subline (MDA/DX). At time 0 (p0) and every 5 passages (p) cells were lysed and subjected to immunoblotting for the indicated proteins. Tubulin was used to check the equal control of protein loading. The figure is representative of 1 out of 3 experiments. Parental MDA-MB-231 (MDA) cells were included as internal control. (B) P-gp mRNA was measured by RT-PCR in triplicates. Data are presented as means  $\pm$  SD (n=3). MDA/DX vs MDA: \*\* p < 0.01; \*\*\* p < 0.001. (C) HIF-1 $\alpha$  activity was measured by ELISA in duplicates. Data are presented as means  $\pm$  SD (n=3). MDA/DX vs MDA: \* p < 0.05; \*\* p < 0.001.

For all the subsequent experiments, we used cells at passage 25, i.e. stably growing in medium containing 500 nM Dox.

As shown in Figure 13A, MDA-MB-231/DX cells had an intermediate expression between parental MDA-MB-231 and JC cells. Consistently, MDA-MB-231/DX cells retained significantly less doxorubicin than parental MDA-MB-231 cells and JC cells had the lowest accumulation of the drug (Figure 13B). In viability assays, 5  $\mu$ M doxorubicin induced a significant reduction of MDA-MB-231 cells, that was less pronounced in MDA-MB-231/DX subline and absent in JC cells (Figure 13C). Similarly, 25  $\mu$ M Dox, that was more accumulated within all cell lines except on JC cells (Figure 13B), produced a moderate decrease in cell viability in MDA-MB-231/DX cells and had no effects on JC cells (Figure 13C). These data suggest that MDA-MB-231/DX subline was able to survive to a dose of doxorubicin (5  $\mu$ M) that typically discriminates sensitive from resistant cells (Riganti *et al.*, 2005), but was damaged by a five-fold higher (5  $\mu$ M) dose of doxorubicin that induced significant damages in most cell lines, except JC cells (Riganti, Gazzano, *et al.*, 2015). This different behavior can be explained by the difference in expression levels of P-gp between MDA-MB-231, MDA-MB-231/DX and JC cells. On the basis of these results, we considered MDA-MB-231, MDA-MB-231/DX and JC cells as doxorubicin-sensitive, moderately doxorubicin-resistant and strongly doxorubicin-resistant cells, respectively.

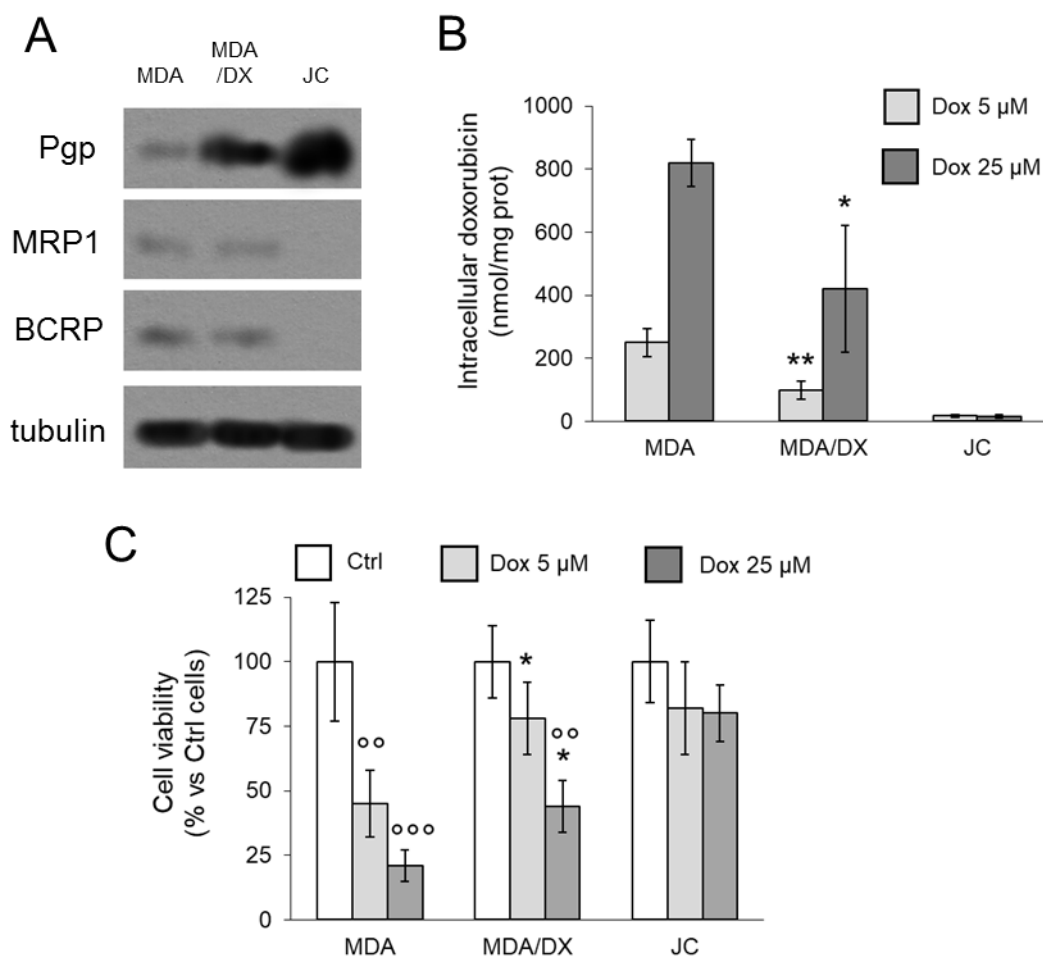


**Figure 13. Doxorubicin accumulation and cytotoxicity in breast cancer cells with different degrees of resistance.**

(A) MDA-MB-231 cells (MDA), MDA-MB-231/DX cells (MDA/DX) and JC cells were lysed and subjected to immunoblotting for the indicated proteins. Tubulin was used to check the equal control of protein loading. The figure is representative of 1 out of 3 experiments. (B) Cells were incubated 24 h with 5 or 25  $\mu$ M doxorubicin (Dox). The intracellular drug accumulation was measured fluorimetrically in duplicates. Data are presented as means  $\pm$  SD (n = 3). MDA-MB-231/DX cells vs. MDA-MB-231 cells: \* p < 0.05; \*\* p < 0.01. (C) Cells were grown 72 h in fresh medium (Ctrl) or in medium with 5 or 25  $\mu$ M Dox. Cell viability was measured by crystal violet staining in quadruplicates. Data are presented as means  $\pm$  SD (n = 3). MDA-MB-231/DX cells vs. MDA-MB-231 cells: \* p < 0.05; Dox vs Ctrl cells: <sup>oo</sup> p < 0.01, <sup>ooo</sup> p < 0.001.

The IC<sub>50</sub> of each compound was > 1 mM in all cell lines, with the exception of Sip, Osh, MLB and Glab in MDA-MB-231/DX and JC cells, where the value was reduced below 250 μM (Table 3).

**Table 3. IC<sub>50</sub> (mM) of natural compounds in breast cancer cells.**

Compound	IC <sub>50</sub> (mM) in MDA-MB- 231 cells	IC <sub>50</sub> (mM) in MDA-MB- 231/DX cells	IC <sub>50</sub> (mM) in JC cells
Neviotine A	> 1	> 1	> 1
Sipholenol N	> 1	0.0238	0.0164
Arctigenin	> 1	> 1	> 1
Delta-Valerolactone	> 1	> 1	> 1
Gamma-Valerolactone	> 1	> 1	> 1
Enterolactone	> 1	> 1	> 1
Bergapten	> 1	> 1	> 1
Iso Bergapten	> 1	> 1	> 1
Osthol	> 1	0.1986	0.0828
Guggulsterone	> 1	> 1	> 1
Magnesium lithospermate B	> 1	0.1963	0.0637
Glabratephrin	> 1	0.2356	0.1378

$1 \times 10^4$  cells were seeded in quadruplicate in 96-well plates, treated at scalar concentrations (from  $10^{-9}$  M to  $10^{-2}$  M) of each compounds for 72 h, then cell viability was calculated by crystal violet staining. IC<sub>50</sub> i.e. the concentration of each compound that decreased the cell viability by 50%, was calculated with the GraphPad Prism (v 6.01) software. Data are means  $\pm$  SD (n = 4).

In preliminary screening, we incubated the three cell lines with Sip, Osh, MLB or Glab at different concentrations (1 nM, 10 nM, 100 nM, 1 μM, 10 μM), with or without 5, 0.5 and 0.05 μM doxorubicin. We measured cell viability using crystal violet after 72 h. In sensitive MDA-MB-231 cells, none of the compounds increased the cytotoxic effects of doxorubicin (Figure 14A). In moderately resistant MDA-MB-231/DX cells, 5, 0.5 and 0.05 μM reduced cell viability no more than 20%, but Sip, Osh,

MLB and Glab increased cell death starting from 10 nM concentration (Figure 14B). In highly -resistant JC cells, doxorubicin did not significantly reduce cells viability, as expected. Interestingly, only Glab rescued the cytotoxicity of doxorubicin when used at 100 nM or higher concentrations (Figure 14C).

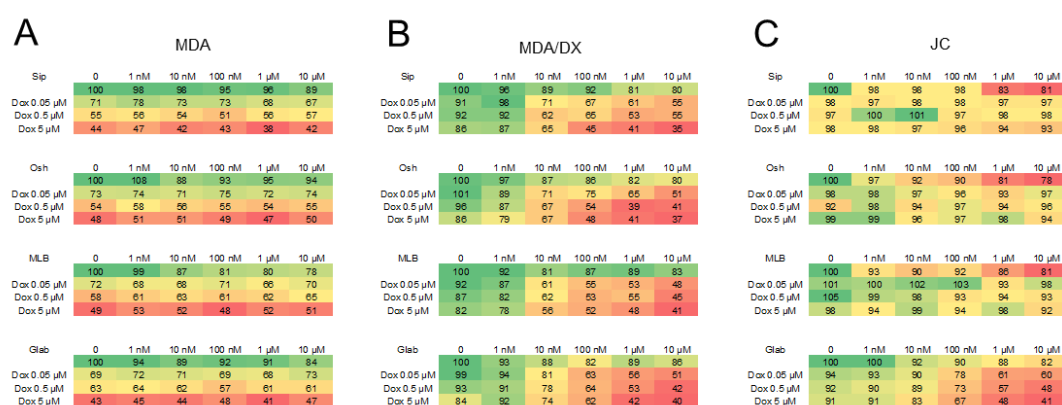


**Figure 14. Effects of selected natural compounds on doxorubicin cytotoxicity in breast cancer cells with different degrees of resistance.**

MDA-MB-231 cells (MDA, panel A), MDA-MB-231/DX cells (MDA/DX, panel B) and JC cells (panel C) were grown for 72 h in fresh medium (0) or in medium containing siphonol N (Sip), Osthol (Osh), Magnesium lithospermate B (MLB) and Glabratephrin (Glab) at 1 nM, 10 nM, 100 nM, 1 μM and 10 μM, alone or in the presence of 0.05 μM, 0.5 μM and 5 μM doxorubicin (Dox). Cell viability was measured by crystal violet staining, in quadruplicate. The heatmaps represent the mean percentage of viable cells in each condition, where the viability of untreated cells was considered 100%, in a colorimetric scale (n = 3 independent experiments). For MDA-MB-231 cells: Dox 0.05 μM vs. untreated cells: \*\* p < 0.01, Dox 0.5 and 5 μM vs. untreated cells: \*\*\* p < 0.01 (all experimental conditions). For MDA-MB-231/DX cells: Dox 0.05, 5 and 5 μM vs. untreated cells: not significant; Dox + 10 nM compounds vs. Dox alone: ° p < 0.05; Dox + 100 nM/1 μM/10 μM compounds vs. Dox alone: °°° p < 0.001. For JC cells: Dox 0.05, 5 and 5 μM vs. untreated cells: not significant; Dox + 100 nM Glab vs. Dox alone: ° p < 0.05; Dox + 1 μM/10 μM compounds vs. Dox alone: °°° p < 0.001.

The effect of Glab was synergistic with Dox as indicated indeed the combination index (CI) was 0.29721 in MDA-MB-231/DX cells and 0.10922 in JC cells (Figure 15).

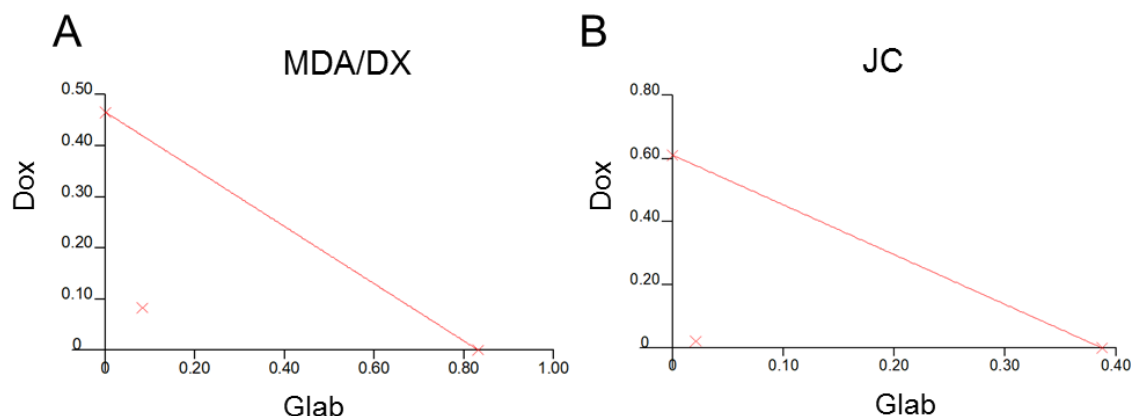


**Figure 15. Isobologram analyses of doxorubicin and Glabratephrin combination.**

MDA-MB-231/DX cells (MDA/DX, panel A) and JC cells (panel B) were grown for 72 h in fresh medium or in medium containing doxorubicin (Dox) and Glabratephrin (Glab), either alone or in combination, in the range of concentrations between  $10^{-9}$  and  $10^{-4}$  M. Cell viability was measured by crystal violet staining in quadruplicates. The isobologram analyses were performed using the CalcuSyn software.

#### 4.2.2 Mechanisms of the chemosensitizing effects of Glabratephrin

We thus investigated whether Glab enhanced doxorubicin cytotoxicity by increasing its intracellular retention and reducing doxorubicin efflux via P-gp. To clarify this point, we first measured the intracellular retention of doxorubicin. After 24 h incubation with doxorubicin and Glab at 100 nM, the anthracycline retention was significantly more accumulated in the P-gp-expressing MDA-MB-231 and JC cells but not in the P-gp-negative MDA-MB-231 cells (Figure 16A). Similarly, Glab increased the retention of rhodamine 123, another substrate of P-gp, in MDA-MB-231 and JC cells when co-incubated (Figure 16B). These data suggest that Glab competes with doxorubicin or rhodamine 123 for the efflux through P-gp, likely modifying its activity.

To further explore this issue, we measured the kinetic parameters of doxorubicin efflux from MDA-MB-231/DX and JC cells. As shown in Figure 16C, MDA-MB-231/DX cells have a lower  $V_{max}$  than JC cells, consistently with lower expression of P-gp of the former. In both cell lines, Glab reduced the  $V_{max}$  of doxorubicin efflux (Figure 16C). These data indicate that Glab reduced the maximal catalytic efficiency of P-gp. Glab did not change the amount of P-gp protein (Figure 16D), suggesting that the reduction of doxorubicin  $V_{max}$  was only caused by a decreased activity of the transporter, not by a different expression. Our hypothesis was proved by the significant decrease of P-gp ATPase activity induced by Glab (Figure 16E). In parallel, Glab increased the  $K_m$  of doxorubicin (Figure 16C), indicating a reduction in doxorubicin affinity for P-gp. This experimental set pointed out that Glab may directly binds to P-gp and alters its catalytic efficiency.



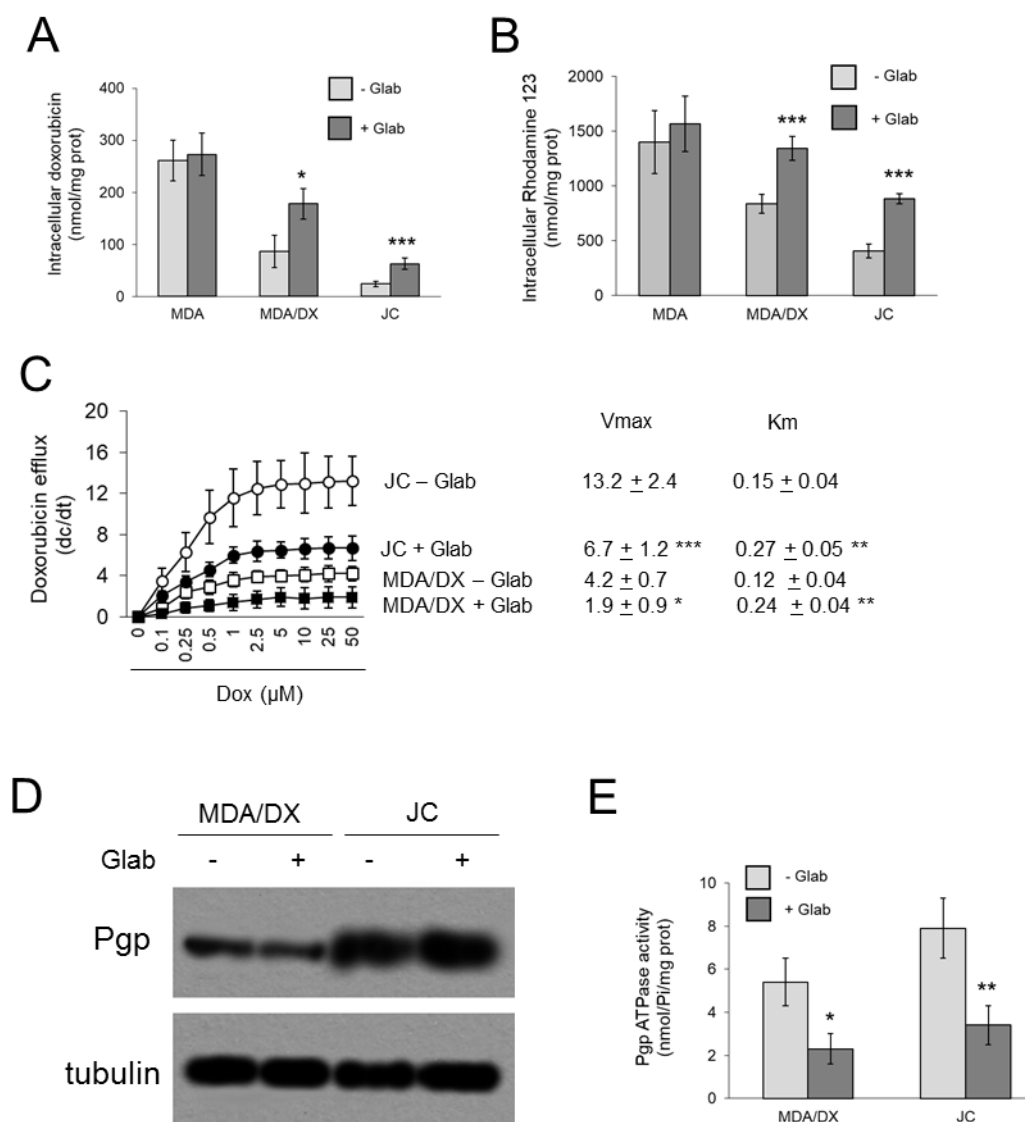


**Figure 16. Glabratephrin reduces doxorubicin efflux by inhibiting P-gp activity.**

(A) MDA-MB-231 cells (MDA), MDA-MB-231/DX cells (MDA/DX) and JC cells were incubated 24 h with 5 µM doxorubicin, in the absence (-) or presence (+) of 100 nM Glabratephrin (Glab). The intracellular drug accumulation was measured fluorimetrically in duplicates. Data are presented as means ± SD (n = 3). Glab-treated vs. untreated cells: \* p < 0.05; \*\*\* p < 0.001. (B) Cells were incubated 20 minutes with 1 µg/mL rhodamine 123, in the absence (-) or presence (+) of 100 nM Glab. The intracellular accumulation of rhodamine 123 was measured fluorimetrically in duplicates. Data are presented as means ± SD (n = 3). Glab-treated vs. untreated cells: \*\*\* p < 0.001. (C) Cells were incubated 10 minute with increasing concentrations of Dox (0.5-50 µM), in the absence (-) or presence (+) of 100 nM Glab. One series of dishes was analyzed for the intracellular doxorubicin concentration (c1); a second series was washed and let in the incubator for additional 10 minutes, then analyzed for the intracellular doxorubicin concentration (c2) as well. The dc/dt value was considered indicative of doxorubicin velocity of efflux. Data are presented as means ± SD (n = 3). Glab-treated vs. untreated cells: \* p < 0.05; \*\* p < 0.01; \*\*\* p < 0.001. (D). Cells were grown 24 h in the absence (-) or presence (+) of 100 nM Glab, then lysed and subjected to immunoblotting for P-gp. Tubulin was used to check the equal control of protein loading. The figure is representative of 1 out of 3 experiments. (E) Cells were grown as in (D). The P-gp ATPase activity was measured spectrophotometrically in duplicates. Data are presented as means ± SD (n = 3). Glab-treated vs. untreated cells: \* p < 0.05; \*\* p < 0.01.

#### 4.2.2.1 Molecular docking studies of glabratephrin on P-gp

To clarify that Glab may effectively binds P-gp, we studied its binding affinity to the protein (PDB: 4M2S) using Molecular Operating Environment (MOE) application for lead optimization and prediction of Glab-P-gp interaction. Docking accuracy was validated by redocking the co-crystallized ligand QZ59-RRR, cyclic-tris-(R)-valineselenazole, into the binding site of 4M2S. The docked ligand was overlying on the native co-crystallized ligand with root mean square deviation (RMSD) 1.31 Å, and binding free energy was (-10.07 kcal/mol) (Figure 17).

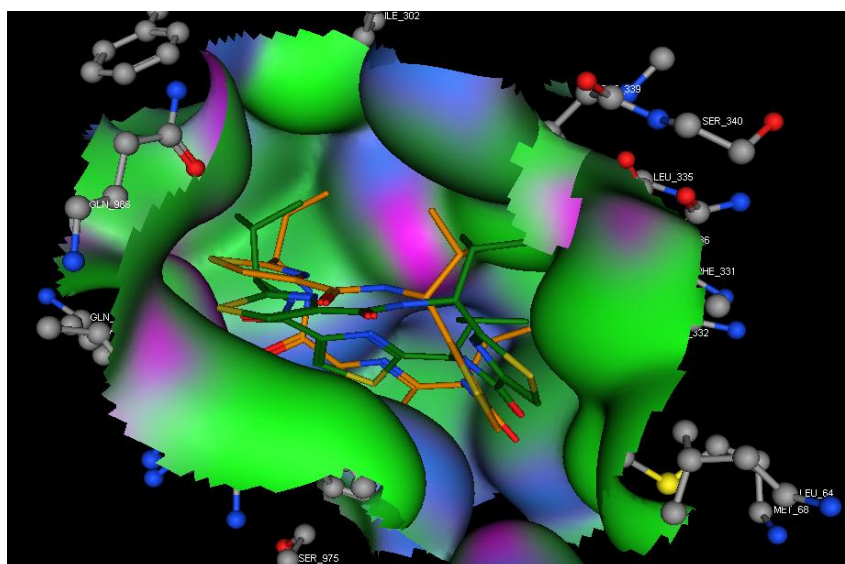


**Figure 17.** Superposition of the co-crystallized ligand QZ59-RRR (orange color) and re-docked ligand QZ59-RRR (green color).

For molecular docking calculation, firstly, the protein structure was separated from the inhibitor, followed by refinement using molecular minimization with the addition of hydrogen bond. Glab docking calculation was carried out using the slandered default variable for the MOE program. Glab was docked into the same groove of the co-crystallized ligand QZ59-RRR (Figure 18).

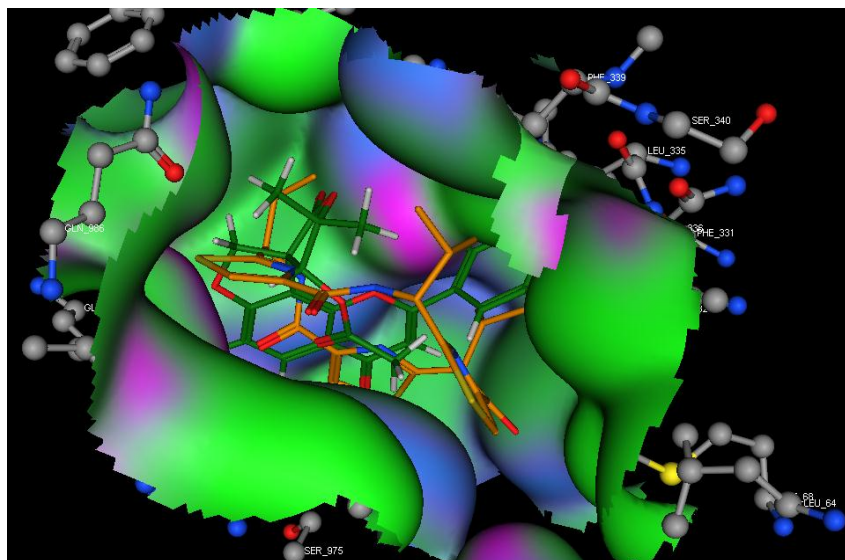


**Figure 18.** Superposition of the co-crystallized ligand QZ59-RRR (orange color) and glabratephrin (green color).

The docking score based on the binding affinity, measured by RMSD values, hydrogen bond and binding free energy (S-score, kcal/mol) (Table 4) was used to evaluate binding affinity.

**Table 4.** Binding affinity evaluation using binding free energy.

Name	Score (Kcal/mol)	No. of H-bond involved	Amino acid involved
Ligand (QZ59-RRR)	-10.07	2	GLN 721 PHE 979
Glabratephrin	-10.95	2	GLN 721 PHE 332

The binding mode of Glab with P-gp exhibited one H-bond donor with Gln 721 at a distance of 3.2 Å and one arene interaction with Phe979 (Figure 19A), one H-bond donor with Gln 721 at a distance of 2.6 Å and one arene interaction Phe 332 (Figure 19B). These results suggest that both the carbonyl group of the acetyl residue and the mono-substituted phenyl moiety of Glab are necessary to interact with P-gp.

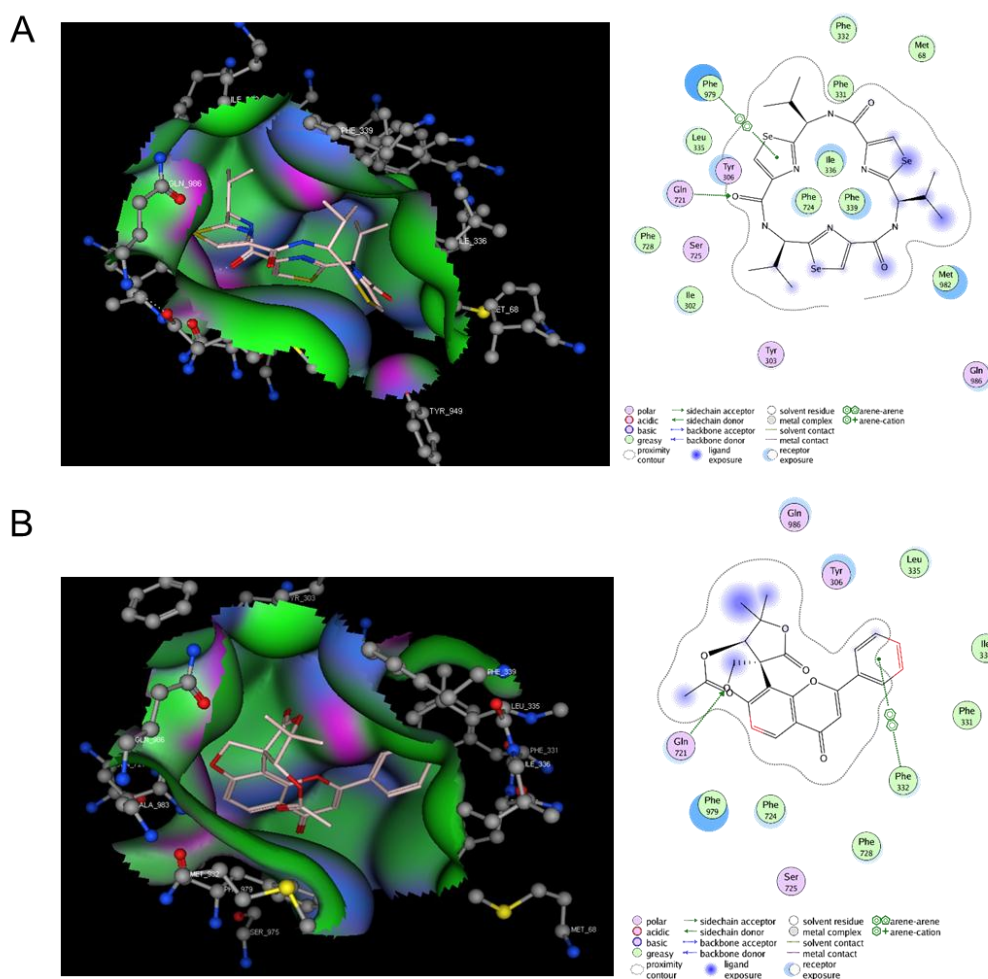


**Figure 19. Modelling of the functional groups involved in the interaction between Glab and P-gp.**

In order to identify a possible mechanism by which Glab interferes with P-gp, we over-expressed wild-type P-gp and five different mutants containing the mutations most commonly annotated in human tumors - Gly185Val, Ser400Asn, Gly412Ala, Ser893Ala, Ser893Thr (ABCMDb/Database for Mutations in ABC proteins; (<http://abcmutations.hegelab.org/>)) - in MDA-MB231 cells. As shown in Figure 20A, both wild-type and mutated P-gp were expressed at comparable levels, higher than the levels of endogenous P-gp. Interestingly, Glab increased doxorubicin accumulation in cells expressing wild-type P-gp and all mutated P-gp, except in cells expressing Gly185Val-

mutated P-gp (Figure 20B). Consistently, Glab reduced the ATPase activity of wild-type and mutated P-gp with the exception of Gly185Val-mutated P-gp (Figure 20C).

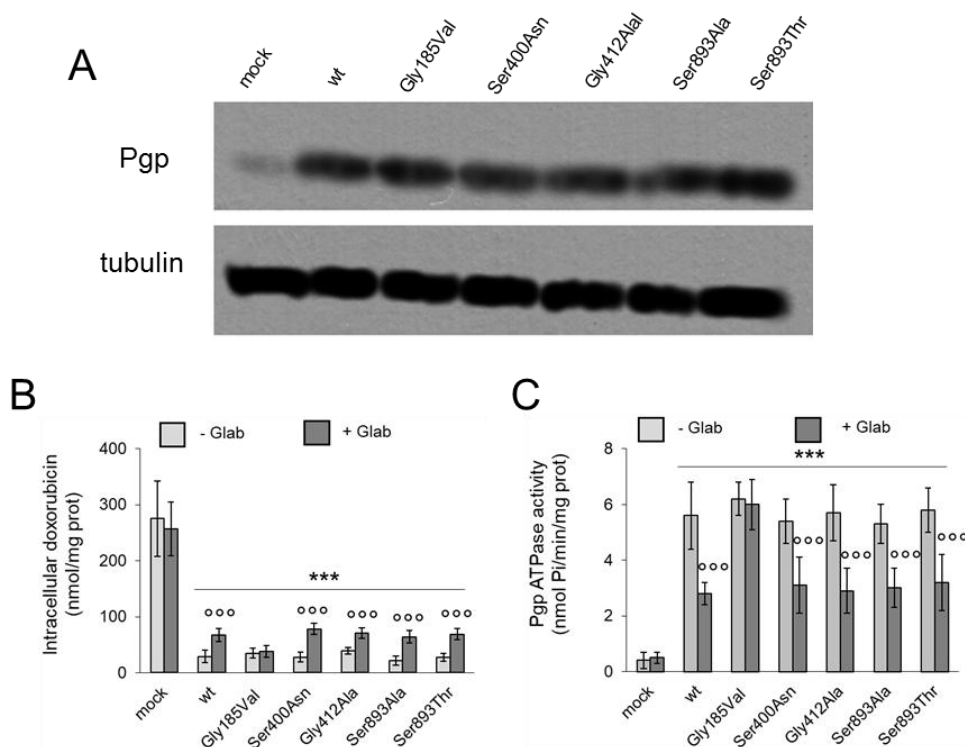


**Figure 20. Glabratephrin loses its efficacy in Gly185Val mutated P-gp.**

MDA-MB-231 cells were transfected with an empty vector (mock) or with expression vectors encoding wild-type (wt) P-gp, or Gly185Val, Ser400Asn, Gly412Ala, Ser893Ala, Ser893Thr-mutated P-gp. (A) Cells were lysed and subjected to immunoblotting for the indicated proteins. Tubulin was used to check the equal control of protein loading. The figure is representative of 1 out of 3 experiments. (B) Cells were incubated 24 h in the absence (-) or presence (+) of 100 nM Glabratephrin (Glab), with 5  $\mu$ M doxorubicin. The intracellular drug accumulation was measured fluorimetrically in duplicates. Data are presented as means  $\pm$  SD (n = 3). MDA-MB-231 cells overexpressing P-gp vs. mock cells: \*\*\* p < 0.001; Glab-treated cells vs corresponding untreated cells: <sup>ooo</sup> p < 0.001. (C) The P-gp ATPase activity was measured spectrophotometrically in duplicates. Data are presented as means  $\pm$  SD (n = 3). MDA-MB-231 cells overexpressing P-gp vs. mock cells: \*\*\* p < 0.001; Glab-treated cells vs corresponding untreated cells: <sup>ooo</sup> p < 0.001.

### 4.2.3 Efficacy of Glabratephrin against drug-resistant JC tumors

We next evaluated the efficacy of Glab in mice bearing JC tumors that were completely refractory to doxorubicin (Figure 21A-B). While Glab alone did not have any effects, the combination of Glab + doxorubicin lowered the rate of tumor growth (Figure 21A) and resulted in smaller tumor masses (Figure 21B). The growth profile was characterized by an initial delay in the growth of tumor, followed by a steady-state in the tumor volumes, suggesting that the effect of Glab + doxorubicin is cytostatic.

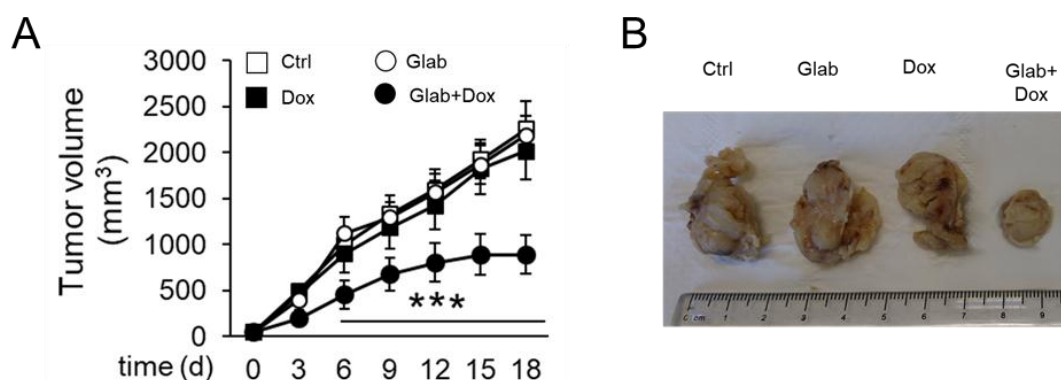


**Figure 21. Glabratephrin effect against drug-resistant JC tumors *in vivo*.**

JC cells were orthotopically implanted into 6 week-old female balb/C mice. When tumor reached the volume of 50 mm<sup>3</sup>, mice (n= 8/group) were randomized and treated as reported in the following groups, treated on day 1, 7, 14 after randomization: 1) vehicle group (Ctrl), treated with 200 μL saline solution intravenously (i.v.); 2) glabratephrin group (Glab), treated with a 200 μL water/10% DMSO solution i.v., containing 5 μM glabratephrin; 3) doxorubicin group (Dox), treated with 5 mg/kg doxorubicin, dissolved in 200 μL water i.v.; 4) glabratephrin + doxorubicin group (Glab+Dox), treated with 100 μL of saline solution i.v. containing 5 μM glabratephrin + 100 μL water solution containing 5 mg/kg doxorubicin. (A) Tumor growth was monitored daily by caliper measurement. Data are presented as means±SD. \*p<0.001: Glab+Dox treatment vs all the other treatment (days 9-18). (B) Photographs of representative tumors of each group.

Most P-gp inhibitors effective *in vitro*, failed in preclinical models for the high systemic toxicity (Callaghan *et al.*, 2014). We thus measured the hematochemical parameters in the treated animals at the time of sacrifice (Table 5). According to these assays, no signs of liver toxicities - indicated by lactate dehydrogenase (LDH), aspartate aminotransferase

(AST), alanine aminotransferase (ALT), alkaline phosphatase (AP) – and kidney toxicities – indicated by creatinine – were detected in Glab-treated animals, alone or in combination with doxorubicin. In our experimental protocol, doxorubicin was used at a the maximum tolerated dose (Gazzano *et al.*, 2018) that did not induce fatal-events related to heart toxicity, but induced a cardiac damage indicated by the increase of creatine phosphokinase (CPK), its cardiac specific isoform CPK-MB, and cardiac troponin T (cTnT). Furthermore, Glab alone did not affect cardiac parameters and did not worsen the damaged elicited by doxorubicin when used in combination.

**Table 5. Hematochemical parameters of the treated mice.**

	Ctrl	Glabratephrin	Doxorubicin	Glabratephrin + Doxorubicin
LDH (U/L)	6578 ± 504	6892 ± 298	6791 ± 471	6792 ± 561
AST (U/L)	193 ± 39	145 ± 35	139 ± 41	127 ± 38
ALT (U/L)	34 ± 7	36 ± 5	38 ± 7	39 ± 10
AP (U/L)	113 ± 31	145 ± 23	139 ± 18	128 ± 27
Creatinine (mg/L)	0.071 ± 0.012	0.065 ± 0.008	0.061 ± 0.008	0.064 ± 0.009
CPK (U/L)	287 ± 77	281 ± 62	542 ± 45 *	591 ± 78 *
CPK-MB (ng/mL)	0.128 ± 0.062	0.110 ± 0.044	0.321 ± 0.076 *	0.296 ± 0.081 *
cTnI (pg/mL)	1.089 ± 0.034	1.028 ± 0.089	1.055 ± 0.041	1.032 ± 0.042
cTnT (pg/mL)	1.983 ± 0.301	1.872 ± 0.217	2.986 ± 0.104 *	3.117 ± 0.285 *

Balb/C mice (n=8 animals/group) were treated as described the Figure 17. Blood was collected immediately after euthanasia and analyzed for lactate dehydrogenase (LDH), aspartate aminotransferase (AST), alanine aminotransferase (ALT), alkaline phosphatase (AP), creatinine, creatine phosphokinase (CPK) and CPK-MB, cardiac troponin I (cTnI) and T (cTnT). Data are presented as means±SD. \* p < 0.05: vs ctrl group.

### 4.3 Aim 3: The use of curcumin-loaded SLN as a nanotechnological approach to inhibit P-gp

#### 4.3.1 Curcumin-loaded SLN effect against drug-resistant cancer cells *in vitro*

In preliminary experiments, we measured the increase of doxorubicin accumulation and cytotoxicity in MDA-MB-231 cells expressing wild-type P-gp (Figure 20). As shown in Figure 22A-B, free curcumin increased doxorubicin retention and doxorubicin-induced cell damage at 25-50  $\mu$ M. However, at these concentrations, curcumin became cytotoxic also without doxorubicin. This is due to the fact that at micromolar concentrations curcumin exerts a cytotoxic activity on cancer cells (Lu *et al.*, 2013) and non-transformed cells (Hollborn *et al.*, 2013). Therein, finding a new strategy to increase the delivery of curcumin at lower concentrations is mandatory in the perspective of setting an effective anticancer strategy (Figure 22B).

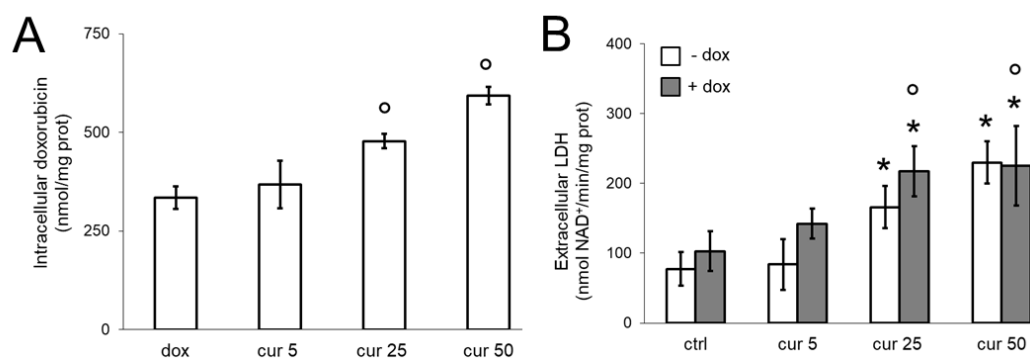


**Figure 22. Dose-dependence free curcumin on doxorubicin accumulation and cytotoxicity in MDA-MB-231-P-gp cells.** MDA-MB-231-P-gp cells were incubated 24 h with fresh medium (ctrl) or with the 5-25-50  $\mu$ M curcumin (cur), in the absence (-) or presence (+) of 5 50 doxorubicin (Dox). (A) Intracellular doxorubicin was measured fluorimetrically in duplicates. Data are presented as means  $\pm$  SD ( $n = 3$ ).  $^{\circ}$   $p < 0.01$ : vs Dox. (B) The release of LDH in the extracellular medium was measured spectrophotometrically in duplicate. Data are presented as means  $\pm$  SD ( $n = 3$ ). \*  $p < 0.05$ : vs untreated cells (ctrl);  $^{\circ}$   $p < 0.05$  vs Dox-treated cells.



In order to reduce the concentration of curcumin below the toxicity threshold, maintaining its ability to increase doxorubicin accumulation, we validated the SLN loaded with curcumin, decorated or not with chitosan. We hypothesized that SLN may allow a higher delivery of curcumin within the cells, enhancing the chemosensitizing effects towards free curcumin.

Preliminary experiments showed that blank SLN, i.e. SLN without curcumin, did not increase the release of LDH in MDA-MB-231-P-gp cells if diluted 1:100 after 24 h (data not shown). This dilution, which corresponded to a final concentration of 5  $\mu$ M curcumin, was used in all the subsequent experiments. Curcumin-loaded SLN and chitosan-containing/curcumin-loaded SLN increased doxorubicin accumulation (Figure 23A) and doxorubicin-induced release of LDH, without being cytotoxic in the absence of doxorubicin (Figure 23B).

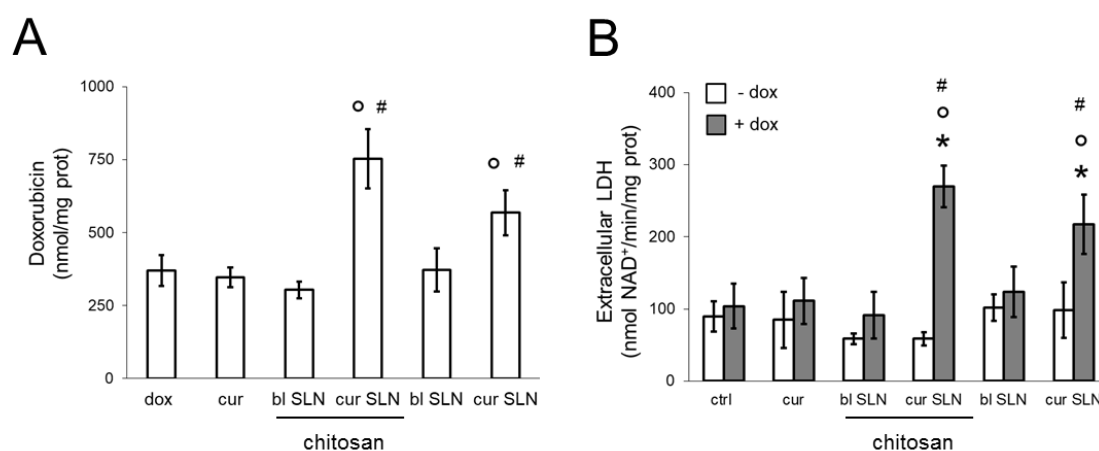


**Figure 23. Effect of curcumin-loaded SLN and chitosan-containing/curcumin-loaded SLN on doxorubicin accumulation and cytotoxicity in MDA-MB-231-P-gp cells.** MDA-MB-231 cells were incubated 24 h with fresh medium (ctrl) or with 5  $\mu$ M curcumin (cur), blank SLN (bl SLN), curcumin-loaded SLN (cur SLN, containing 5  $\mu$ M cur), (without and with chitosan. When indicated, 5  $\mu$ M doxorubicin (Dox) was added. (A) Intracellular doxorubicin was measured fluorimetrically in duplicates. Data are presented as means  $\pm$  SD (n = 3).  $^{\circ}$  p < 0.001: vs Dox; # p < 0.001 vs cur. (B) The release of LDH in the extracellular medium was measured spectrophotometrically in duplicate. Data are presented as means  $\pm$  SD (n = 3). \* p < 0.001: vs ctrl;  $^{\circ}$  p < 0.001: vs Dox; # p < 0.001 vs cur

Similar effects were obtained on the highly P-gp-expressing murine JC cells (Figure 24A-B).

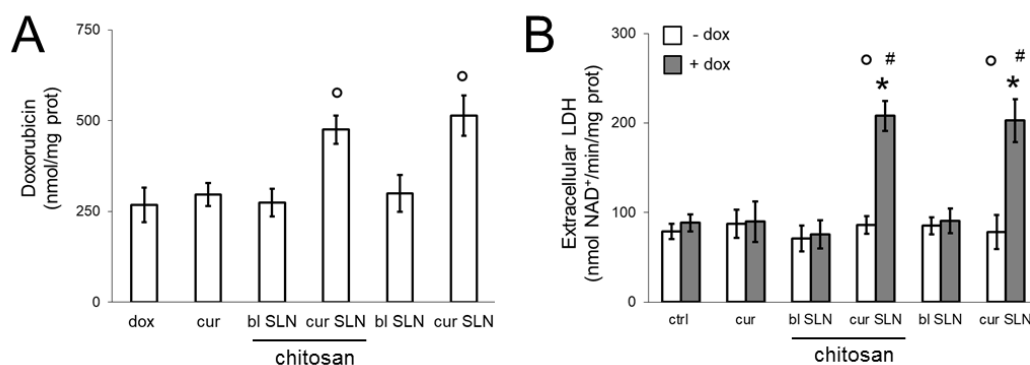


**Figure 24. Effect of curcumin-loaded SLN and chitosan-containing/curcumin-loaded SLN on doxorubicin accumulation and cytotoxicity in JC cells.** JC were incubated 24 h with fresh medium (ctrl) or with 5  $\mu$ M curcumin (cur), blank SLN (bl SLN), curcumin-loaded SLN (cur SLN, containing 5  $\mu$ M cur), without and with chitosan. When indicated, 5  $\mu$ M doxorubicin (Dox) was added. (A) Intracellular doxorubicin was measured fluorimetrically in duplicates. Data are presented as means  $\pm$  SD ( $n = 3$ ). <sup>°</sup>  $p < 0.001$ : vs Dox; #  $p < 0.001$  vs cur. (B) The release of LDH in the extracellular medium was measured spectrophotometrically in duplicate. Data are presented as means  $\pm$  SD ( $n = 3$ ). \*  $p < 0.001$ : vs ctrl; <sup>°</sup>  $p < 0.001$ : vs Dox; #  $p < 0.001$  vs cur.

To clarify whether the effects of SLN were due to changes in P-gp expression or activity, we first measured whether curcumin released from SLN may act as inhibitor of P-gp efflux activity, measuring the retention of rhodamine 123, a typical P-gp substrate. In long-term assays – (i.e. after a 24 h incubation of curcumin, curcumin-loaded SLN and chitosan-containing/curcumin-loaded SLN followed by a 20 min incubation with rhodamine 123) we observed an increased retention of rhodamine, indicative of a diminished efflux via P-gp, in cells treated with curcumin-loaded SLN and chitosan-containing/curcumin-loaded SLN (Figure 25A). In the short-term assays (i.e. curcumin and curcumin-loaded SLN co-incubated with rhodamine 123 for 20 min) we did not detect any changes in rhodamine efflux (Figure 25B).

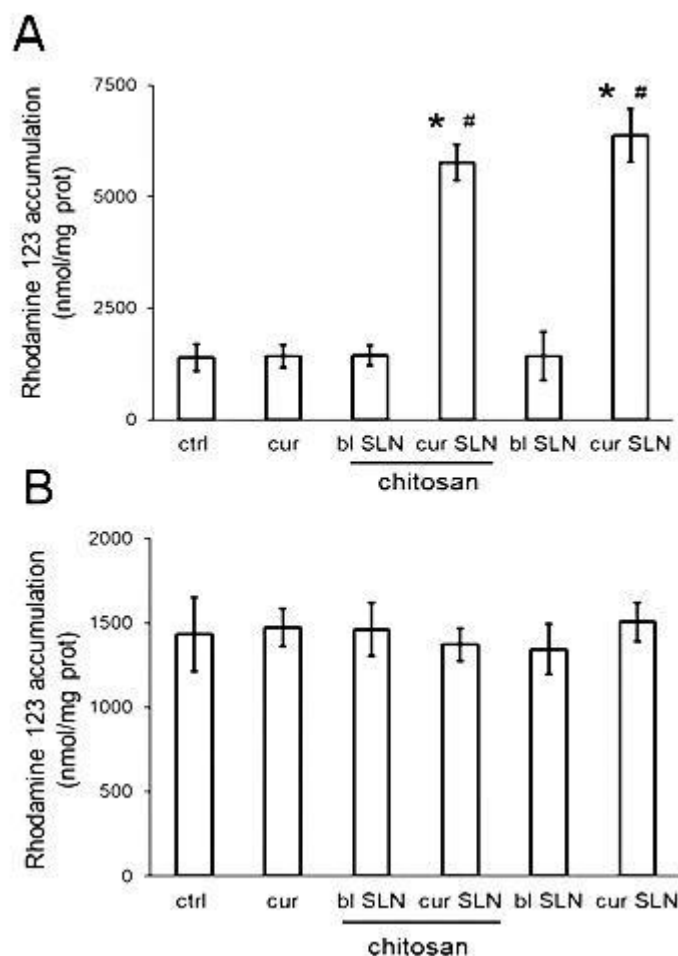


**Figure 25. Effect of curcumin-loaded SLN and chitosan-containing/curcumin-loaded SLN treated cells on P-gp activity.** (A) MDA-MB-231-P-gp cells were incubated 24 h with fresh medium (ctrl) or with 5  $\mu$ M curcumin (cur), blank SLN (bl SLN), curcumin-loaded SLN (cur SLN, containing 5  $\mu$ M cur), without and with chitosan. The P-gp substrate rhodamine 123 was added in the last 20 minutes. (B) Cells were co-incubated for 20 min with fresh medium (ctrl) or blank SLN (bl SLN), curcumin-loaded SLN (cur SLN, containing 5  $\mu$ M cur), without and with chitosan, together with rhodamine 123. In both assays, the intracellular accumulation of rhodamine 123 was measured fluorimetrically in duplicates. Measurements were performed in triplicate and data are presented as means  $\pm$  SD (n = 3). \* p < 0.001: vs ctrl; # p < 0.001 vs cur.

This experimental set suggests that it is unlikely that SLN loaded with curcumin act as competitive inhibitors of P-gp. We hypothesize that the increase in doxorubicin and rhodamine 123 retention was due to changes in P-gp expression. To investigate this issue, we first measured the amount of P-gp on cell surface, corresponding to the active form of the protein. As shown in Figure 26A-B, curcumin-loaded SLN and chitosan-containing/curcumin-loaded SLN slightly decreased the amount of surface

P-gp in MDA-MB-231-P-gp cells. Doxorubicin increased P-gp, likely as a consequence of the increased transcription of P-gp/ABCB1/MDR1 gene induced by active HIF-1 $\alpha$  upon doxorubicin exposure (Kopecka *et al.*, 2015). This increase was not reversed by free curcumin or blank SLN; but only by curcumin loaded SLN. No changes in untreated cells were detected in any experimental conditions.

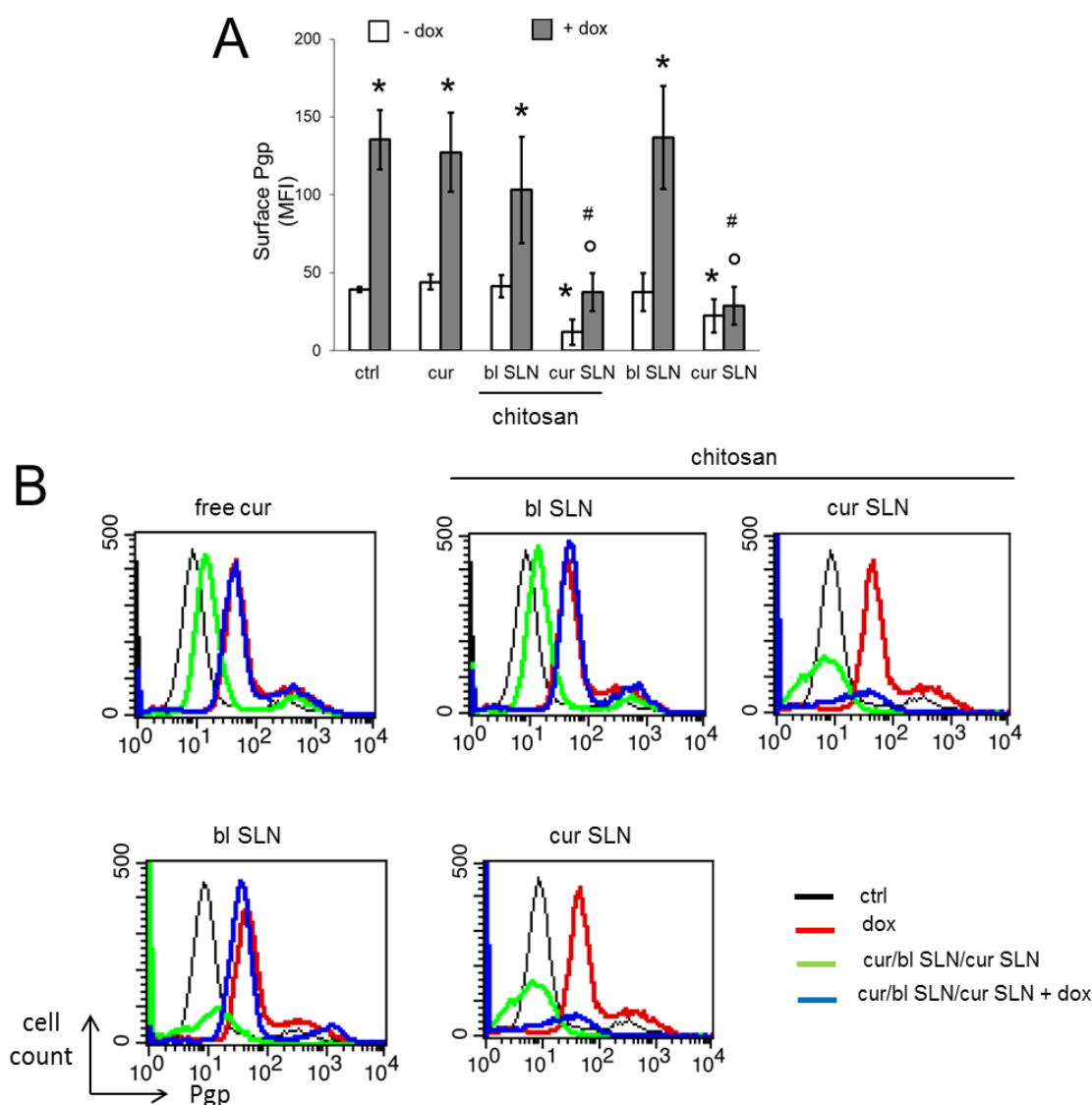


**Figure 26. Surface P-gp in curcumin-loaded SLN and chitosan-containing /curcumin-loaded SLN treated cells.** MDA-MB-231 cells were incubated 24 h with fresh medium (ctrl) or with 5  $\mu$ M curcumin (cur), blank SLN (bl SLN), curcumin-loaded SLN (cur SLN, containing 5  $\mu$ M cur), without and with chitosan. When indicated, 5  $\mu$ M doxorubicin (Dox) was added. (A) Mean fluorescence intensity (MFI). (B) P-gp on cell surface was measured by flow cytometry. Measurements were performed in triplicate and data are presented as means  $\pm$  SD (n = 3). \* p < 0.01: vs ctrl; <sup>o</sup> p < 0.001: vs Dox; # p < 0.001 vs cur.

The changes in the surface P-gp proteins were paralleled by changes in the mRNA of P-gp/ABCB1/MDR1; while in cells not exposed to doxorubicin, we did not detect any significant changes in P-gp mRNA, and doxorubicin treatment hugely increased it. Curcumin-loaded SLN and chitosan-containing/curcumin-loaded SLN, but not free curcumin or blank SLN, reduced such increase (Figure 27A). By contrast, neither doxorubicin nor the other treatments changed the mRNA level of MRP1/ABCC1 (Figure 27B) and BCRP/ABCG2 (Figure 27C), two transporters involved in doxorubicin efflux, suggesting that effect of SLN carrying curcumin is specific for P-gp transcription.

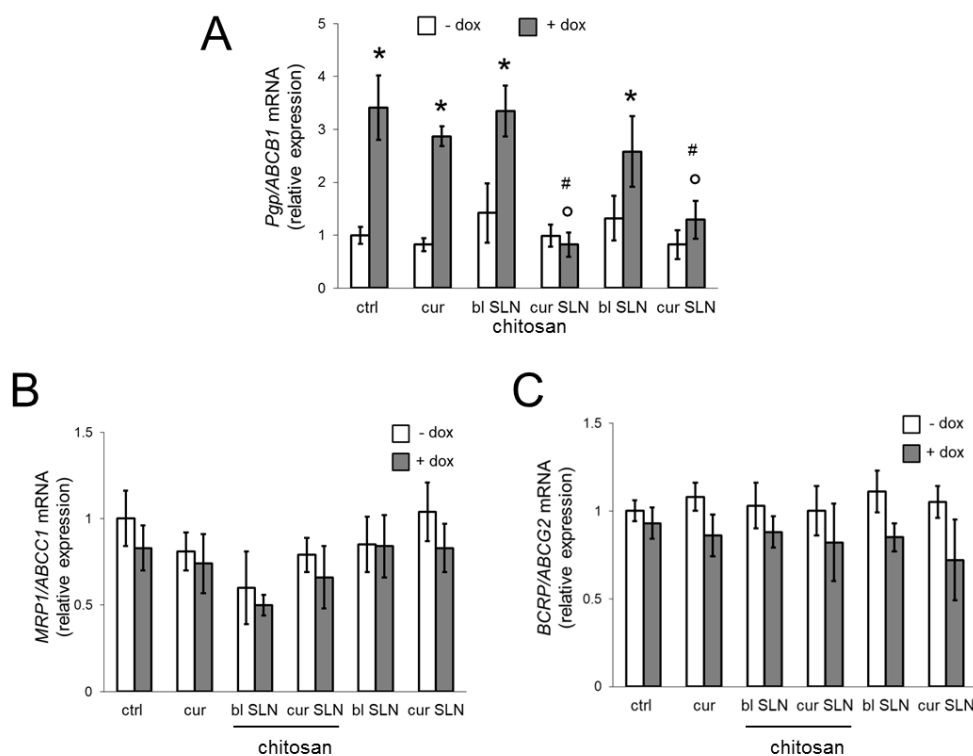


**Figure 27. P-gp, MRP1 and BCRP mRNA in curcumin-loaded SLN and chitosan-containing/curcumin-loaded SLN treated cells.** MDA-MB-231-P-gp cells were incubated 24 h with fresh medium (ctrl) or blank SLN (bl SLN), curcumin-loaded SLN (cur SLN, containing 5  $\mu$ M cur), without and with chitosan. When indicated, 5  $\mu$ M doxorubicin (Dox) was added. The expression of the P-gp (panel A), MRP1 (panel B) and BCRP (panel C) mRNAs was measured by qRT-PCR in triplicates. Data are presented as means  $\pm$  SD (n = 3). \* p < 0.01: vs ctrl; ° p < 0.001: vs Dox; # p < 0.001 vs cur.

We next investigated the potential mechanisms of curcumin-loaded SLN in reducing P-gp transcription after doxorubicin exposure. Doxorubicin is known to increase ROS in treated cells (Kim *et al.*, 2006; Pilco-Ferreto and Calaf, 2016) and curcumin has been reported to prevent such increase, limiting the side-effects related to oxidative stress in non-transformed cells (Mohajeri and Sahebkar, 2018). We thus investigated how ROS levels change in MDA-MB-231-P-gp cells exposed to doxorubicin and curcumin. As expected, doxorubicin increased intracellular ROS. Free curcumin did not prevent ROS increase, whereas curcumin-loaded SLN, either with or without chitosan, significantly reduced ROS (Figure 28).

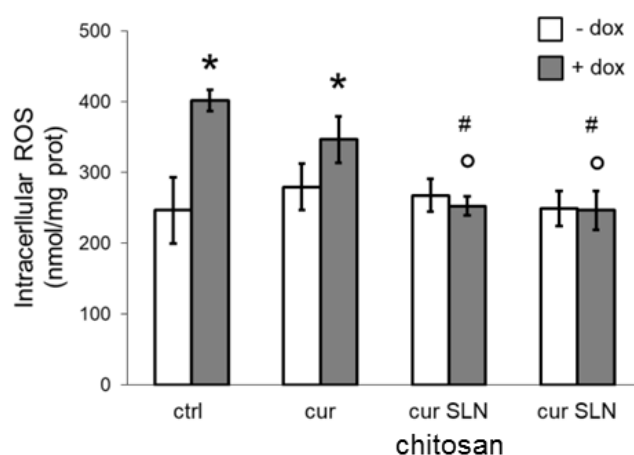


**Figure 28. Effect of curcumin-loaded SLN and chitosan-containing/curcumin-loaded SLN in ROS levels.** MDA-MB-231-P-gp cells were incubated with fresh medium (ctrl) or with 5  $\mu$ M curcumin (cur), curcumin-loaded SLN (cur SLN, containing 5  $\mu$ M cur), without and with chitosan. When indicated, 5  $\mu$ M doxorubicin (Dox) was added. ROS levels were measured fluorimetrically in triplicates. Data are presented as means  $\pm$  SD (n = 3). \* p < 0.05: vs ctrl; ° p < 0.001: vs Dox; # p < 0.01 vs cur.

Intracellular ROS can mediate the activation of several transcription factors. Among these redox-sensitive factors, HIF-1 $\alpha$  (Comerford *et al.*, 2002; Kopecka *et al.*, 2015) and NF- $\kappa$ B (Bentires-Alj *et al.*, 2003; Karabay *et al.*, 2018) are well known transcriptional inducers of P-gp/ABCB1/MDR1. We thus investigated whether the effects of curcumin were due to the changes in transcriptional activity in these factors.

HIF-1 $\alpha$  activity was increased by doxorubicin, as already reported (Kopecka *et al.*, 2015), but nor free curcumin neither curcumin-loaded SLN formulations affect its activity in doxorubicin-treated and untreated cells (Figure 29).

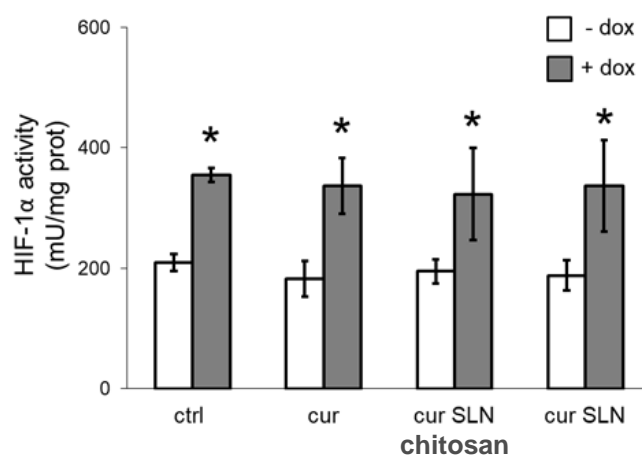


**Figure 29. Effect of curcumin-loaded SLN and chitosan-containing/curcumin-loaded SLN on HIF-1 $\alpha$  activation.** MDA-MB-231 cells were incubated with fresh medium (ctrl) or with 5  $\mu$ M curcumin (cur), curcumin-loaded SLN (cur SLN, containing 5  $\mu$ M cur), without and with chitosan. When indicated, 5  $\mu$ M doxorubicin (Dox) was added. HIF-1 $\alpha$  activation was measured by ELISA in triplicates. Data are presented as means  $\pm$  SD (n = 3). \* p < 0.001: vs ctrl.

In keeping with the higher ROS levels, doxorubicin-treated cells displayed a higher activation of NF-kB that was not reduced by free curcumin and blank SLN. NF-kB activity was instead blunted in doxorubicin-treated cells by curcumin-loaded SLN either without or with chitosan (Figure 30) that reduced ROS levels (Figure 28).

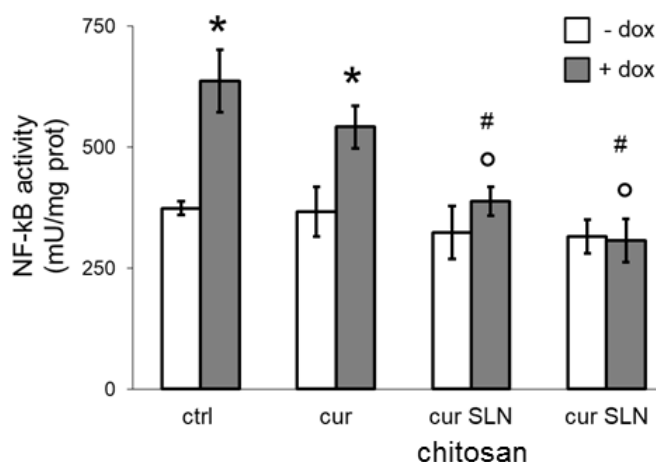


**Figure 30. Effect of curcumin-loaded SLN and chitosan-containing/ curcumin-loaded SLN in NF-kB levels.** MDA-MB-231 cells were incubated with fresh medium (ctrl) or with 5  $\mu$ M curcumin (cur), curcumin-loaded SLN (cur SLN, containing 5  $\mu$ M cur), without and with chitosan. When indicated, 5  $\mu$ M doxorubicin (Dox) was added. NF-kB activation was measured by ELISA in duplicates. Data are presented as means  $\pm$  SD (n = 3) \* p < 0.05: vs ctrl; ° p < 0.001: vs Dox; # p < 0.01 vs cur.

NF-kB is a multimeric transcription factor that can form heterodimers between each components, including p65, p50, p52, Rel-A, c-Rel, characterized by different transcriptional effects (Orlowski and Baldwin, 2002; Christian *et al.*, 2016). p65 has been described to bind to MDR1 promoter and activate the transcription of P-gp/ABCB1/MDR1 (Karabay *et al.*, 2018).

NF-kB dimers, in particular p50/p65, are sequestered in cytoplasm in an inactive form by I $\kappa$ B- $\alpha$  inhibitor. However, the phosphorylation of I $\kappa$ B- $\alpha$  on serine 32 primes the latter for ubiquitination and proteasomal



degradation, freeing NF- $\kappa$ B dimers to translocate in the nucleus and become active transcription factors (Hinz *et al.*, 2012). The master regulator of I $\kappa$ B- $\alpha$  phosphorylation is the IKK- $\alpha/\beta$  complex that becomes activated after the phosphorylation on serine 176 and 180 (Israel, 2010). Among the multiple kinases activating IKK  $\alpha/\beta$ , there is Akt that is active when phosphorylated on serine 473 (Zhao *et al.*, 2017). ROS are known activators of Akt and downstream IKK- $\alpha/\beta$ /NF- $\kappa$ B cascade (Liu *et al.*, 2019) that is often constitutively activated in cancer cells (Mu and Liu, 2017; Zhao *et al.*, 2017; Liu *et al.*, 2019).

We thus investigated which NF- $\kappa$ B components were involved in P-gp/ABCB1/MDR1 transcription and eventually targeted by curcumin-loaded SLN. Doxorubicin increased p50 (Figure 31A), p65 (Figure 31B) and at lesser extent c-Rel (Figure 31C) binding to target DNA sequences in nuclear extracts. In accord with previous evidences (Christian *et al.*, 2016), p50, p65 and – at smaller extent – c-Rel binding activity was reduced by curcumin-loaded SLN, without or with chitosan (Figure 31A-C). Of note, curcumin-loaded SLN reduced the basal activity of p50 and p65 also in the absence of doxorubicin, suggesting particularly strong and specific effects for this dimer.

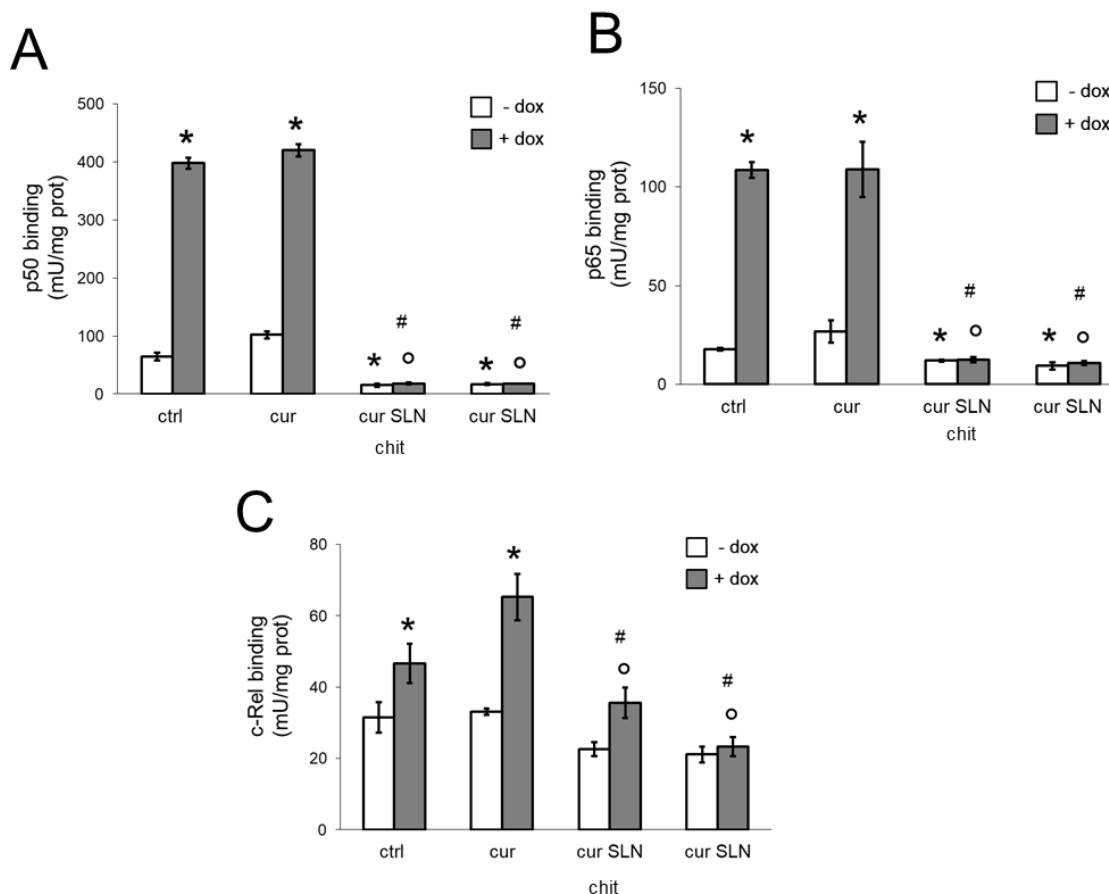


**Figure 31. Effect of curcumin-loaded SLN and chitosan-containing/ curcumin-loaded SLN on the activity of NF- $\kappa$ B subunits.** MDA-MB-231 cells were incubated with fresh medium (ctrl) or with 5  $\mu$ M curcumin (cur), curcumin-loaded SLN (cur SLN, containing 5  $\mu$ M cur), without and with chitosan. When indicated, 5  $\mu$ M doxorubicin (Dox) was added. The binding activity of p50 (A), p65 (B) or c-Rel (C) was measured by ELISA, in duplicates. Data are presented as means  $\pm$  SD (n = 3). \* p < 0.001: vs ctrl; ° p < 0.02: vs Dox; # p < 0.01 vs cur.

To confirm that the nuclear translocation and binding of p50/p65 to DNA target sequences, was responsible of the transcription of P-gp/ABCB1/MDR1 gene, we immunoprecipitated p50 and p65 bound to DNA and amplified the immunoprecipitated DNA with primers specific for MDR1 promoter. This ChIP assays indicated that doxorubicin increases the transcription of MDR1 gene mediated by p50 (Figure 32A) and p65 (Figure 32B). SLN-loaded curcumin, both with and without chitosan, but non free curcumin, decreased p50- and p65-induced transcription of the gene, both

in the absence or in the presence of doxorubicin (Figure 32A-B), confirming the results of the activation of p50 and p65 obtained in the ELISA (Figure 31A-B).

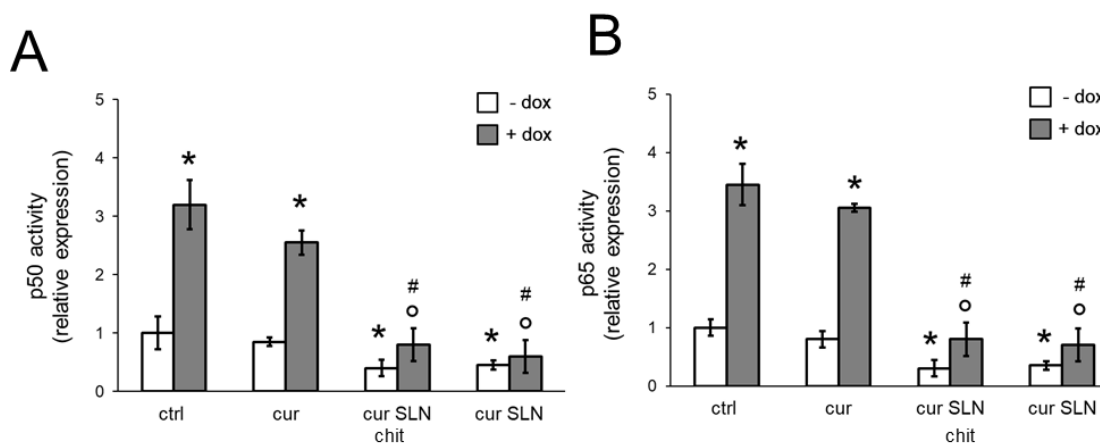


**Figure 32. Effect of curcumin-loaded SLN and chitosan-containing/ curcumin-loaded SLN on p50 and p65 transcriptional activation of MDR1 gene.** MDA-MB-231 cells were incubated with fresh medium (ctrl) or with 5  $\mu$ M curcumin (cur), curcumin-loaded SLN (cur SLN, containing 5  $\mu$ M cur), without and with chitosan. When indicated, 5  $\mu$ M doxorubicin (Dox) was added. The binding of p50 (A) or p65 (B) to MDR1 promoter was measured by ChIP. The immunoprecipitated DNA was measured amplified by qRT-PCR in triplicates. Data are presented as means  $\pm$  SD (n = 3). \* p < 0.01: vs ctrl; ° p < 0.001: vs Dox; # p < 0.01 vs cur.

The expression of upstream activators of p50/p65 dimer - Akt, phospho-Akt, IKK $\alpha/\beta$ , phospho-IKK $\alpha/\beta$ - and inhibitor I $\kappa$ B- $\alpha$  was measured by immunoblotting. While doxorubicin increased the active form of Akt (phospho (Ser473) Akt) and IKK $\alpha/\beta$  (phospho (Ser176/180) IKK $\alpha/\beta$ ), curcumin-loaded SLN, with or without chitosan, decreased these events, contrarily to free curcumin or blank SLN that were devoid of effects. Consistently, doxorubicin decreased the total amount of I $\kappa$ B- $\alpha$ ; this decrease was restored by curcumin-loaded SLN with or without chitosan, not by free curcumin or blank SLN. Neither curcumin nor SLN affected the expression of total Akt or IKK $\alpha/\beta$ . Moreover, no changes were detected in cells not treated with doxorubicin (Figure 33).

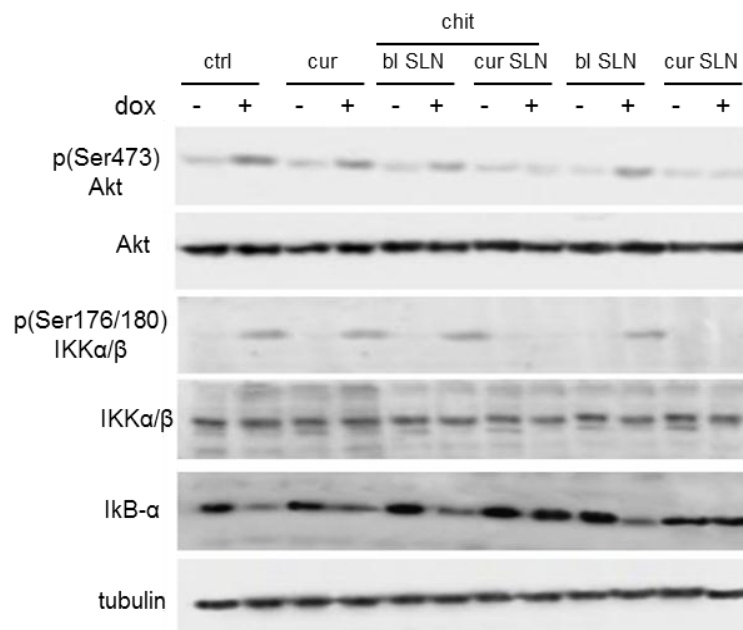


**Figure 33. Effect of curcumin-loaded SLN and chitosan-containing/curcumin-loaded SLN on the expression of Akt, phospho-Akt, IKK $\alpha/\beta$ , phospho-IKK $\alpha/\beta$  and I $\kappa$ B- $\alpha$ .** MDA-MB-231-P-gp cells were incubated 24 h with fresh medium (ctrl) or blank SLN (bl SLN), curcumin-loaded SLN (cur SLN, containing 5  $\mu$ M cur), without and with chitosan. When indicated, 5  $\mu$ M doxorubicin (Dox) was added. Cells were lysed and probed with the indicated antibodies. Tubulin was used as control of equal protein loading. The figure is representative of 1 out of 3 experiments with similar results.

#### 4.3.2 Curcumin-loaded SLN is effective against drug-resistant JC tumors *in vivo*

We next evaluated the efficacy of curcumin-loaded SLN, with or without chitosan, alone or in combination with doxorubicin, in mice bearing doxorubicin-resistant/P-gp-expressing JC. While free curcumin did not reduce tumor growth (Figure 34A, upper panel) and masses (Figure 34B), both curcumin-loaded SLN decreased the rates of growth (Figure 34A, upper panel). Doxorubicin, alone and in combination with free curcumin, was completely ineffective (Figure 34A, lower panel; Figure 34B), in line with the high resistance of these tumors to the drug. By contrast, the combinations of curcumin-loaded SLN, with or without chitosan, plus doxorubicin were the most effective in reducing tumor growth (Figure 34A, lower panel) and massed (Figure 34B). These

combinations were significantly more effective than doxorubicin or curcumin alone, or than curcumin-loaded SLN without doxorubicin (Figure 34A).

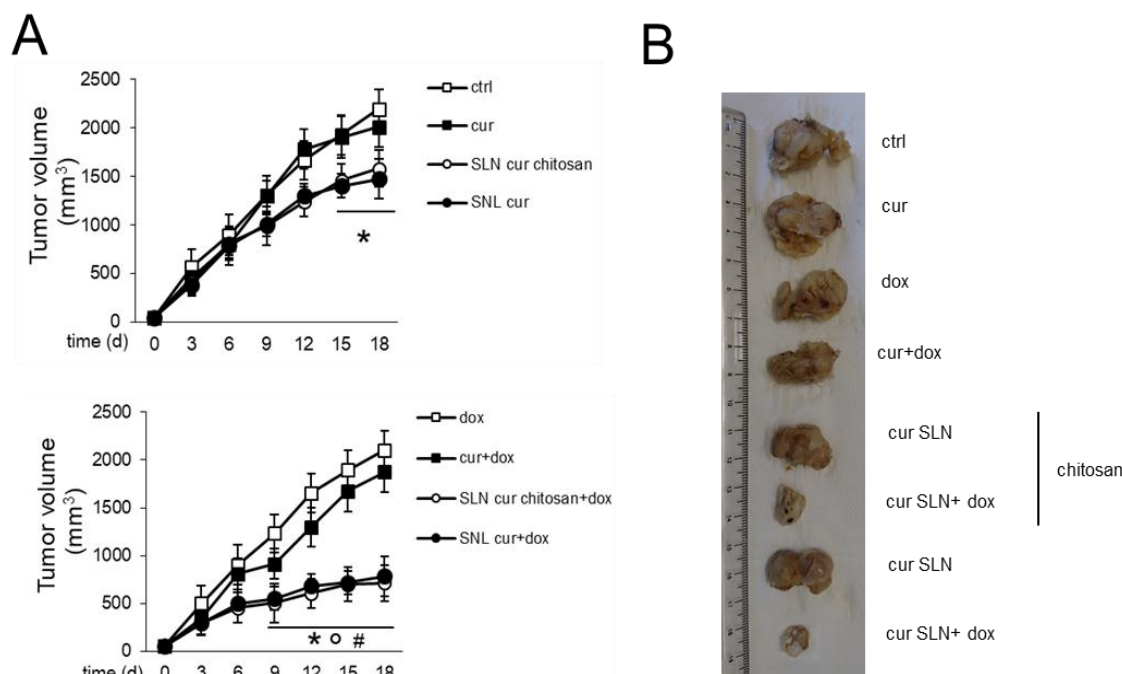


**Figure 34. Curcumin-loaded SLN effect against drug-resistant JC tumors *in vivo*.**

JC cells were orthotopically implanted into 6 week-old female balb/C mice. When tumor reached the volume of 50 mm<sup>3</sup>, mice (n= 8 mice/group) were randomized and treated as reported in the following groups, on day 1, 7, 14 after randomization: 1) vehicle group (ctrl), treated with 200 µl saline solution intravenously (i.v.); 2) curcumin group (cur), treated with 5 mg/kg curcumin, dissolved in 200 µl water/10% DMSO solution i.v.; 3) doxorubicin group (Dox), treated with 5 mg/kg doxorubicin, dissolved in 200 µl water i.v.; 4) curcumin + doxorubicin group (cur+Dox), treated with 100 µl of water/10% DMSO solution containing with 5 mg/kg curcumin + 100 µl water solution containing 5 mg/kg doxorubicin; 5) chitosan coated-SLN carrying curcumin group (cur SLN chitosan), treated i.v. with 200 µl of saline solution containing 5 mg/kg curcumin; 6) chitosan coated-SLN carrying curcumin + doxorubicin group (cur SLN + Dox chitosan), treated i.v. with 100 µl of saline solution. containing 5 mg/kg curcumin + 100 µl water solution containing 5 mg/kg doxorubicin; 7) uncoated-SLN carrying curcumin group (cur SLN), treated i.v. with 100 µL of saline solution containing 5 mg/kg curcumin; 8) uncoated-SLN carrying curcumin + doxorubicin group (cur SLN + Dox), treated i.v with 200 µl of saline solution containing 5 mg/kg curcumin + 100 µl water solution containing 5 mg/kg doxorubicin. (A) Tumor growth was monitored daily by caliper measurement. Data are presented as means±SD. \*p<0.01: vs. ctrl; \*p<0.001: vs. Dox; #p<0.001: vs. cur. (B) Photographs of representative tumors of each group.

Furthermore, we measured hematocemical parameters in the treated animals at the time of sacrifice, i.e. the liver toxicity parameters LDH, AST, ALT, AP, the kidney toxicity parameter creatinine, the heart toxicity parameters CPK, CPK-MB, cTnI and cTnT. Free curcumin and curcumin-

loaded SLN did not worsen these hematochemical parameters indicative of cardiotoxicity (Table 6).

**Table 6. Hematochemical parameters of the treated mice.**

- Doxorubicin	Ctrl	Curcumin	Chitosan-coated SLN curcumin	Uncoated SLN curcumin
LDH (U/L)	7091 ± 639	7189 ± 409	6781 ± 1021	7112 ± 678
AST (U/L)	89 ± 54	101 ± 43	121 ± 48	99 ± 29
ALT (U/L)	38 ± 8	41 ± 8	37 ± 10	34 ± 8
AP (U/L)	134 ± 49	139 ± 41	129 ± 29	139 ± 18
Creatinine (mg/L)	0.056 ± 0.005	0.062 ± 0.010	0.062 ± 0.009	0.054 ± 0.008
CPK (U/L)	314 ± 99	312 ± 83	382 ± 56	334 ± 39
CPK-MB (ng/mL)	0.109 ± 0.058	0.118 ± 0.032	0.129 ± 0.045	0.118 ± 0.041
cTnI (pg/mL)	1.011 ± 0.082	1.019 ± 0.032	1.008 ± 0.062	1.024 ± 0.029
cTnT (pg/mL)	2.182 ± 0.213	2.178 ± 0.101	2.189 ± 0.123	1.897 ± 0.162
+ Doxorubicin	Ctrl	Curcumin	Chitosan-coated SLN curcumin	Uncoated SLN curcumin
LDH (U/L)	7561 ± 761	7192 ± 506	7821 ± 821	6523 ± 801
AST (U/L)	103 ± 44	132 ± 45	105 ± 36	137 ± 89
ALT (U/L)	36 ± 15	41 ± 18	39 ± 13	56 ± 19
AP (U/L)	138 ± 25	167 ± 56	139 ± 44	168 ± 41
Creatinine (mg/L)	0.083 ± 0.009	0.082 ± 0.009	0.093 ± 0.011	0.093 ± 0.010
CPK (U/L)	556 ± 89 *	571 ± 89 *	562 ± 81 *	504 ± 81 *
CPK-MB (ng/mL)	0.302 ± 0.71 *	0.287 ± 0.045 *	0.297 ± 0.062 *	0.322 ± 0.016 *
cTnI (pg/mL)	1.021 ± 0.039	1.033 ± 0.046	1.031 ± 0.067	1.019 ± 0.052
cTnT (pg/mL)	3.197 ± 0.209 *	2.882 ± 0.172 *	2.904 ± 0.209 *	2.821 ± 0.178 *

Balb/C mice (n=8 mice/group) were treated as described the Figure 30. Blood was collected immediately after euthanasia and analyzed for lactate dehydrogenase (LDH), aspartate aminotransferase (AST), alanine aminotransferase (ALT), alkaline phosphatase (AP), creatinine, creatine phosphokinase (CPK) and CPK-MB, cardiac troponin I (cTnI) and T (cTnT). Data are presented as means±SD. \* p < 0.05: vs ctrl group.

In all the assays *in vitro* and *in vivo* we did not notice any significant difference between the SLN with or without chitosan.

## **5. DISCUSSION**

In the first part of this thesis the goal was to apply a physical-based approach to reverse doxorubicin resistance. To this aim, we used photoexcitable/NO-releasing doxorubicins (PNODOXOs), i.e. doxorubicins able to release NO when irradiated with a specific wavelength, power and irradiance. We chose the human melanoma M14 cells since they express multiple ABC transporters, thus representing a model of strongly chemoresistant cells.

The source of NO in cells treated with PNODOXOs can origin from the upregulation of iNOS induced by doxorubicin (Riganti *et al.*, 2005; De Boo *et al.*, 2009) or by the release of NO by the NO-donor conjugated with the anthracycline (Chegaev *et al.*, 2011; Riganti *et al.*, 2013; Gazzano *et al.*, 2016). The ability of doxorubicin to induce iNOS is proportional to the drug's intracellular accumulation: this event usually occurs in doxorubicin-sensitive cells, but not in doxorubicin-resistant cells where the drug is rapidly effluxed by ABC transporters (De Boo *et al.*, 2009). Since melanoma cells express at least three transporters involved in doxorubicin efflux (e.g. P-gp, MRP1, BCRP), it is unlikely that the drug reaches an intracellular concentration sufficient to induce iNOS. We hypothesize instead that the increase of nitrite is due to the release of NO from PNODOXOs, because: 1) it occurs only after irradiation; 2) the value of nitrite released by compounds 4, 12 and 13 in acellular systems are compatible with the amounts of nitrite measured in the supernatants of cells treated with those compounds.

Since P-gp, MRP1 and BCRP are the main transporters involved in doxorubicin efflux; their nitration may explain the increased intracellular retention of Dox observed in irradiated cells treated with compound 4.



The reversion of doxorubicin resistance using NO donors or NO-releasing doxorubicin that nitrate ABC transporters is not new. However, the first novel aspect of this work is the use of doxorubicin and NOPD (compound 4) at equimolar concentration, i.e. 5  $\mu$ M. Previous works demonstrated an effective nitration and inhibition of ABC transporters activity only when classical NO donors (such as SNAP, SNP, GSNO) were used at significantly higher concentrations, i.e. 100  $\mu$ M (Riganti *et al.*, 2005; De Boo *et al.*, 2009), difficult to reach *in vivo*. Moreover, each NO donor has a different kinetics of NO release: this makes necessary to increase high concentrations and/or prolong incubation time to reach the intracellular concentration of NO-derivatives sufficient for proteins nitration (Ischiropoulos, 2003). A second novelty of this work is the use of photoexcitable/NO releasing doxorubicins, where NOPD and doxorubicin are equimolar, i.e. 5  $\mu$ M. The use of PNODOXOs offers the advantage to finely tune the amount of NO released, allowing reaching nitrating concentrations in a strictly controlled manner and period, enabling to reduce the amount of NOPD used. Not all the ABC transporters present in M14 cells were nitrated. The amount and localization of target proteins, the amount and accessibility of tyrosines, the type of amino acids surrounding tyrosines critically influence nitration (Ischiropoulos, 2003). We cannot exclude that changing tumor type and/or incubation conditions we may obtain a different spectrum of nitrated ABC transporters.

As expected, doxorubicin did not induce any cell damage in M14 cells, in line with what was observed in other resistant cancer cells with low intracellular accumulation of doxorubicin and high drug efflux rate via ABC transporters (Riganti *et al.*, 2005, 2013; De Boo *et al.*, 2009; Chegaev *et al.*, 2011; Gazzano *et al.*, 2016). Of note, the NOPD compound 4 and the PNODOXs compounds 12 and 13 were not toxic either in non-irradiated

cells: the amount of NO released is indeed in the nanomolar range, i.e. below the cytotoxic micromolar range of NO (Wink and Mitchell, 1998). By contrast, the co-incubation of doxorubicin and compound 4 significantly induced cytotoxicity upon irradiation. A similar effect was exerted by the stronger PNODOXO 12, while no toxicity was elicited by the weaker PNODOXO 13. The significant increase in NO released by 12 together with the cytotoxic effect of doxorubicin itself is the likely reason for this cytotoxic effect.

In not-transformed cells, fibroblasts and cardiomyocytes, a well-known target of doxorubicin, the absence of toxicity of 4 and 13 was confirmed. As expected, doxorubicin was toxic in both cell populations. Interestingly the co-incubation with 4 did not increase further the doxorubicin's cytotoxicity. Compound 12, which was cytotoxic against melanoma cells, was less toxic than parental doxorubicin on not-transformed cells, suggesting a preferential toxicity of PNODOXOs towards cancer cells. These observations point out the possibility of a therapeutic window of using PNODOXOs maximizing the therapeutic benefits against the tumors, reducing the side toxicities on non-transformed tissues. The possibility to selectively irradiate accessible tumors, such as melanoma, further increases the specificity of the therapeutic effects of PNODOXOs on tumor cells.

As conclusion of this first part, we can state that the use of combined doxorubicin and NOPD or PNODOXOs offers the advantage to finely tune the amount of NO released, allowing reducing the amount of NO donors used to reverse chemoresistance. By modulating the ratio between NOPD and doxorubicin, a different amount of NO can be released, allowing to switch from a “not-toxic/ABC-transporters nitrating” to a “highly cytotoxic” concentration of NO, and to explore the pleiotropic anti-tumor

effects exerted by different NOPD/ doxorubicin ratios. On the other hand, PNODOXOs – that have a fixed ratio between NOPD and doxorubicin – are expected to have more favourable kinetics and less drug-drug unfavourable interactions than the co-administration of NOPD and doxorubicin. Overall, both approaches grant a high flexibility in the field of anti-tumor strategies based on NO donors. Melanoma is a highly chemoresistant tumor expressing multiple ABC transporters: it has been demonstrated that inhibiting only one transporter is not sufficient to effectively reverse chemoresistance (Chen *et al.*, 2009). Our strategy inhibits at the same time the activity of different ABC transporters. In this way, the NO photorelease increases the accumulation of doxorubicin by reducing the extrusion activity of the dedicated transporters (e.g. P-gp, MRP1, BCRP). Such broad-spectrum inhibition of ABC transporters may result in the increased retention and cytotoxicity of several other chemotherapeutic drugs, determining an efficient reversion of chemoresistance not limited to doxorubicin.

In the second part of the Thesis we used natural products to overcome doxorubicin resistance in human and murine TNBC cell lines.

Starting from the human TNBC MDA-MB-231 cells, which had a low expression of P-gp, we generated a doxorubicin-resistant subline, namely MDA-MB-231/DX, using a classical stepwise selection protocol in medium with increasing concentration of doxorubicin. This selection up-regulate P-gp following the progressive activation of the transcription factor HIF-1 $\alpha$  even in normoxic conditions. The activation of HIF-1 $\alpha$  after acute (Doublier *et al.*, 2012) or prolonged (Kopecka *et al.*, 2015) exposure to doxorubicin is an event occurring in ER/PR-positive breast cancer

(Doublier *et al.*, 2012) or in colon cancer (Kopecka *et al.*, 2015), suggesting that is a process common to different cancer cell types during the acquisition of resistance. The generated subline MDA-MB-231/DX cells has an intermediate resistance to doxorubicin between the sensitive MDA-MB-231 cells and the highly resistant JC cells.

In a first preliminary screening of 12 natural products selected for their different biological activity on proliferation and redox metabolism, we identified four compounds - Sip, Osh, MLB and Glab – that showed a preferential cytotoxicity against resistant cells. The peculiar cytotoxicity of a compound on highly P-gp-expressing cells is known as “collateral sensitivity” (Pluchino *et al.*, 2012) and is considered an innovative way to eradicate drug-resistant cells. Thiosemicarbazones, 1,10-phenanthrolines, as well as natural-product-derived sesquiterpenic benzoquinones and flavonoids have been recently identified as potent inducers of collateral sensitivity (Szakács *et al.*, 2014). Curiously, the four natural products with the lowest IC<sub>50</sub> against JC cells contain benzoquinone- or flavonoid-derivatives within their structure. We thus focused on these compounds and tested their ability to reverse doxorubicin resistance in our models, by combining each compound with doxorubicin at different concentrations. The results of cytotoxicity screening indicated that when combined with Dox - the four compounds exerted a selective toxicity against cells expressing moderate levels of P-gp, such as MDA-MB-231/DX cells. Glab was the unique compound that maintained its sensitizing efficacy against highly expressing P-gp cells. As suggested by the different CI index between MDA-MB-231/DX and JC cells, the higher P-gp level is, the higher synergism is observed. We thus hypothesized that Glab may directly interfere with the expression or activity of P-gp, reducing the efflux of Dox. This interference may explain the synergic effect induced by the

combination of Dox and Glab in P-gp-expressing cells only. Indeed, Glab reduced the  $V_{max}$  of doxorubicin efflux, in line with the decreased efficiency of catalytic activity of P-gp exerted by the compound. Moreover, Glab increased the  $K_m$  of doxorubicin, suggesting a reduced affinity of the drug towards P-gp.

These data support the hypothesis that Glab may interfere with the doxorubicin binding or release from P-gp, or with the NBDs that bind and hydrolyse ATP. Since P-gp has multiple drug binding pockets and the binding and releasing sites for doxorubicin have been not yet identified, we produced different mutated constructs of P-gp, bearing the clinically relevant mutations already reported in human tumors and affecting protein stability, conformation or drug efflux (ABCMDb/Database for Mutations in ABC proteins; <http://abcmutations.hegelab.org/>), in order to get more information on the putative site of interaction between Glab and P-gp. Ser400Asn, Gly412Ala, Ser893Ala, Ser893Thr, Gly185Val-mutated P-gp were expressed in parental MDA-MB-231 cells and showed the same expression level and ATPase activity than wild-type P-gp. Ser400 and Gly412 mutations have no reported clinical significance; these amino acids are located in exons 12 and 13 that are components of the nucleotide binding domain (NBD) at the N-terminal side (Raymond and Gross, 1989) of P-gp (Raymond and Gross, 1989). Ser893 is located between the 10<sup>th</sup> and 11<sup>th</sup> transmembrane domain <sup>TM</sup> of P-gp; its mutation alters the efflux of lipophilic drugs, such as simvastatin (Becker *et al.*, 2009), ondansetron (Choi *et al.*, 2010) and paclitaxel (Gréen *et al.*, 2006). Gly185 is located in a large hydrophobic domain of P-gp and is involved in drug binding and subsequent release outside the cell (Chen *et al.*, 1986). Moreover, Gly185 dictates the conformation changes occurring between the hydrolysis of ATP and the release of the efflux of the drugs; its mutation into Val

determines a more efficient coupling between these two processes (Omote *et al.*, 2004). Interestingly, Gly185Val has been involved in the resistance to lipophilic drugs such as colchicine, epipodophyllotoxins (Safa *et al.*, 1990). Moreover, this mutation impairs the effects of P-gp allosteric inhibitors, such as distearoyl-phosphatidylethanolamine-polyethylene glycol (DSPE-PEG), which increases the  $K_m$  of doxorubicin and reduces ATPase activity in wild-type P-gp, not in Gly185Val-mutated P-gp (Kopecka *et al.*, 2014). Of note, Glab shows the same properties of DSPE-PEG, since it increased doxorubicin  $K_m$  and decreased P-gp ATPase activity, but lose its efficacy in cells mutated at Gly185. We may hypothesize that Glab binds and/or interacts indirectly with Gly185, and that this interaction disrupts the efficient coupling between ATP hydrolysis and doxorubicin efflux. In consequence of the decreased catalytic activity of P-gp, the release of doxorubicin towards the external side is less efficient, as suggested by the increased  $K_m$  of the drug. In consequence of the decreased catalytic cycle of P-gp, doxorubicin is also effluxed with a reduced  $V_{max}$ .

We finally validated the efficacy and safety of Glab *in vivo*, treating balb/C mice bearing JC tumors that were completely unresponsive to doxorubicin. In line with the results obtained *in vitro*, Glab restored the efficacy of doxorubicin, without displaying additional side-toxicities according to the hematochemical parameters measured. Given the huge reduction in tumor growth elicited by the combination of Glab and doxorubicin, the addition of Glab could be an option in reducing the dose of doxorubicin, preserving a good efficacy against P-gp/expressing tumors and limiting the dose/dependent cardiotoxicity.

Overall this second part of the thesis demonstrates that natural products may offer a safe and effective alternative to small molecules

---

designed for inhibiting P-gp (Callaghan *et al.*, 2014) or selectively killing P-gp-expressing cells (Pluchino *et al.*, 2012), that are often effective *in vitro* but not in preclinical models, for the low efficacy and/or the undesired toxicities. We identified Glab as a chemosensitizing agent, whose efficacy is higher in strongly P-gp-expressing JC cells than in moderately P-gp-expressing MDA-MB-231/DX cells, suggesting that it can be tested as an effective chemosensitizer in breast cancers strongly resistant to doxorubicin.

In the third part of the thesis, I coupled the use of a natural product, curcumin, with a nanotechnological approach, based on its encapsulation within SLN. Curcumin has recently shown several anti-tumor properties, including the inhibition of oncogenic factors such as STAT-3 and NF- $\kappa$ B, the inhibition of the pro-invasive factor Sp-1 and the inhibition of chronic pro-tumor inflammation. Interestingly, these effects are accompanied by a low toxicity against non-transformed cells (Vallianou *et al.*, 2015), suggesting that it could be a selective agent against tumor cells. It has been already reported that curcumin down-regulate P-gp expression (Choi *et al.*, 2008), by downregulating NF- $\kappa$ B activation, a strong inducer of P-gp. Indeed, free curcumin has synergized with paclitaxel, a typical P-gp substrate, in different cancer cell lines (Hossain *et al.*, 2012).

The main disadvantages of curcumin are the poor water-solubility, the unfavorable pharmacokinetic, the easy degradation at slightly alkaline pH, that limit curcumin efficacy in clinical practice. To increase the bioavailability of curcumin, it has been proposed the use of nanocarriers that may decrease curcumin degradation and increase its uptake within tumor cells (Sun *et al.*, 2013). In my thesis, I tested the efficacy of curcumin encapsulated in SLN designed to achieve a high biocompatibility in the perspective of a systemic administration of the formulation *in vivo*.

---

Indeed the cold dilution of microemulsion method (Chirio *et al.*, 2018) followed in the SLN preparation granted :

- a good hydrophilicity avoiding the use of organic solvents that can have an unacceptable toxicity or interfere with the drug encapsulation;
- stable  $\zeta$  potential, low PI index;
- high and reproducible encapsulation efficacy.

In parallel, other SLNs have been produced by introducing in the microemulsion system chitosan, a polymer that coats SLN surface and further increases the hydrophilic properties of the SLN. Moreover, chitosan is highly biodegradable, granting a good biocompatibility, and has strong adhesive properties to epithelial cells, that are supposed to favor the uptake of the coated SLN within the cell.

In a preliminary comparison of free curcumin, curcumin-loaded SLN and chitosan-containing/curcumin-loaded SLN, we observed that the latter formulations produced the same retention of doxorubicin and doxorubicin-induced toxicity at a concentration (i.e. 5  $\mu$ M) five to ten-fold lower than free curcumin. These results suggested that SLN likely elicited a higher delivery of curcumin within the cells, allowing to curcumin to exert its chemosensitizing effects on TNBC human MDA-MB-231 expressing wild-type P-gp and murine JC cells at a concentration at which curcumin was ineffective. Therefore the encapsulation of curcumin within SLN improved the cellular uptake of the drug. Moreover, at this concentration, neither blank SLN nor curcumin-loaded SLN and chitosan-containing/curcumin-loaded SLN were cytotoxic for the cells. To achieve the same chemosensitizing efficacy, free curcumin had to be used at 25-50  $\mu$ M, a



range of concentrations that elicits cytotoxicity *in vitro* and was difficult to reach *in vivo*. These data indicate the superior efficacy and safety curcumin-loaded SLN over free curcumin.

Mechanistically, curcumin delivered by SLN did not act as a competitive inhibitor of P-gp, since it did not increase the retention of rhodamine 123, a classical P-gp substrate, if co-incubated at short term. By contrast, a 24 h incubation of curcumin-loaded SLN and chitosan-containing/curcumin-loaded SLN increased the accumulation of both doxorubicin and rhodamine 123. This event was paralleled to the decrease in P-gp mRNA and protein and was evident in cells treated with doxorubicin that increases P-gp expression, as expected (Maitra *et al.*, 2001). This result looks promising because it suggests that curcumin-loaded SLN reduced P-gp expression only in cancer cells after exposure to chemotherapy, without affecting the basal expression of the transporter. This means that likely the physiological effects of P-gp in non-transformed tissues are less affected than the activity of P-gp within the tumor, leading to expect a lower rate of undesired side-toxicities. Moreover, no changes in MRP1 and BCRP mRNA levels were detected, suggesting that curcumin-loaded SLN effects were specific for P-gp. Such specificity for P-gp may further contribute to limit the undesired toxicity due to the non-selective inhibition of other ABC transporters.

Unexpectedly, Intracellular doxorubicin accumulation and cytotoxicity, levels of P-gp, MRP1 and BCRP mRNAs, amount of P-gp surface and activity showed the same trends for chitosan-containing/curcumin-loaded SLN than for the curcumin-loaded SLN without chitosan. Chitosan-containing SLN are known for their higher hydrophilic properties. It is likely that the good solubility in cell culture medium achieved by uncoated curcumin-loaded SLN is sufficient to reach

the maximal curcumin delivery necessary to induce a chemosensitizing effect. On the other hand, our data suggest that chitosan coating likely did not change significantly the amount of released curcumin within the cells.

To further investigate the mechanism at the basis of the down-regulation of the doxorubicin-induced P-gp transcription, we focused on three events elicited by doxorubicin in cancer cells and involved in P-gp up-regulation: the increase in intracellular ROS, the activation of the transcription factors HIF-1 $\alpha$  and NF-kB, which are both inducers of P-gp and activated in response to increased ROS. Our data indicated that doxorubicin increased ROS levels, HIF-1 $\alpha$  and NF-kB activity, as expected; curcumin-loaded SLN and chitosan-containing/curcumin-loaded SLN reduced ROS and NF-kB activation, without any effects on HIF-1 $\alpha$ . We identify p50, p65 and – at lesser extent – c-Rel as the NF-kB components inhibited by curcumin. Our results are in accord to previous findings, demonstrating that p65, which commonly dimerizes with p50 (Christian *et al.*, 2016), is the leading NF-kB binds MDR1 promoter and activates the transcription of P-gp (Karabay *et al.*, 2018). By reducing both p65 and p56 binding to MDR1 promoter, curcumin delivered by SLN strongly reduced the levels of P-gp mRNA. Our studies on the signalling upstream NF-kB suggest that the effects of curcumin are due to a decreased activation of Akt and IKK- $\alpha$ /  $\beta$  complex upon doxorubicin treatment, leading to a reduced expression of I $\kappa$ B- $\alpha$  that finally allowed the nuclear translocation and transcriptional activity of p65/p50 dimer. Since ROS activate the Akt/IKK- $\alpha$ / $\beta$ /NF-kB axis (Zhao *et al.*, 2017; Liu *et al.*, 2019), we hypothesize that the prime mover of P-gp reduction was the decrease in intracellular ROS induced by curcumin and the consequence down-regulation of Akt/IKK- $\alpha$ / $\beta$ /NF-kB/P-gp pathway. This may explain why the effects of curcumin-loaded SLN and chitosan-containing/curcumin-loaded

---

SLN were more pronounced in cells treated with doxorubicin, where there are high levels of intracellular doxorubicin, and less pronounced in untreated cells, where ROS levels were significantly lower.

The effects of curcumin-loaded SLN and chitosan-containing/curcumin-loaded SLN were not cell line or species-specific, since they were shared by both human and murine doxorubicin-resistant cells. Moreover, our *in vivo* experiment proved that both curcumin-loaded SLN and chitosan-containing/curcumin-loaded SLN were effective against doxorubicin-resistant JC tumors. Consistently with the anti-tumor properties of curcumin (Vallianou *et al.*, 2015), both SLN reduced the growth of tumors in the absence of doxorubicin at a dosage at which free curcumin was ineffective. These profiles indirectly suggest the better bioavailability and delivery to tumor of curcumin when carried by SLN than when administered as free drug. Most importantly, the effects of curcumin-loaded SLN and chitosan-containing/curcumin-loaded SLN were most pronounced in doxorubicin-treated animals, where the anti-tumor effects of doxorubicin were rescued by the combination treatments. This is consistent with the mechanism of increased intracellular accumulation of doxorubicin, due to the down-regulation of P-gp, observed *in vitro*. Furthermore, both SLN formulations did not display signs of systemic toxicities and did not worsen the cardiac damage, indicated by the increase in CPK, CPK-MB and cTnT, induced by doxorubicin.

As already observed for *in vitro* assays, there were no differences between curcumin-loaded SLN and chitosan-containing/curcumin-loaded SLN, although chitosan should grant a higher stability and biocompatibility of the nanocarriers. It is likely that uncoated SLN had a good pharmacokinetic profile and a good hydrophilicity sufficient to elicit anti-tumor property, and a good biocompatibility that avoids side-toxicities.

As a conclusion of this third part, we produced two nanocarriers loaded with curcumin, able to down-regulate P-gp expression and rescue doxorubicin efficacy against resistant TNBC tumors at lower and non-toxic doses than free curcumin. After systemic co-administration with doxorubicin, our formulations were effective in reducing the growth of highly resistant tumors, revealing a good safety profile.

## **6. CONCLUSION AND FUTURE PERSPECTIVES**

The main goal of this thesis is testing different approaches to increase the efficacy of doxorubicin in ABC transporters expressing tumors. 40 to 70% of tumors are resistant to chemotherapy and targeted-therapy at the diagnosis as a consequence of the constitutive expression of ABC transporters. This percentage increases after the treatment with chemotherapy that increases the expression of ABC transporters. Until now, inhibiting these transporters, in particular P-gp that recognizes the broadest spectrum of substrates is a still unmet clinical need. Since small chemical inhibitors effective *in vitro* have repeatedly failed in preclinical models for the high toxicity and the low specificity, we tested alternative approaches.

The first one was a physico-chemical approach based on the use of hybrid doxorubicins containing the anthracycline moiety and a photoexcitable NO-releasing group, i.e. a group able to release NO, a non-competitive inhibitor of ABC transporters including P-gp, only upon irradiation at specific wavelength. The innovation of this approach is the highly temporal and spatial controlled inhibition of ABC transporters that increases the effects on tumor tissue only, sparing non-transformed tissues. This is a strong innovation compared to systemically administered inhibitors of ABC transporters. The main disadvantage is that the irradiation-based approach can be used for superficial tumors (e.g. skin cancers) or endoscopically accessible tumors (e.g. gastrointestinal tumors, bronchial tumors, prostate tumors), due to the low penetration - i.e. few millimetres - of the light used. Changing the wavelength used, moving from violet toward a green or red light increases the light penetration, allowing the targeting of internal tumors. This implies the design of different photoexcitable NO donors, their stable conjugation with

doxorubicin or other chemotherapeutic drugs, the validation *in vitro* and *in vivo* of the new hybrids. These steps represent the future development of our first work.

Another alternative to the small chemical inhibitors tested in the past to inhibit P-gp is the use of natural products, characterized by low toxicity on non-transformed tissue and by a preferential toxicity on P-gp-expressing cancer cells. Glab is an example of this category of compounds, exerting the maximal efficacy on moderately P-gp-expressing and highly-P-gp-expressing cells thanks to the ability to impair the catalytic cycle of P-gp. Thanks to the experiments with mutants P-gp we hypothesized that Glab inhibits P-gp by interacting with the domain centred around Glycine185, a domain that is involved in the release of hydrophobic drugs including doxorubicin from the pump. Despite these indications, we did not completely clarify the exact binding site of Glab. Modelling studies are currently on going to clarify this point.

Until now, few chemical small molecules displayed a selective toxicity against P-gp-expressing tumors, i.e. induce a collateral sensitivity. To the best of our knowledge, Glab is the first natural product inducer of collateral sensitivity and of chemosensitizing effects. In depth studies of molecular modelling may led to identify the key groups of Glab responsible for the inhibition of P-gp. This may pave the way to the design of small libraries of Glab analogues, both inducers of collateral sensitivity and inhibitors of P-gp, with higher specificity and selectivity.

Not always natural products as free compounds are able to reach a satisfactory bioavailability, as in the case of curcumin that reversed doxorubicin resistance *in vitro* only when used at toxic concentrations and was devoid of effects *in vivo*, likely as a consequence of its low solubility

and stability in hydrophilic biological fluids. Nanobiomaterials can overcome these limitations by offering a wide range of biocompatible carriers, able to improve the pharmacokinetics and pharmacodynamics profile of the natural products. In our hand, curcumin-loaded SLN proved to be five to ten-fold more potent than free curcumin, able to overcome doxorubicin resistance by downregulating P-gp and targeting a pro-survival pathway - Akt/IKK- $\alpha/\beta$ /NF- $\kappa$ B – typically activated in cancer cells. After having demonstrated the anti-tumor efficacy *in vivo*, we are currently performed immunohistochemistry-based analysis of the collected tumors to verify that the molecular events observed *in vitro* also occur within the tumor mass. Moreover, although curcumin-loaded SLN associated with doxorubicin was not more toxic than doxorubicin alone according to the hematochemical parameters analysed, an in depth analysis of the target organs - liver, kidney, heart, lung, bone marrow, central nervous system - is required to check the lack of toxicity undetectable with the hematochemical parameters. Another study that we plan to perform is a detailed distribution and pharmacokinetic profile of the curcumin-loaded SLN. This will allow an optimization in the scheduled treatment and in the route of administration, in order to further increase the anti-tumor benefits and the safety.

A limitation of our work is that Glab and curcumin-loaded SLN have been tested on commercial cell lines, not in primary samples. The promising results obtained, however, may pave the way to test these approaches in patient-derived TNBC cells and tumor xenografts, in order to identify subset of patients – unresponsive to doxorubicin for the presence of high levels of P-gp and characterized by poor prognosis – who may benefit from the use of Glab or curcumin as potential adjuvant agents in doxorubicin-based treatments.



Overall, our results with natural compounds are clinically relevant because chemotherapy based on anthracyclines such as doxorubicin is the first therapeutic option in TNBC (Harbeck and Gnant, 2017). Unluckily, this type of breast cancer results less responsive to doxorubicin than other breast cancer types (Székely *et al.*, 2017). One of the main reasons for this low success is the abundant presence of P-gp in breast cancer cells (Iris C. Salaroglio *et al.*, 2018). Increasing doxorubicin efficacy in TNBC is still an unmet need. We suggest that the use of natural compounds may help to achieve this goal.

In conclusion, my thesis work collected a series of proof of concepts on alternative, effective and safe approaches, based on multidisciplinary approaches combining physics, medicinal chemistry, nanotechnology and pharmacology. Such multidisciplinary may represent a significant advancement in overcoming MDR related to ABC transporters.

## **7. LIST OF FIGURES**

Figure	Title	Page
1	Schematic representation of the function of ABC transporters.	12
2	Inhibitory mechanisms of P-glycoprotein.	16
3	Molecular structure of doxorubicin (Dox) and Nitric Oxide Photodonor (NOPD).	21
4	Schematic transition from curcumin to curcumin nanoformulations.	25
5	<sup>1</sup> H-NMR analysis of compound 1 (glabratephrin)	35
6	NO release by compounds 1, 11, 12 and 13 upon irradiation in PBS.	50
7	ABC transporters expression in melanoma cells.	51
8	Nitrites amount in melanoma cells treated with NOPD and PNODOXOs	52
9	Nitration and ATPase activity of ABC transporters by NOPD and PNODOXOs.	53
10	Cytotoxicity of NOPD and PNODOXOs.	54
11	Cytotoxicity on human fibroblasts and rat H9c2 cardiomyocytes.	55
12	MDA-MB-231/DX subline generation.	57
13	Doxorubicin accumulation and cytotoxicity in breast cancer cells with different degrees of resistance.	59
14	Effects of selected natural compounds on doxorubicin cytotoxicity in breast cancer cells with different degrees of resistance.	61
15	Isobologram analyses of doxorubicin and Glabratephrin combination.	62
16	Glabratephrin reduces doxorubicin efflux by inhibiting P-gp activity.	64
17	Superposition of the co-crystallized ligand QZ59-RRR (orange color) and re-docked ligand QZ59-RRR (green color).	65

18	Superposition of the co-crystallized ligand QZ59-RRR (orange color) and glabratephrin (green color).	66
19	Modelling of the functional groups involved in the interaction between Glab and P-gp.	67
20	Glabratephrin loses its efficacy in Gly185Val mutated P-gp.	68
21	Glabratephrin effect against drug-resistant JC tumors <i>in vivo</i> .	69
22	Dose-dependence free curcumin on doxorubicin accumulation and cytotoxicity in MDA-MB-231-P-gp cells.	71
23	Effect of curcumin-loaded SLN and chitosan-containing/curcumin-loaded SLN on doxorubicin accumulation and cytotoxicity in MDA-MB-231-P-gp cells.	72
24	Effect of curcumin-loaded SLN and chitosan-containing/curcumin-loaded SLN on doxorubicin accumulation and cytotoxicity in JC cells.	73
25	Effect of curcumin-loaded SLN and chitosan-containing/curcumin-loaded SLN treated cells on P-gp activity.	74
26	Surface P-gp in curcumin-loaded SLN and chitosan-containing /curcumin-loaded SLN treated cells.	75
27	P-gp, MRP1 and BCRP mRNA in curcumin-loaded SLN and chitosan-containing/curcumin-loaded SLN treated cells.	76
28	Effect of curcumin-loaded SLN and chitosan-containing/curcumin-loaded SLN in ROS levels.	77
29	Effect of curcumin-loaded SLN and chitosan-containing/curcumin-loaded SLN on HIF-1 $\alpha$ activation.	78
30	Effect of curcumin-loaded SLN and chitosan-containing/curcumin-loaded SLN in NF-kB levels.	79
31	Effect of curcumin-loaded SLN and chitosan-containing/curcumin-loaded SLN on the activity of NF-kB subunits.	81
32	Effect of curcumin-loaded SLN and chitosan-containing/curcumin-loaded SLN on p50 and p65 transcriptional activation of MDR1 gene.	82

33	Effect of curcumin-loaded SLN and chitosan-containing/curcumin-loaded SLN on the expression of Akt, phospho-Akt, IKK $\alpha/\beta$ , phospho-IKK $\alpha/\beta$ and I $\kappa$ B- $\alpha$ .	83
34	SLN-curcumin effect against drug-resistant JC tumors <i>in vivo</i> .	84

## **8. LIST OF TABLES**

Table	Title	Page
1	Tested natural pure compounds.	33
2	The stability of the target products 11-13 was evaluated by HPLC.	49
3	IC <sub>50</sub> (mM) of natural compounds in breast cancer cells.	60
4	Binding affinity evaluation using binding free energy.	66
5	Hematochemical parameters of the treated mice.	70
6	Hematochemical parameters of the treated mice.	85

## **9. LIST OF SCHEMES**



<b>Scheme</b>	<b>Title</b>	<b>Page</b>
1	a) KF, DMF, room temperature; b) THF, HCl in dry dioxane.	31

## **10. LIST OF ABBREVIATIONS**

---

MDR	Multidrug resistance
ABC	Adenosine triphosphate-binding cassette
P-gp/ABCB1/MDR1	Permeability glycoprotein
Wt P-gp	Wild-type P-gp
Mu P-gp	Mutant-type P-gp
MRPs	Multidrug associated proteins
MRP1/ABCC1	MDR-associated protein 1
MRP2/ABCC2	MDR-associated protein 2
BCRP/ABCG2/MXR	Breast cancer resistance protein
TMDs	Transmembrane domains
NBDs	Nucleotide-binding domains
ANOVA	Analysis of variance
ROS	Reactive oxygen species
RB1	Retinoblastoma
LRP	lung resistance protein
PDT	Photodynamic therapy
NO	Nitric oxide
NOS	Nitric oxide synthase
nNOS	Neuronal nitric oxide synthase
eNOS	Endothelial nitric oxide synthase
iNOS	Inducible nitric oxide synthase
NOPDs	NO-photodonors
SLNs	Solid lipid nanoparticles
i.v.	Intravenously
LDH	Lactate dehydrogenase
AST	Aspartate aminotransferase
ALT	Alanine aminotransferase
AP	Alkaline phosphatase
DMSO	Dimethylsulphoxide

CPK	Creatine phosphokinase
cTnI	Cardiac troponin I
cTnT	Cardiac troponin T
qRT-PCR	Quantitative real time-PCR
BSA	Bovine serum albumin
FBS	Fetal bovine serum
FITC	Flurescence isothiocyanate
SPSS	Statistical package for social science
Dox	Doxorubicin
Nev	Neviotine A
Sip	Sipholenol N
Arc	Arctigenin
D-Val	Delta-Valerolactone
G-Val	Gamma-Valerolactone
Ent	Enterolactone
Ver	Bergapten
Iso-B	Iso Bergapten
Osh	Osthol
Gug	Guggulsterone
MLB	Magnesium lithospermate B
Glab	Glabratephrin
MDA	MDA-MB-231 cell line
MDA/DX	MDA-MB-231 cell line/doxorubicin
IC <sub>50</sub>	Half-maximal inhibitory concentration
CI	Combination Index
ChIP	Chromatin Immunoprecipitation
HIF-1 $\alpha$	Hypoxia Inducible Factor 1 $\alpha$
RMSD	Root mean square deviation

## **11. REFERENCES**

- Afzal, F., Khurshid, R., Ashraf, M. and Gul Kazi, A. (2014) 'Reactive Oxygen Species and Antioxidants in Response to Pathogens and Wounding', in *Oxidative Damage to Plants: Antioxidant Networks and Signaling*. Elsevier, pp. 397–424. doi: 10.1016/B978-0-12-799963-0.00013-7.
- Agarwal, S., et al. (2011) 'Breast Cancer Resistance Protein and P-Glycoprotein in Brain Cancer: Two Gatekeepers Team Up', *Current Pharmaceutical Design*, 17(26), pp. 2793–2802.
- Agnihotri, S. A., Mallikarjuna, N. N. and Aminabhavi, T. M. (2004) 'Recent advances on chitosan-based micro- and nanoparticles in drug delivery', *Journal of Controlled Release*, pp. 5–28. doi: 10.1016/j.jconrel.2004.08.010.
- Akhtar, N., Ahad, A., Khar, R. K., et al. (2011) 'The emerging role of P-glycoprotein inhibitors in drug delivery: A patent review', *Expert Opinion on Therapeutic Patents*, 21(4), pp. 561–576. doi: 10.1517/13543776.2011.561784.
- Ammar, M. I., Nenaah, G. E. and Mohamed, A. H. H. (2013) 'Antifungal activity of prenylated flavonoids isolated from *Tephrosia apollinea* L. against four phytopathogenic fungi', *Crop Protection*. Elsevier Ltd, 49, pp. 21–25. doi: 10.1016/j.cropro.2013.02.012.
- Baek, J. S., Na, Y. G. and Cho, C. W. (2018) 'Sustained cytotoxicity of wogonin on breast cancer cells by encapsulation in solid lipid nanoparticles', *Nanomaterials*, 8(3). doi: 10.3390/nano8030159.
- Bansal, T., Jaggi, M., Khar, R. K. and Talegaonkar, S. (2009) 'Emerging significance of flavonoids as P-glycoprotein inhibitors in cancer chemotherapy.', *Journal of pharmacy & pharmaceutical sciences : a publication of the Canadian Society for Pharmaceutical Sciences, Societe canadienne des sciences pharmaceutiques*, 12(1), pp. 46–78. Available at: <http://www.ncbi.nlm.nih.gov/pubmed/19470292> (Accessed: 23 August 2019).
- Becker, M. L., Visser, L. E., Van Schaik, R. H. N., Hofman, A., Uitterlinden, A. G. and Stricker, B. H. (2009) 'Common genetic variation in the ABCB1 gene is associated with the cholesterol-lowering effect of simvastatin in males', *Pharmacogenomics*, 10(11), pp. 1743–1751. doi: 10.2217/pgs.09.105.
- Bentires-Alj, M., Barbu, V., Fillet, M., et al. (2003) 'NF- $\kappa$ B transcription

- factor induces drug resistance through MDR1 expression in cancer cells', *Oncogene*, 22(1), pp. 90–97. doi: 10.1038/sj.onc.1206056.
- Bodó, A., Bakos, É., Szeri, F., Váradi, A. and Sarkadi, B. (2003) 'The role of multidrug transporters in drug availability, metabolism and toxicity', *Toxicology Letters*, 140–141, pp. 133–143. doi: 10.1016/S0378-4274(02)00497-6.
- De Boo, S., Kopecka, J., Brusa, D., *et al.* (2009) 'INOS activity is necessary for the cytotoxic and immunogenic effects of doxorubicin in human colon cancer cells', *Molecular Cancer*, 8, pp. 1–18. doi: 10.1186/1476-4598-8-108.
- Bray, F., Ferlay, J., Soerjomataram, I., Siegel, R. L., Torre, L. A. and Jemal, A. (2018) 'Global cancer statistics 2018: GLOBOCAN estimates of incidence and mortality worldwide for 36 cancers in 185 countries', *CA: A Cancer Journal for Clinicians*, 68(6), pp. 394–424. doi: 10.3322/caac.21492.
- Brown, J. S., O'Carrigan, B., Jackson, S. P. and Yap, T. A. (2017) 'Targeting DNA repair in cancer: Beyond PARP inhibitors', *Cancer Discovery*, 7(1), pp. 20–37. doi: 10.1158/2159-8290.CD-16-0860.
- Brózik, A., Hegedüs, C., Erdei, Z., *et al.* (2011) 'Tyrosine kinase inhibitors as modulators of ATP binding cassette multidrug transporters: substrates, chemosensitizers or inducers of acquired multidrug resistance?', *Expert Opinion on Drug Metabolism & Toxicology*, 7(5), pp. 623–642. doi: 10.1517/17425255.2011.562892.
- Callaghan, R., Luk, F. and Bebawy, M. (2014) 'Inhibition of the multidrug resistance P-glycoprotein: Time for a change of strategy?', *Drug Metabolism and Disposition*. American Society for Pharmacology and Experimental Therapy, pp. 623–631. doi: 10.1124/dmd.113.056176.
- Callari, F. L. and Sortino, S. (2008) 'Amplified nitric oxide photorelease in DNA proximity', *Chemical Communications*, 1(17), pp. 1971–1973. doi: 10.1039/b800132d.
- Caruso, E. B., Petralia, S., Conoci, S., Giuffrida, S. and Sortino, S. (2007) 'Photodelivery of Nitric Oxide from Water-Soluble Platinum Nanoparticles', *Journal of the American Chemical Society*, 129(3), pp. 480–481. doi: 10.1021/ja067568d.
- Chandra Pal, H., Marchiony Hunt, K., Diamond, A., A. Elmetts, C. and Afaq, F. (2016) 'Phytochemicals for the Management of Melanoma', *Mini-*

*Reviews in Medicinal Chemistry*, 16(12), pp. 953–979. doi: 10.2174/1389557516666160211120157.

Chegaev, K., Riganti, C., Lazzarato, L., *et al.* (2011) ‘Nitric oxide donor doxorubicins accumulate into doxorubicin-resistant human colon cancer cells inducing cytotoxicity’, *ACS Medicinal Chemistry Letters*, 2(7), pp. 494–497. doi: 10.1021/ml100302t.

Chegaev, K., Fraix, A., Gazzano, E., *et al.* (2017) ‘Light-Regulated NO Release as a Novel Strategy To Overcome Doxorubicin Multidrug Resistance’, *ACS Medicinal Chemistry Letters*, 8(3), pp. 361–365. doi: 10.1021/acsmchemlett.7b00016.

Chen, C. jie, Chin, J. E., Ueda, K., *et al.* (1986) ‘Internal duplication and homology with bacterial transport proteins in the *mdr1* (P-glycoprotein) gene from multidrug-resistant human cells’, *Cell*, 47(3), pp. 381–389. doi: 10.1016/0092-8674(86)90595-7.

Chen, K. G., Valencia, J. C., Gillet, J.-P., Hearing, V. J. and Gottesman, M. M. (2009) ‘Involvement of ABC transporters in melanogenesis and the development of multidrug resistance of melanoma’, *Pigment Cell & Melanoma Research*, 22(6), pp. 740–749. doi: 10.1111/j.1755-148X.2009.00630.x.

Chen, Z., Shi, T., Zhang, L., *et al.* (2016) ‘Mammalian drug efflux transporters of the ATP binding cassette (ABC) family in multidrug resistance: A review of the past decade’, *Cancer Letters*. Elsevier Ireland Ltd, 370(1), pp. 153–164. doi: 10.1016/j.canlet.2015.10.010.

Cheng, X., Li, D., Sun, M., *et al.* (2019) ‘Co-delivery of DOX and PDTC by pH-sensitive nanoparticles to overcome multidrug resistance in breast cancer’, *Colloids and Surfaces B: Biointerfaces*, 181(May), pp. 185–197. doi: 10.1016/j.colsurfb.2019.05.042.

Chirio, D., Gallarate, M., Peira, E., Battaglia, L., Serpe, L. and Trotta, M. (2011) ‘Formulation of curcumin-loaded solid lipid nanoparticles produced by fatty acids coacervation technique’, *Journal of Microencapsulation*, 28(6), pp. 537–548. doi: 10.3109/02652048.2011.590615.

Chirio, D., Peira, E., Sapino, S., *et al.* (2018) ‘Stearoyl-chitosan coated nanoparticles obtained by microemulsion cold dilution technique’, *International Journal of Molecular Sciences*. MDPI AG, 19(12). doi: 10.3390/ijms19123833.

Chirio, D., Peira, E., Dianzani, C., *et al.* (2019) ‘Development of Solid



- Lipid Nanoparticles by Cold Dilution of Microemulsions: Curcumin Loading, Preliminary In Vitro Studies, and Biodistribution’, *Nanomaterials*, 9(2), p. 230. doi: 10.3390/nano9020230.
- Choi, B. H., Kim, C. G., Lim, Y., Shin, S. Y. and Lee, Y. H. (2008) ‘Curcumin down-regulates the multidrug-resistance *mdr1b* gene by inhibiting the PI3K/Akt/NFκB pathway’, *Cancer Letters*, 259(1), pp. 111–118. doi: 10.1016/j.canlet.2007.10.003.
- Choi, E. M., Lee, M. G., Lee, S. H., Choi, K. W. and Choi, S. H. (2010) ‘Association of ABCB1 polymorphisms with the efficacy of ondansetron for postoperative nausea and vomiting’, *Anaesthesia*, 65(10), pp. 996–1000. doi: 10.1111/j.1365-2044.2010.06476.x.
- Christian, F., Smith, E. and Carmody, R. (2016) ‘The Regulation of NF-κB Subunits by Phosphorylation’, *Cells*. MDPI AG, 5(1), p. 12. doi: 10.3390/cells5010012.
- Comerford, K. M., Wallace, T. J., Karhausen, J., Louis, N. A., Montalto, M. C. and Colgan, S. P. (2002) ‘Hypoxia-inducible factor-1-dependent regulation of the multidrug resistance (MDR1) gene.’, *Cancer research*, 62(12), pp. 3387–94. Available at: <http://www.ncbi.nlm.nih.gov/pubmed/12067980> (Accessed: 9 September 2019).
- Conoci, S., Petralia, S. and Sortino, S. (2013) ‘Use of nitroaniline derivatives for the production of nitric oxide’. United States. Available at: <https://patents.google.com/patent/US8440849B2/en>.
- Dantzig, A. H., Shepard, R. L., Law, K. L., *et al.* (1999) ‘Selectivity of the multidrug resistance modulator, LY335979, for P-glycoprotein and effect on cytochrome P-450 activities.’, *The Journal of pharmacology and experimental therapeutics*, 290(2), pp. 854–62. Available at: <http://www.ncbi.nlm.nih.gov/pubmed/10411602> (Accessed: 18 August 2019).
- Dean, M. (2009) ‘ABC Transporters , Drug Resistance , and Cancer Stem Cells’, (December 2008), pp. 3–9. doi: 10.1007/s10911-009-9109-9.
- Deshpande, S. S., Shah, G. B. and Parmar, N. S. (2003) ‘Antiulcer activity of *Tephrosia purpurea* in rats’, *Indian Journal of Pharmacology*, 35(3), pp. 168–172.
- Doublier, S., Riganti, C., Voena, C., *et al.* (2008) ‘RhoA silencing reverts the resistance to doxorubicin in human colon cancer cells’, *Molecular*

*Cancer Research*, 6(10), pp. 1607–1620. doi: 10.1158/1541-7786.MCR-08-0251.

Doublier, S., Belisario, D. C., Polimeni, M., *et al.* (2012) ‘HIF-1 activation induces doxorubicin resistance in MCF7 3-D spheroids via P-glycoprotein expression: a potential model of the chemo-resistance of invasive micropapillary carcinoma of the breast.’, *BMC cancer*, 12, p. 4. doi: 10.1186/1471-2407-12-4.

El-Beih, A. A., El-Desoky, A. H., Al-hammady, M. A., *et al.* (2018) ‘New inhibitors of RANKL-induced Osteoclastogenesis from the marine sponge *Siphonochalina siphonella*’, *Fitoterapia*. Elsevier B.V., 128, pp. 43–49. doi: 10.1016/j.fitote.2018.05.001.

El-Hawary, A. K., Abbas, A. S., Elsayed, A. A. and Zalata, K. R. (2012) ‘Molecular subtypes of breast carcinoma in Egyptian women: Clinicopathological features’, *Pathology - Research and Practice*. Elsevier GmbH., 208(7), pp. 382–386. doi: 10.1016/j.prp.2012.03.011.

Ford, P. C. (2008) ‘Polychromophoric metal complexes for generating the bioregulatory agent nitric oxide by single- and two-photon excitation’, *Accounts of Chemical Research*, 41(2), pp. 190–200. doi: 10.1021/ar700128y.

Ford, P. C. (2013) ‘Photochemical delivery of nitric oxide’, *Nitric Oxide - Biology and Chemistry*. Elsevier Inc., 34, pp. 56–64. doi: 10.1016/j.niox.2013.02.001.

Freimund, A. E., Beach, J. A., Christie, E. L. and Bowtell, D. D. L. (2018) ‘Mechanisms of Drug Resistance in High-Grade Serous Ovarian Cancer’, *Hematology/Oncology Clinics of North America*, pp. 983–996. doi: 10.1016/j.hoc.2018.07.007.

Fruttero, R., Crosetti, M., Chegaev, K., *et al.* (2010) ‘Phenylsulfonylfuroxans as modulators of multidrug-resistance-associated protein-1 and P-glycoprotein’, *Journal of Medicinal Chemistry*, 53(15), pp. 5467–5475. doi: 10.1021/jm100066y.

Fry, N. L. and Mascharak, P. K. (2011) ‘Photoactive ruthenium nitrosyls as NO donors: How to sensitize them toward visible light’, *Accounts of Chemical Research*, 44(4), pp. 289–298. doi: 10.1021/ar100155t.

Gazzano, E., Chegaev, K., Rolando, B., *et al.* (2016) ‘Overcoming multidrug resistance by targeting mitochondria with NO-donating doxorubicins’, *Bioorganic and Medicinal Chemistry*. Elsevier Ltd, 24(5),

pp. 967–975. doi: 10.1016/j.bmc.2016.01.021.

Gazzano, E., Rolando, B., Chegaev, K., *et al.* (2018) ‘Folate-targeted liposomal nitrooxy-doxorubicin: An effective tool against P-glycoprotein-positive and folate receptor-positive tumors’, *Journal of Controlled Release*. Elsevier, 270(September 2017), pp. 37–52. doi: 10.1016/j.jconrel.2017.11.042.

Gottesman, M. M., Fojo, T. and Bates, S. E. (2002) ‘Multidrug resistance in cancer: role of ATP-dependent transporters’, *Nature Reviews Cancer*, 2(1), pp. 48–58. doi: 10.1038/nrc706.

Granados-Principal, S., Quiles, J. L., Ramirez-Tortosa, C. L., Sanchez-Rovira, P. and Ramirez-Tortosa, Mc. (2010) ‘New advances in molecular mechanisms and the prevention of adriamycin toxicity by antioxidant nutrients’, *Food and Chemical Toxicology*, pp. 1425–1438. doi: 10.1016/j.fct.2010.04.007.

Gréen, H., Söderkvist, P., Rosenberg, P., Horvath, G. and Peterson, C. (2006) ‘mdr-1 single nucleotide polymorphisms in ovarian cancer tissue: G2677T/A correlates with response to paclitaxel chemotherapy’, *Clinical Cancer Research*, 12(3 I), pp. 854–859. doi: 10.1158/1078-0432.CCR-05-0950.

Guerrero, S., Inostroza-Riquelme, M., Contreras-Orellana, P., *et al.* (2018) ‘Curcumin-loaded nanoemulsion: A new safe and effective formulation to prevent tumor recurrence and metastasis’, *Nanoscale*. Royal Society of Chemistry, 10(47), pp. 22612–22622. doi: 10.1039/c8nr06173d.

Gulecha, V., Sivakumar, T., Upaganlawar, A., Khandare, R. and Upasani, C. (2011) ‘Tephrosia purpurea Linn leaves attenuate pain and inflammation in experimental animals’, *International journal of Nutrition, Pharmacology, Neurological Diseases*. Medknow, 1(2), p. 146. doi: 10.4103/2231-0738.84205.

Guri, A., Gülseren, I. and Corredig, M. (2013) ‘Utilization of solid lipid nanoparticles for enhanced delivery of curcumin in cocultures of HT29-MTX and Caco-2 cells’, *Food & Function*, 4(9), p. 1410. doi: 10.1039/c3fo60180c.

Hakkim, F. L., Bakshi, H. A., Khan, S., *et al.* (2019) ‘Frankincense essential oil suppresses melanoma cancer through down regulation of Bcl-2/Bax cascade signaling and ameliorates hepatotoxicity via phase I and II drug metabolizing enzymes’, *Oncotarget*, 10(37), pp. 3472–3490. doi:

10.18632/oncotarget.26930.

Harbeck, N. and Gnant, M. (2017) 'Breast cancer.', *Lancet (London, England)*, 389(10074), pp. 1134–1150. doi: 10.1016/S0140-6736(16)31891-8.

Hegazy, M. E. F., Abd El-Razek, M. H., Nagashima, F., Asakawa, Y. and Paré, P. W. (2009) 'Rare prenylated flavonoids from *Tephrosia purpurea*', *Phytochemistry*. Elsevier Ltd, 70(11–12), pp. 1474–1477. doi: 10.1016/j.phytochem.2009.08.001.

Higgins, C. F., Callaghan, R., Linton, K. J., Rosenberg, M. F. and Ford, R. C. (1997) 'Structure of the multidrug resistance P-glycoprotein', *Seminars in Cancer Biology*, 8(3), pp. 135–142. doi: 10.1006/scbi.1997.0067.

Hinz, M., Arslan, S. Ç. and Scheidereit, C. (2012) 'It takes two to tango: IκBs, the multifunctional partners of NF-κB', *Immunological Reviews*, 246(1), pp. 59–76. doi: 10.1111/j.1600-065X.2012.01102.x.

Holland, I. B. (2011) 'ABC transporters, mechanisms and biology: an overview', *Essays In Biochemistry*, 50, pp. 1–17. doi: 10.1042/bse0500001.

Hollborn, M., Chen, R., Wiedemann, P., Reichenbach, A., Bringmann, A. and Kohen, L. (2013) 'Cytotoxic Effects of Curcumin in Human Retinal Pigment Epithelial Cells', *PLoS ONE*. Public Library of Science, 8(3). doi: 10.1371/journal.pone.0059603.

Holohan, C., Van Schaeybroeck, S., Longley, D. B. and Johnston, P. G. (2013) 'Cancer drug resistance: An evolving paradigm', *Nature Reviews Cancer*. Nature Publishing Group, 13(10), pp. 714–726. doi: 10.1038/nrc3599.

Hosni, M., Abnane, I., Idri, A., *et al.* (2019) 'Computer Methods and Programs in Biomedicine Reviewing ensemble classification methods in breast cancer', *Computer Methods and Programs in Biomedicine*. Elsevier B.V., 177, pp. 89–112. doi: 10.1016/j.cmpb.2019.05.019.

Hossain, M. M., Banik, N. L. and Ray, S. K. (2012) 'Synergistic anti-cancer mechanisms of curcumin and paclitaxel for growth inhibition of human brain tumor stem cells and LN18 and U138MG cells', *Neurochemistry International*, 61(7), pp. 1102–1113. doi: 10.1016/j.neuint.2012.08.002.

Housman, G., Byler, S., Heerboth, S., *et al.* (2014) 'Drug resistance in cancer: An overview', *Cancers*, 6(3), pp. 1769–1792. doi:

10.3390/cancers6031769.

Hu, C. M. J. and Zhang, L. (2012) ‘Nanoparticle-based combination therapy toward overcoming drug resistance in cancer’, *Biochemical Pharmacology*. Elsevier Inc., 83(8), pp. 1104–1111. doi: 10.1016/j.bcp.2012.01.008.

Huerta, S., Chilka, S. and Bonavida, B. (2008) ‘Nitric oxide donors: Novel cancer therapeutics (review)’, *International Journal of Oncology*, pp. 909–927. doi: 10.3892/ijo\_00000079.

Hyafil, F., Vergely, C., Du Vignaud, P. and Grand-Perret, T. (1993) ‘In vitro and in vivo reversal of multidrug resistance by GF120918, an acridonecarboxamide derivative.’, *Cancer research*, 53(19), pp. 4595–602. Available at: <http://www.ncbi.nlm.nih.gov/pubmed/8402633> (Accessed: 18 August 2019).

Ibrahim, A. S., Khaled, H. M., Mikhail, N. N., Baraka, H. and Kamel, H. (2014) ‘Cancer Incidence in Egypt: Results of the National Population-Based Cancer Registry Program’, *Journal of Cancer Epidemiology*, 2014, pp. 1–18. doi: 10.1155/2014/437971.

Ischiropoulos, H. (2003) ‘Biological selectivity and functional aspects of protein tyrosine nitration.’, *Biochemical and biophysical research communications*, 305(3), pp. 776–83. doi: 10.1016/s0006-291x(03)00814-3.

Israel, A. (2010) ‘The IKK Complex, a Central Regulator of NF- $\kappa$ B Activation’, *Cold Spring Harbor Perspectives in Biology*, 2(3), pp. a000158–a000158. doi: 10.1101/cshperspect.a000158.

Jani, M., Ambrus, C., Magnan, R., *et al.* (2014) ‘Structure and function of BCRP, a broad specificity transporter of xenobiotics and endobiotics’, *Arch Toxicol*, 88, pp. 1205–1248. doi: 10.1007/s00204-014-1224-8.

Jiang, P., Mukthavavam, R., Chao, Y., *et al.* (2014) ‘Novel anti-glioblastoma agents and therapeutic combinations identified from a collection of FDA approved drugs’, *Journal of Translational Medicine*, 12(1), p. 13. doi: 10.1186/1479-5876-12-13.

Jin, J.-S., Zhao, Y.-F., Nakamura, N., Akao, T., Kakiuchi, N. and Hattori, M. (2007) ‘Isolation and characterization of a human intestinal bacterium, Eubacterium sp. ARC-2, capable of demethylating arctigenin, in the essential metabolic process to enterolactone.’, *Biological & pharmaceutical bulletin*, 30(5), pp. 904–11. doi: 10.1248/bpb.30.904.

- Jin, J. S. and Hattori, M. (2010) 'Human intestinal bacterium, strain END-2 is responsible for demethylation as well as lactonization during plant lignan metabolism', *Biological and Pharmaceutical Bulletin*, pp. 1443–1447. doi: 10.1248/bpb.33.1443.
- Jones, D., Kamel-Reid, S., Bahler, D., *et al.* (2009) 'Laboratory practice guidelines for detecting and reporting BCR-ABL drug resistance mutations in chronic myelogenous leukemia and acute lymphoblastic leukemia', *Journal of Molecular Diagnostics*. American Society for Investigative Pathology and Association for Molecular Pathology, 11(1), pp. 4–11. doi: 10.2353/jmoldx.2009.080095.
- Juliano, R. L. and Ling, V. (1976) 'A surface glycoprotein modulating drug permeability in Chinese hamster ovary cell mutants', *BBA - Biomembranes*, 455(1), pp. 152–162. doi: 10.1016/0005-2736(76)90160-7.
- Karabay, A. Z., Koc, A., Ozkan, T., *et al.* (2018) 'Expression analysis of Akirin-2, NFκB-p65 and β-catenin proteins in imatinib resistance of chronic myeloid leukemia', *Hematology*. Taylor and Francis Ltd., 23(10), pp. 765–770. doi: 10.1080/10245332.2018.1488795.
- Kathawala, R. J., Gupta, P., Ashby, C. R. and Chen, Z. S. (2015) 'The modulation of ABC transporter-mediated multidrug resistance in cancer: A review of the past decade', *Drug Resistance Updates*. Elsevier Ltd, 18, pp. 1–17. doi: 10.1016/j.drug.2014.11.002.
- Khalafallah, A. K., Suleiman, S. A., Yousef, A. H., El-kanzi, N. A. A. and Mohamed, A. E. H. H. (2009) 'Prenylated flavonoids from *Tephrosia apollinea*', *Chinese Chemical Letters*, 20(12), pp. 1465–1468. doi: 10.1016/j.ccllet.2009.05.025.
- Khavari, P. A. (2006) 'Modelling cancer in human skin tissue', *Nature Reviews Cancer*, 6(4), pp. 270–280. doi: 10.1038/nrc1838.
- Kim, S. Y., Kim, S. J., Kim, B. J., *et al.* (2006) 'Doxorubicin-induced reactive oxygen species generation and intracellular Ca<sup>2+</sup> increase are reciprocally modulated in rat cardiomyocytes', *Experimental and Molecular Medicine*. Korean Society of Med. Biochemistry and Mol. Biology, 38(5), pp. 535–545. doi: 10.1038/emm.2006.63.
- Kim, T. H., Shin, S., Yoo, S. D. and Shin, B. S. (2018) 'Effects of phytochemical P-glycoprotein modulators on the pharmacokinetics and tissue distribution of doxorubicin in mice', *Molecules*, 23(2). doi: 10.3390/molecules23020349.

- Kitamura, K., Kawaguchi, M., Ieda, N., Miyata, N. and Nakagawa, H. (2016) 'Visible Light-Controlled Nitric Oxide Release from Hindered Nitrobenzene Derivatives for Specific Modulation of Mitochondrial Dynamics', *ACS Chemical Biology*, 11(5), pp. 1271–1278. doi: 10.1021/acscchembio.5b00962.
- Koboldt, D. C., Fulton, R. S., McLellan, M. D., *et al.* (2012) 'Comprehensive molecular portraits of human breast tumours', *Nature*, 490(7418), pp. 61–70. doi: 10.1038/nature11412.
- Kopecka, J., Salzano, G., Campia, I., *et al.* (2014) 'Insights in the chemical components of liposomes responsible for P-glycoprotein inhibition', *Nanomedicine: Nanotechnology, Biology, and Medicine*, 10(1), pp. 77–87. doi: 10.1016/j.nano.2013.06.013.
- Kopecka, J., Campia, I., Jacobs, A., *et al.* (2015) 'Carbonic anhydrase XII is a new therapeutic target to overcome chemoresistance in cancer cells', *Oncotarget*. Impact Journals LLC, 6(9), pp. 6776–6793. doi: 10.18632/oncotarget.2882.
- Kopecka, J., Salaroglio, I. C., Righi, L., *et al.* (2018) 'Loss of C/EBP-beta LIP drives cisplatin resistance in malignant pleural mesothelioma.', *Lung cancer (Amsterdam, Netherlands)*. Ireland, 120, pp. 34–45. doi: 10.1016/j.lungcan.2018.03.022.
- Kumar, A. and Jaitak, V. (2019) 'Natural products as multidrug resistance modulators in cancer', *European Journal of Medicinal Chemistry*. Elsevier Masson SAS, 176, pp. 268–291. doi: 10.1016/j.ejmech.2019.05.027.
- Lee, B. D., French, K. J., Zhuang, Y. and Smith, C. D. (2003) 'Development of a syngeneic in vivo tumor model and its use in evaluating a novel P-glycoprotein modulator, PGP-4008.', *Oncology research*, 14(1), pp. 49–60. Available at: <http://www.ncbi.nlm.nih.gov/pubmed/14552591> (Accessed: 9 September 2019).
- Lehmann, B. D., Jovanovi, B., Chen, X., *et al.* (2016) 'Refinement of Triple-Negative Breast Cancer Molecular Subtypes : Implications for Neoadjuvant Chemotherapy Selection', pp. 1–22. doi: 10.1371/journal.pone.0157368.
- Li, W., Zhang, H., Assaraf, Y. G., *et al.* (2016) 'Overcoming ABC transporter-mediated multidrug resistance: Molecular mechanisms and novel therapeutic drug strategies', *Drug Resistance Updates*. Elsevier Ltd, 27, pp. 14–29. doi: 10.1016/j.drug.2016.05.001.

- Li, Z., Wang, C., Cheng, L., *et al.* (2013) 'PEG-functionalized iron oxide nanoclusters loaded with chlorin e6 for targeted, NIR light induced, photodynamic therapy', *Biomaterials*. Elsevier Ltd, 34(36), pp. 9160–9170. doi: 10.1016/j.biomaterials.2013.08.041.
- Lim, Y. A., Kojima, S., Nakamura, N., *et al.* (1997) 'Inhibitory effects of *Cordia spinescens* extracts and their constituents on reverse transcriptase and protease from human immunodeficiency virus', *Phytotherapy Research*, 11(7), pp. 490–495. doi: 10.1002/(SICI)1099-1573(199711)11:7<490::AID-PTR134>3.0.CO;2-Y.
- Limtrakul, P., Anuchapreeda, S. and Bhudsuk, D. (2005) 'Modulation of human multidrug-resistance MDR-1 gene by natural curcuminoids', *Acta Horticulturae*, 678, pp. 75–83. doi: 10.1186/1471-2407-4-13.
- Limtrakul, P., Anuchapreeda, S. and Buddhasukh, D. (2004) 'Modulation of human multidrug-resistance MDR-1 gene by natural curcuminoids', *BMC Cancer*, 4(1), p. 13. doi: 10.1186/1471-2407-4-13.
- Liu, C., He, X., Liu, X., *et al.* (2019) 'RPS15A promotes gastric cancer progression via activation of the Akt/IKK- $\beta$ /NF- $\kappa$ B signalling pathway', *Journal of Cellular and Molecular Medicine*. Blackwell Publishing Inc., 23(3), pp. 2207–2218. doi: 10.1111/jcmm.14141.
- Llano, S., Gómez, S., Londoño, J. and Restrepo, A. (2019) 'Antioxidant activity of curcuminoids', *Physical Chemistry Chemical Physics*, 21(7), pp. 3752–3760. doi: 10.1039/c8cp06708b.
- Lopes-Rodrigues, V., Sousa, E. and Vasconcelos, M. (2016) 'Curcumin as a Modulator of P-Glycoprotein in Cancer: Challenges and Perspectives', *Pharmaceuticals*, 9(4), p. 71. doi: 10.3390/ph9040071.
- López-Lázaro, M. (2008) 'Anticancer and carcinogenic properties of curcumin: Considerations for its clinical development as a cancer chemopreventive and chemotherapeutic agent', *Molecular Nutrition and Food Research*, 52(SUPPL. 1), pp. 103–127. doi: 10.1002/mnfr.200700238.
- López, S. B., López, M. L., Aragón, L. M., *et al.* (2011) 'Composition and anti-insect activity of essential oils from *Tagetes L.* species (Asteraceae, Helenieae) on *Ceratitis capitata* Wiedemann and *Triatoma infestans* Klug.', *Journal of agricultural and food chemistry*, 59(10), pp. 5286–92. doi: 10.1021/jf104966b.
- Lovitt, C. J., Shelper, T. B. and Avery, V. M. (2018) 'Doxorubicin



- resistance in breast cancer cells is mediated by extracellular matrix proteins', *BMC Cancer*. *BMC Cancer*, 18(1), pp. 1–11. doi: 10.1186/s12885-017-3953-6.
- Lu, W.-D., Qin, Y., Yang, C. and Li, L. (2013) 'Effect of curcumin on human colon cancer multidrug resistance in vitro and in vivo', *Clinics*. Hospital das Clinicas da Faculdade de Medicina da Universidade de Sao Paulo, 68(5), p. 694.
- Maitra, R., Halpin, P. A., Karlson, K. H., *et al.* (2001) 'Differential effects of mitomycin C and doxorubicin on P-glycoprotein expression', *Biochemical Journal*. Portland Press Ltd, 355(3), pp. 617–624. doi: 10.1042/bj3550617.
- Maldini, M., Montoro, P., MacChia, M., Pizza, C. and Piacente, S. (2011) 'Profiling of phenolics from *Tephrosia cinerea*', *Planta Medica*, 77(16), pp. 1861–1864. doi: 10.1055/s-0030-1271190.
- Mansoori, B., Mohammadi, A., Davudian, S., Shirjang, S. and Baradaran, B. (2017) 'The Different Mechanisms of Cancer Drug Resistance: A Brief Review', *Advanced Pharmaceutical Bulletin*, 7(3), pp. 339–348. doi: 10.15171/apb.2017.041.
- Menon, V. P. and Sudheer, A. R. (2007) 'Antioxidant and anti-inflammatory properties of curcumin', *Advances in Experimental Medicine and Biology*. Boston, MA: Springer US, pp. 105–125. doi: 10.1007/978-0-387-46401-5\_3.
- Meselhy, M. R. (2003) 'Inhibition of LPS-induced NO production by the oleogum resin of *Commiphora wightii* and its constituents.', *Phytochemistry*, 62(2), pp. 213–8. Available at: <http://www.ncbi.nlm.nih.gov/pubmed/12482459> (Accessed: 27 August 2019).
- Minotti, G. (2004) 'Anthracyclines: Molecular Advances and Pharmacologic Developments in Antitumor Activity and Cardiotoxicity', *Pharmacological Reviews*, 56(2), pp. 185–229. doi: 10.1124/pr.56.2.6.
- Mistry, P., Stewart, A. J., Dangerfield, W., *et al.* (2001) 'In vitro and in vivo reversal of P-glycoprotein-mediated multidrug resistance by a novel potent modulator, XR9576', 'Addition of gabapentin to a modified FOLFOX regimen does not reduce oxaliplatin-induced neurotoxicity', *Cancer Research*, 61(2), pp. 749–758.
- Mo, W. and Zhang, J. (2012) 'Human ABCG2 : structure , function , and

its role in multidrug resistance', 3(1), pp. 1–27.

Mohajeri, M. and Sahebkar, A. (2018) 'Protective effects of curcumin against doxorubicin-induced toxicity and resistance: A review', *Critical Reviews in Oncology/Hematology*. Elsevier Ireland Ltd, pp. 30–51. doi: 10.1016/j.critrevonc.2017.12.005.

Mohamed, A. E. H. H., Khalafallah, A. K. and Yousof, A. H. (2008) 'Biotransformation of glabratephrin, a rare type of isoprenylated flavonoids, by *Aspergillus niger*', *Zeitschrift fur Naturforschung - Section C Journal of Biosciences*, 63(7–8), pp. 561–564. doi: 10.1515/znc-2008-7-816.

Moscow, J., Morrow, C. S. and Cowan, K. H. (2003) *General Mechanisms of Drug Resistance. Holland-Frei Cancer Medicine. 6th edition. Hamilton (ON): BC Decker; 2003.* 6th edn. Edited by K. DW et al. Available at: <https://www.ncbi.nlm.nih.gov/books/NBK12424/>.

Mu, W. and Liu, L. Z. (2017) 'Reactive Oxygen Species Signaling in Cancer Development', *Reactive Oxygen Species*, 4(10), pp. 251–265. doi: 10.20455/ros.2017.843.

Nabekura, T., Kamiyama, S. and Kitagawa, S. (2005) 'Effects of dietary chemopreventive phytochemicals on P-glycoprotein function', *Biochemical and Biophysical Research Communications*, 327(3), pp. 866–870. doi: 10.1016/j.bbrc.2004.12.081.

Nakhlband, A., Eskandani, M., Saeedi, N., *et al.* (2018) 'Marrubiin-loaded solid lipid nanoparticles' impact on TNF- $\alpha$  treated umbilical vein endothelial cells: A study for cardioprotective effect', *Colloids and Surfaces B: Biointerfaces*. Elsevier B.V., 164, pp. 299–307. doi: 10.1016/j.colsurfb.2018.01.046.

Neophytou, C., Boutsikos, P. and Papageorgis, P. (2018) 'Molecular Mechanisms and emerging Therapeutic Targets of Triple-negative Breast Cancer Metastasis', *Frontiers in oncology*, 8(February), p. 31. doi: 10.3389/fonc.2018.00031.

Obaid, G., Broekgaarden, M., Bulin, A. L., *et al.* (2016) 'Photonanomedicine: A convergence of photodynamic therapy and nanotechnology', *Nanoscale*. Royal Society of Chemistry, 8(25), pp. 12471–12503. doi: 10.1039/c5nr08691d.

Oellers, P., Wolkow, N., Jakobiec, F. A. and Kim, I. K. (2018) 'Hemorrhagic choroidal melanoma', *American Journal of Ophthalmology*

*Case Reports*. Elsevier, 10(November 2017), pp. 105–107. doi: 10.1016/j.ajoc.2018.02.001.

Omar, S., Khaled, H., Gaafar, R., Zekry, A. R., Eissa, S. and el-Khatib, O. (2003) ‘Breast cancer in Egypt: a review of disease presentation and detection strategies.’, *Eastern Mediterranean health journal = La revue de sante de la Mediterranee orientale = al-Majallah al-sihhiyah li-sharq al-mutawassit*, 9(3), pp. 448–63. Available at: <http://www.ncbi.nlm.nih.gov/pubmed/15751939> (Accessed: 2 August 2019).

Omote, H., Figler, R. A., Polar, M. K. and Al-Shawi, M. K. (2004) ‘Improved Energy Coupling of Human P-glycoprotein by the Glycine 185 to Valine Mutation’, *Biochemistry*, 43(13), pp. 3917–3928. doi: 10.1021/bi035365l.

Orelle, C., Gubellini, F., Durand, A., *et al.* (2008) ‘Conformational change induced by ATP binding in the multidrug ATP-binding cassette transporter BmrA’, *Biochemistry*. American Chemical Society, 47(8), pp. 2404–2412. doi: 10.1021/bi702303s.

Orlowski, R. Z. and Baldwin, A. S. (2002) ‘NF-kappaB as a therapeutic target in cancer.’, *Trends in molecular medicine*, 8(8), pp. 385–9. Available at: <http://www.ncbi.nlm.nih.gov/pubmed/12127724> (Accessed: 9 September 2019).

Paharia, A. K. and Pandurangan, A. (2013) ‘Evaluation of Hepatoprotective activity of Ethanolic Extract of *Nymphaea alba* Linn Flower in experimental rats’, *International Journal of Biomedical Research*. Scholar Science Journals, 4(7), p. 349. doi: 10.7439/ijbr.v4i7.326.

Pavana, P., Sethupathy, S., Santha, K. and Manoharan, S. (2008) ‘Effects of tephrosia purpurea aqueous seed extract on blood glucose and antioxidant enzyme activities in streptozotocin induced diabetic rats’, *African Journal of Traditional, Complementary and Alternative Medicines*, 6(1), pp. 78–86. doi: 10.4314/ajtcam.v6i1.57077.

Pelter, A., Ward, R. S., Rao, E. V. and Raju, N. R. (1981) ‘8-Substituted flavonoids and 3'-substituted 7-oxygenated chalcones from *Tephrosia purpurea*’, *Journal of the Chemical Society, Perkin Transactions 1*, pp. 2491–2498. doi: 10.1039/P19810002491.

Perou, C. M. (2011) ‘Molecular Stratification of Triple-Negative Breast

- Cancers', *The Oncologist*, 16(Supplement 1), pp. 61–70. doi: 10.1634/theoncologist.2011-s1-61.
- Pilco-Ferreto, N. and Calaf, G. M. (2016) 'Influence of doxorubicin on apoptosis and oxidative stress in breast cancer cell lines.', *International journal of oncology*, 49(2), pp. 753–62. doi: 10.3892/ijo.2016.3558.
- Pluchino, K. M., Hall, M. D., Goldsborough, A. S., Callaghan, R. and Gottesman, M. M. (2012) 'Collateral sensitivity as a strategy against cancer multidrug resistance', *Drug Resistance Updates*. Churchill Livingstone, 15(1–2), pp. 98–105. doi: 10.1016/j.drug.2012.03.002.
- Qureshi, S., Shah, A. and Ageel, A. (1992) 'Toxicity studies on *Alpinia galanga* and *Curcuma longa*', *Planta Medica*, 58(02), pp. 124–127. doi: 10.1055/s-2006-961412.
- Raymond, M. and Gross, P. (1989) 'Mammalian multidrug-resistance gene: Correlation of exon organization with structural domains and duplication of an ancestral gene', *Proceedings of the National Academy of Sciences of the United States of America*, 86(17), pp. 6488–6492. doi: 10.1073/pnas.86.17.6488.
- Rehman, M. U., Khan, M. A., Khan, W. S., Shafique, M. and Khan, M. (2018) 'Fabrication of Niclosamide loaded solid lipid nanoparticles: in vitro characterization and comparative in vivo evaluation', *Artificial Cells, Nanomedicine and Biotechnology*. Informa UK Limited, trading as Taylor & Francis Group, 46(8), pp. 1926–1934. doi: 10.1080/21691401.2017.1396996.
- Ren, F., Shen, J., Shi, H., Hornicek, F. J., Kan, Q. and Duan, Z. (2016) 'Novel mechanisms and approaches to overcome multidrug resistance in the treatment of ovarian cancer', *Biochimica et Biophysica Acta - Reviews on Cancer*. Elsevier B.V., 1866(2), pp. 266–275. doi: 10.1016/j.bbcan.2016.10.001.
- Renzi, M., Schimmel, J., Decker, A. and Lawrence, N. (2019) 'Management of Skin Cancer in the Elderly', *Dermatologic Clinics*. Elsevier Inc, 37(3), pp. 279–286. doi: 10.1016/j.det.2019.02.003.
- Rice, A. J., Park, A. and Pinkett, H. W. (2014) 'Diversity in ABC transporters: Type I, II and III importers', *Critical Reviews in Biochemistry and Molecular Biology*, 49(5), pp. 426–437. doi: 10.3109/10409238.2014.953626.
- Riganti, C., Miraglia, E., Viarisio, D., *et al.* (2005a) 'Nitric oxide reverts

the resistance to doxorubicin in human colon cancer cells by inhibiting the drug efflux.’, *Cancer research*, 65(2), pp. 516–25. Available at: <http://www.ncbi.nlm.nih.gov/pubmed/15695394> (Accessed: 27 August 2019).

Riganti, C., Miraglia, E., Viarisio, D., *et al.* (2005b) ‘Nitric oxide reverts the resistance to doxorubicin in human colon cancer cells by inhibiting the drug efflux’, *Cancer Research*, 65(2), pp. 516–525.

Riganti, C., Costamagna, C., Doublier, S., *et al.* (2008) ‘The NADPH oxidase inhibitor apocynin induces nitric oxide synthesis via oxidative stress’, *Toxicology and Applied Pharmacology*, 228(3), pp. 277–285. doi: 10.1016/j.taap.2007.12.013.

Riganti, C., Voena, C., Kopecka, J., *et al.* (2011) ‘Liposome-encapsulated doxorubicin reverses drug resistance by inhibiting P-glycoprotein in human cancer cells’, *Molecular Pharmaceutics*, 8(3), pp. 683–700. doi: 10.1021/mp2001389.

Riganti, C., Rolando, B., Kopecka, J., *et al.* (2013a) ‘Mitochondrial-targeting nitrooxy-doxorubicin: A new approach to overcome drug resistance’, *Molecular Pharmaceutics*, 10(1), pp. 161–174. doi: 10.1021/mp300311b.

Riganti, C., Rolando, B., Kopecka, J., *et al.* (2013b) ‘Mitochondrial-targeting nitrooxy-doxorubicin: A new approach to overcome drug resistance’, *Molecular Pharmaceutics*, 10(1), pp. 161–174. doi: 10.1021/mp300311b.

Riganti, C., Kopecka, J., Panada, E., Barak, S. and Rubinstein, M. (2015) ‘The role of C/EBP- $\beta$  LIP in multidrug resistance’, *Journal of the National Cancer Institute*, 107(5), pp. 1–14. doi: 10.1093/jnci/djv046.

Riganti, C., Gazzano, E., Gulino, G. R., Volante, M., Ghigo, D. and Kopecka, J. (2015) ‘Two repeated low doses of doxorubicin are more effective than a single high dose against tumors overexpressing P-glycoprotein’, *Cancer Letters*. Elsevier Ireland Ltd, 360(2), pp. 219–226. doi: 10.1016/j.canlet.2015.02.008.

Safa, A. R., Stern, R. K., Choi, K., *et al.* (1990) ‘Molecular basis of preferential resistance to colchicine in multidrug-resistant human cells conferred by Gly-185  $\rightarrow$  Val-185 substitution in P-glycoprotein’, *Proceedings of the National Academy of Sciences of the United States of America*. National Academy of Sciences, 87(18), pp. 7225–7229. doi:

10.1073/pnas.87.18.7225.

Sakil, H. A. M., Stantic, M., Wolfsberger, J., Brage, S. E., Hansson, J. and Wilhelm, M. T. (2017) 'ΔNp73 regulates the expression of the multidrug-resistance genes ABCB1 and ABCB5 in breast cancer and melanoma cells - a short report', *Cellular Oncology*. Cellular Oncology, 40(6), pp. 631–638. doi: 10.1007/s13402-017-0340-x.

Salaroglio, Iris C, Gazzano, E., Abdullrahman, A., *et al.* (2018) 'Increasing intratumor C/EBP-β LIP and nitric oxide levels overcome resistance to doxorubicin in triple negative breast cancer', *Journal of Experimental & Clinical Cancer Research*. Journal of Experimental & Clinical Cancer Research, 37(1), p. 286. doi: 10.1186/s13046-018-0967-0.

Salaroglio, Iris C., Gazzano, E., Abdullrahman, A., *et al.* (2018) 'Increasing intratumor C/EBP-β LIP and nitric oxide levels overcome resistance to doxorubicin in triple negative breast cancer', *Journal of Experimental & Clinical Cancer Research*, 37(1), p. 286. doi: 10.1186/s13046-018-0967-0.

Salehan, M. R. and Morse, H. R. (2013) 'DNA damage repair and tolerance: a role in chemotherapeutic drug resistance', *British Journal of Biomedical Science*, 70(1), pp. 31–40. doi: 10.1080/09674845.2013.11669927.

Saraf, M., Soni, K. and Kumar, Ps. (2006) 'Antioxidant activity of fraction of Tephrosia purpurea linn', *Indian Journal of Pharmaceutical Sciences*. OMICS Publishing Group, 68(4), p. 456. doi: 10.4103/0250-474x.27817.

Saraswathy, M. and Gong, S. (2013) 'Different strategies to overcome multidrug resistance in cancer', *Biotechnology Advances*. Elsevier Inc., 31(8), pp. 1397–1407. doi: 10.1016/j.biotechadv.2013.06.004.

Shair, I., He, W. and Yin, L. (2018) 'Understanding of human ATP binding cassette superfamily and novel multidrug resistance modulators to overcome MDR', *Biomedicine and Pharmacotherapy*. Elsevier, 100(December 2017), pp. 335–348. doi: 10.1016/j.biopha.2018.02.038.

Shankar, T. N., Shantha, N. V, Ramesh, H. P., Murthy, I. A. and Murthy, V. S. (1980) 'Toxicity studies on turmeric (*Curcuma longa*): acute toxicity studies in rats, guineapigs & monkeys.', *Indian journal of experimental biology*, 18(1), pp. 73–5. Available at: <http://www.ncbi.nlm.nih.gov/pubmed/6772551> (Accessed: 20 August 2019).

- Shapira, A., Livney, Y. D., Broxterman, H. J. and Assaraf, Y. G. (2011) 'Nanomedicine for targeted cancer therapy : Towards the overcoming of drug resistance', *Drug Resistance Updates*. Elsevier Ltd, 14(3), pp. 150–163. doi: 10.1016/j.drug.2011.01.003.
- Sharma, K., Sengupta, K. and Chakrapani, H. (2013) 'Nitroreductase-activated nitric oxide (NO) prodrugs', *Bioorganic & Medicinal Chemistry Letters*. Elsevier Ltd, 23(21), pp. 5964–5967. doi: 10.1016/j.bmcl.2013.08.066.
- Stuart, E. C., Jarvis, R. M. and Rosengren, R. J. (2010) 'In vitro mechanism of action for the cytotoxicity elicited by the combination of epigallocatechin gallate and raloxifene in MDA-MB-231 cells', *Oncol Rep.*, 24(3), pp. 779–785. doi: 10.3892/or.
- Sun, J., Bi, C., Chan, H. M., Sun, S., Zhang, Q. and Zheng, Y. (2013) 'Curcumin-loaded solid lipid nanoparticles have prolonged in vitro antitumour activity, cellular uptake and improved in vivo bioavailability', *Colloids and Surfaces B: Biointerfaces*. Elsevier B.V., 111, pp. 367–375. doi: 10.1016/j.colsurfb.2013.06.032.
- Suzuki, T., Nagae, O., Kato, Y., Nakagawa, H., Fukuhara, K. and Miyata, N. (2005) 'Photoinduced nitric oxide release from nitrobenzene derivatives', *Journal of the American Chemical Society*, 127(33), pp. 11720–11726. doi: 10.1021/ja0512024.
- Szakács, G., Paterson, J. K., Ludwig, J. A., Booth-Genthe, C. and Gottesman, M. M. (2006) 'Targeting multidrug resistance in cancer', *Nature Reviews Drug Discovery*, 5(3), pp. 219–234. doi: 10.1038/nrd1984.
- Szakács, G., Hall, M. D., Gottesman, M. M., *et al.* (2014) 'Targeting the achilles heel of multidrug-resistant cancer by exploiting the fitness cost of resistance', *Chemical Reviews*. American Chemical Society, pp. 5753–5774. doi: 10.1021/cr4006236.
- Székely, B., Silber, A. L. M. and Pusztai, L. (2017) 'New Therapeutic Strategies for Triple-Negative Breast Cancer.', *Oncology (Williston Park, N.Y.)*, 31(2), pp. 130–7. Available at: <http://www.ncbi.nlm.nih.gov/pubmed/28205193> (Accessed: 9 September 2019).
- Szöllösi, D., Rose-Sperling, D., Hellmich, U. A. and Stockner, T. (2018) 'Comparison of mechanistic transport cycle models of ABC exporters', *Biochimica et Biophysica Acta - Biomembranes*, 1860(4), pp. 818–832. doi:

10.1016/j.bbamem.2017.10.028.

Tacar, O., Sriamornsak, P. and Dass, C. R. (2013) 'Doxorubicin: an update on anticancer molecular action, toxicity and novel drug delivery systems', *Journal of Pharmacy and Pharmacology*, 65(2), pp. 157–170. doi: 10.1111/j.2042-7158.2012.01567.x.

Tajbakhsh, A., Rivandi, M., Abedini, S. and Pasdar, A. (2019) 'Critical Reviews in Oncology / Hematology Regulators and mechanisms of anoikis in triple-negative breast cancer ( TNBC ): A review', *Critical Reviews in Oncology / Hematology*. Elsevier, 140(May), pp. 17–27. doi: 10.1016/j.critrevonc.2019.05.009.

Thomas, H. and Coley, H. M. (2003) 'Overcoming multidrug resistance in cancer: An update on the clinical strategy of inhibiting P-glycoprotein', *Cancer Control*, 10(2), pp. 159–165. doi: 10.1177/107327480301000207.

Toia, F., Garbo, G., Tripoli, M., Rinaldi, G., Moschella, F. and Cordova, A. (2015) 'A systematic review on external ear melanoma', *Journal of Plastic, Reconstructive and Aesthetic Surgery*. Elsevier Ltd, 68(7), pp. 883–894. doi: 10.1016/j.bjps.2015.04.003.

Umsumarng, S., Pitchakarn, P., Yodkeeree, S., *et al.* (2017) 'Modulation of P-glycoprotein by Stemona alkaloids in human multidrug resistance leukemic cells and structural relationships', *Phytomedicine*. Elsevier, 34(June), pp. 182–190. doi: 10.1016/j.phymed.2017.08.004.

Vadlapatla, R. K., Vadlapudi, A. D., Pal, D. and Mitra, A. K. (2013) 'Mechanisms of Drug Resistance in Cancer Chemotherapy : Coordinated Role and Regulation of Efflux Transporters and Metabolizing Enzymes', pp. 7126–7140.

Vallianou, N. G., Evangelopoulos, A., Schizas, N. and Kazazis, C. (2015) 'Potential anticancer properties and mechanisms of action of curcumin.', *Anticancer research*, 35(2), pp. 645–51. Available at: <http://www.ncbi.nlm.nih.gov/pubmed/25667441> (Accessed: 9 September 2019).

Vleggaar, R., Kruger, G. J., Smalberger, T. M. and Van Den Berg, A. J. (1978) 'Flavonoids from tephrosia—XI: The structure of glabratephrin', *Tetrahedron*, 34(9), pp. 1405–1408. doi: 10.1016/0040-4020(78)88338-0.

Wang, P., Yang, H. L., Yang, Y. J., Wang, L. and Lee, S. C. (2015) 'Overcome Cancer Cell Drug Resistance Using Natural Products', *Evidence-Based Complementary and Alternative Medicine*. Hindawi



- Publishing Corporation, 2015, pp. 1–14. doi: 10.1155/2015/767136.
- Wang, W., Chen, T., Xu, H., *et al.* (2018) ‘Curcumin-loaded solid lipid nanoparticles enhanced anticancer efficiency in breast cancer’, *Molecules*, 23(7), pp. 1–13. doi: 10.3390/molecules23071578.
- Wang, X. (2014) *Studies of Overcoming Acquired Resistance : Molecular Mechanisms and Development of Novel Drugs*.
- Wang, X., Zhang, H. and Chen, X. (2019) ‘Drug resistance and combating drug resistance in cancer’, *Cancer Drug Resistance*, 2, pp. 141–160. doi: 10.20517/cdr.2019.10.
- Ween, M. P., Armstrong, M. A., Oehler, M. K. and Ricciardelli, C. (2015) ‘The role of ABC transporters in ovarian cancer progression and chemoresistance’, *Critical Reviews in Oncology/Hematology*. Elsevier Ireland Ltd, 96(2), pp. 220–256. doi: 10.1016/j.critrevonc.2015.05.012.
- Willers, C., Svitina, H., Rossouw, M. J., Swanepoel, R. A., Hamman, J. H. and Gouws, C. (2019) ‘Models used to screen for the treatment of multidrug resistant cancer facilitated by transporter-based efflux’, *Journal of Cancer Research and Clinical Oncology*. Springer Berlin Heidelberg, 145(8), pp. 1949–1976. doi: 10.1007/s00432-019-02973-5.
- Wink, D. A. and Mitchell, J. B. (1998) ‘Chemical biology of nitric oxide: insights into regulatory, cytotoxic, and cytoprotective mechanisms of nitric oxide’, *Free Radical Biology and Medicine*, 25(4–5), pp. 434–456. doi: 10.1016/S0891-5849(98)00092-6.
- Wink, M., Ashour, M. L. and El-Readi, M. Z. (2012) ‘Secondary metabolites from plants inhibiting ABC transporters and reversing resistance of cancer cells and microbes to cytotoxic and antimicrobial agents’, *Frontiers in Microbiology*, 3(APR), pp. 1–15. doi: 10.3389/fmicb.2012.00130.
- Wu, C., Hsieh, C. and Wu, Y. (2011) ‘The Emergence of Drug Transporter-Mediated Multidrug Resistance to Cancer Chemotherapy’, pp. 1996–2011.
- Wu, F., Zhu, J., Li, G., *et al.* (2019) ‘Biologically synthesized green gold nanoparticles from *Siberian ginseng* induce growth-inhibitory effect on melanoma cells (B16)’, *Artificial Cells, Nanomedicine, and Biotechnology*. Taylor & Francis, 47(1), pp. 3297–3305. doi: 10.1080/21691401.2019.1647224.

- Wu, Q., Yang, Z., Nie, Y., Shi, Y. and Fan, D. (2014) 'Multi-drug resistance in cancer chemotherapeutics: Mechanisms and lab approaches', *Cancer Letters*. Elsevier Ireland Ltd, 347(2), pp. 159–166. doi: 10.1016/j.canlet.2014.03.013.
- Xiao, P. and Liu, C. (2005) 'Pharmacology , pharmacokinetics and toxicology of Chinese traditional medicine for stroke therapy', 5(2), pp. 83–124.
- Xu, Y. chao, Liu, X., Li, M., *et al.* (2018) 'A Novel Mechanism of Doxorubicin Resistance and Tumorigenesis Mediated by MicroRNA-501-5p-Suppressed BLID', *Molecular Therapy - Nucleic Acids*. Elsevier Ltd., 12(September), pp. 578–590. doi: 10.1016/j.omtn.2018.06.011.
- Yallapu, M. M., Nagesh, P. K. B., Jaggi, M. and Chauhan, S. C. (2015) 'Therapeutic Applications of Curcumin Nanoformulations', *The AAPS Journal*, 17(6), pp. 1341–1356. doi: 10.1208/s12248-015-9811-z.
- Yallapu, M. M., Jaggi, M. and Chauhan, S. C. (2012) 'Curcumin nanoformulations: a future nanomedicine for cancer', *Drug Discovery Today*, 17(1–2), pp. 71–80. doi: 10.1016/j.drudis.2011.09.009.
- Yallapu, M. M., Jaggi, M. and Chauhan, S. C. (2013) 'Curcumin nanomedicine: a road to cancer therapeutics.', *Current pharmaceutical design*, 19(11), pp. 1994–2010. doi: 10.2174/138161213805289219.
- Yu, J., Zhou, P., Asenso, J., Yang, X. D., Wang, C. and Wei, W. (2016) 'Advances in plant-based inhibitors of P-glycoprotein', *Journal of Enzyme Inhibition and Medicinal Chemistry*, 31(6), pp. 867–881. doi: 10.3109/14756366.2016.1149476.
- Zhang, S. and Morris, M. E. (2003) 'Effects of the flavonoids biochanin A, morin, phloretin, and silymarin on P-glycoprotein-mediated transport', *Journal of Pharmacology and Experimental Therapeutics*, 304(3), pp. 1258–1267. doi: 10.1124/jpet.102.044412.
- Zhao, Y., Hu, X., Liu, Y., *et al.* (2017) 'ROS signaling under metabolic stress: Cross-talk between AMPK and AKT pathway', *Molecular Cancer*. BioMed Central Ltd. doi: 10.1186/s12943-017-0648-1.
- Zinzi, L., Capparelli, E., Cantore, M., Contino, M., Leopoldo, M. and Colabufo, N. A. (2014) 'Small and Innovative Molecules as New Strategy to Revert MDR', *Frontiers in Oncology*, 4(January), pp. 1–12. doi: 10.3389/fonc.2014.00002.

Zorofchian Moghadamtousi, S., Abdul Kadir, H., Hassandarvish, P., Tajik, H., Abubakar, S. and Zandi, K. (2014) 'A review on antibacterial, antiviral, and antifungal activity of curcumin', *BioMed Research International*. Hindawi Publishing Corporation, 2014. doi: 10.1155/2014/186864.

## **12. LIST OF PUBLICATIONS**

**List of publications:**

- 1- Salaroglio, I.C., Gazzano, E., Abdullrahman, A., Mungo, E., Castella, B., **Abd, G.E.F.A.E.**, Massaia, M., Donadelli, M., Rubinstein, M., Riganti, C., Kopecka, J., 2018. Increasing intratumor C/EBP- $\beta$  LIP and nitric oxide levels overcome resistance to doxorubicin in triple negative breast cancer. *Journal of Experimental & Clinical Cancer Research*, 37(1), p.286.
- 2- **Abd-Ellatef, G.E.F.**, Ahmed, O.M., Abdel-Reheim, E.S. and Abdel-Hamid, A.H.Z., 2017. *Ulva lactuca* polysaccharides prevent Wistar rat breast carcinogenesis through the augmentation of apoptosis, enhancement of antioxidant defense system, and suppression of inflammation. *Breast Cancer: Targets and Therapy*, 9, p.67-83.
- 3- Chegaev, K., Fraix, A., Gazzano, E., **Abd-Ellatef, G.E.F.**, Blangetti, M., Rolando, B., Conoci, S., Riganti, C., Fruttero, R., Gasco, A. and Sortino, S., 2017. Light-regulated NO release as a novel strategy to overcome doxorubicin multidrug resistance. *ACS medicinal chemistry letters*, 8(3), pp.361-365.
- 4- Walaa, A., Hamed, A.R., El-Raey, M., Elshamy, A.I. and **Abd-Ellatef, G.E.F.**, 2016. Antiproliferative, antioxidant and antimicrobial activities of phenolic compounds from *Acrocarpus fraxinifolius*. *Journal of Chemical and Pharmaceutical Research*, 8(3), pp.520-528.
- 5- Yahya, S.M., Hamed, A.R., Emara, M., Soltan, M.M., **Abd-Ellatef, G.E.F.** and Abdelnasser, S.M., 2016. Differential effects of c-myc and ABCB1 silencing on reversing drug resistance in HepG2/Dox cells. *Tumor Biology*, 37(5), pp.5925-5932.
- 6- **Fathy Abd-Ellatef G.E.**, Gazzano, E., Chirio, D., Hamed, A.R., Belisario, D.C., Zuddas, C., Peira, E., Rolando, B., Kopecka, J., ... and Riganti, C., 2020. Curcumin-Loaded Solid Lipid Nanoparticles Bypass P-Glycoprotein Mediated Doxorubicin Resistance in Triple Negative Breast Cancer Cells. *Pharmaceutics*, 12(2), 96.

**Manuscripts in preparation:**

- 7- **Abd-Ellatef, G.E.F.**, El-Desoky, A.H., Hamed, A.R., M. R., Belisario, D.C., Marie, M.A.S., Fahmy, S.R., Abdel-Hamid, A.Z., Riganti, C. Glabratephrin reverses doxorubicin resistance mediated by P-glycoprotein in breast cancer cells. *Submitted to Biochemical Pharmacology*.

## **13. ACKNOWLEDGMENTS**

*First and foremost, I would like to express my great praise and most sincere thanks to ALLAH (God), to whom every success should be attributed.*

*I am deeply grateful and totally indebted to my Italian supervisor, Prof. Dr. Chiara Riganti for her keen supervision, positive criticism and enthusiasm, for her patience and understanding, generous assistance, endless tolerance and sincere guidance, for her encouragement during my progress, her great help and valuable hints during writing, revising and finishing this thesis.*

*I owe great debt of gratitude and special thanks to my Egyptian supervisors, Prof. Dr. Abdel-Hamid Zakī Abdel-Hamid from National Research Centre, Prof. Dr. Mohamed Assem. S. Marie and Prof. Dr. Sohair Ramadan Fahmy from Cairo University; for their constructive supervision, fruitful help, continuous support and encouragement during the progress of this work, A special word of gratefulness is directed to all my Professors and my Colleagues in National Research Centre, Cairo University in Egypt and the University of Torino in Italy specially Oncology Department, who have provided their assistance to me; for their kind cooperation, sincere help and encouragement. My deep special thanks and appreciation to my Professors and my Colleagues in Zoology Department, Faculty of Science, Beni-Suef University in Egypt for their supporting and encouragement.*

*I must offer my truly deepest appreciation, sincere gratitude and heartily thanks to my great father, I pray to ALLAH for him to be in the highest degree of Paradise, my compassionate mother, my respected brother, my pretty sisters, my lovely wife, my cute daughter, my dear twins and my confidant friends for their endless love, prayers for me, great help and support. I appreciate their encouragement and patience not only during the fulfillment of this thesis but also through my life.*

*Gamal Eldein Fathy Abd-Elatef Abd-Elrahman*

## **14. PhD ACTIVITIES**



### **Conferences attendance**

- 1- Guido Tarone study day (D-Day), University of Turin, Molecular Biotechnology Center, Torino, Italy, 16 May, 2018.
- 2- International Conference on Recent Applications in medical Sciences (ICRAMS), Syndicate of Scientific Professions, Egypt, 1 February, 2019.

### **Conferences organization**

1. 6th International Euro-Mediterranean Conference and Expo Life Sciences (BioNat 6), Pharma and Bio-medicine, which held in 1-2 April, 2019 (Member of the management committee).
2. 1st NRC-Grenoble INP International Conference on Science and Sustainable Development under the theme of “There can never be sustainable development without science” which held in 16-18 September, 2019 (Member of the organizing committee).

### **Workshop & Symposium attendance**

- 1- Workshop on Metabolomics in Drug Discovery and Bio-informatics held in Potchefstroom, South Africa, North-West University, 1-3 February, 2016.
- 2- Graphene and its Amazing Applications, The Egyptian Materials Research Society, Faculty of Science, Beni-suef University, Beni-Suef, Egypt, 22 December, 2018.
- 3- Workshop on Poisoning: Diagnosis and Treatment, National Committee of Toxicology, Academy of Scientific Research and Technology, Egypt, 26 December, 2018.
- 4- Workshop on Introduction to Scholarly Publishing, Elsevier Research Academy on Campus, National Research Centre, Egypt, 9 January, 2019.
- 5- Workshop on Biomedical Applications of Marine and Terrestrial Microorganisms Derived Compounds, National Research Centre, Egypt, 10 January, 2019.

- 6- BioNat workshop on Bio-safety and Bio-security Management, BioNat International Conference, Animal Health Research Institute, Egypt, 2 February, 2019.
- 7- Symposium on Biological Sciences and Human Efforts Towards Development and Progress, National Committee for Biochemistry and Molecular Biology, Academy of Scientific Research and Technology, Egypt, 16 March, 2019.
- 8- 1st BioNat workshop on Scientific Writing (Mastering the Art of Clarity and Style), BioNat International Conference, Convention Center, Cairo University, Egypt, 31 March, 2019.
- 9- 1st BioNat Nano Mini-Symposium (The Knowledge of Nanoscience and Nanotechnology), BioNat International Conference, Convention Center, Cairo University, Egypt, 3 April, 2019.
- 10- Workshop on New Trends in Biotechnology, Therapeutic Chemistry Department, National Research Centre, Egypt, 14 April, 2019.

### **Attended courses**

- 1- Italian language course in correspondence with the level A2, C.P.I.A. 2-Torino, Italy, 22 March, 2017.
- 2- Courses of PhD Program, Integrated Molecular Physiology, Zoology Department, Faculty of Science, Cairo University, Egypt, from 1<sup>st</sup> October, 2015 to 1<sup>st</sup> October, 2019: Cancer Biology, Cytokines, Cell signaling and regulation, Stem cell biology, Physiology of sense organs, Biology of regeneration, Seminar and Bioinformatics.

### **Reviewing activity**

I participated as a reviewer in Tumor Biology Journal; I reviewed two manuscripts in 2017.

### **Patents**

- Currently applying for two patents in the Academy of Scientific Research and Technology, through the National Research Centre in Egypt in:

- 1- Glabratephrin reverses doxorubicin resistance mediated by P-glycoprotein in breast cancer cells. (Patent number: 371/2020)
- 2- Curcumin-loaded solid lipid nanoparticles bypasses P-glycoprotein mediated doxorubicin resistance in triple negative breast cancer cells. (Patent number: 1953/2019)

المخلص العربي

## 15. ARABIC SUMMARY

تُعرف مقاومة الخلايا السرطانية لمجموعة واسعة من الأدوية المضادة للسرطان باسم مقاومة الأدوية المتعددة، والتي تشكل عائقاً قوياً أمام نجاح العلاج الكيميائي في التغلب على السرطان مما يؤدي إلى تطور الورم. و يتعرض لهذه المقاومة المرضى الذين يعانون من أورام الدم والأورام الصلبة بما في ذلك سرطان الثدي والمبيض والرئة والجلد وسرطان الجهاز الهضمي. ويعد المسؤول الرئيسي عن النمط الظاهري للمقاومة للأدوية المتعددة هو الناقلات (ATP Binding Cassette) (ABC) ، وهي ناقلات مرتبطة بأغشية البلازما والتي تدفق الأدوية المتعددة خارج الخلايا والتي لا علاقة لها بالهيكل والنشاط ، مما يحد من تراكم هذه الأدوية داخل الخلايا وبالتالي يحد من تأثيرها السام على الخلايا. يعتبر الناقل الرئيسي ABC المتعلق بمقاومة الأدوية المتعددة هو ال بي جليكوبروتين. حتى الآن ، تم اختبار جزيئات صغيرة مختلفة مثبتة للبي جليكوبروتين، على الرغم من أنها فعالة في خطوط الخلايا السرطانية خارج الكائن الحي، إلا أنها فشلت في النماذج قبل السريرية نظراً لسميتها العالية وافتقارها للتخصصية. في هذه الدراسة تم بحث ثلاثة طرق بديلة لتنشيط البي جليكوبروتين بطريقة فعالة وآمنة:

أولاً: استخدام الجزيئات الديناميكية الضوئية، وهي جزيئات قادرة على إطلاق دواء الدوكسوروبيسين كعلاج كيميائي وأكسيد النيتريك كمثبط للبي جليكوبروتين وذلك فقط إذا تم تشعبه بأطوال موجية مناسبة داخل الخلايا السرطانية. ثانياً: استخدام المنتجات الطبيعية ضعيفة السمية على الخلايا الطبيعية الغير محولة والغير مسرطنة وفي نفس الوقت لها انتقائية عالية للخلايا السرطانية التي لديها نسبة عالية من البي جليكوبروتين. ثالثاً: استخدام طرق نانو تكنولوجية، مبنية على المشاركة بين الدوكسوروبيسين ومنتج طبيعي مثير للحساسية الكيميائية وهو الكركمين والذي تم تحميله في جسيمات نانوية دهنية صلبة متوافقة حيويًا.

في الجزء الأول من الرسالة ، قمت بالتحقق من صنف جديد من أكسيد النيتريك المثار ضوئياً والمطلق للدوكسوروبيسين، حيث يرتبط مركب مناسب مانح لأكسيد النيتريك بواسطة جسر حساس للضوء متصل بالدوكسوروبيسين PNODOXOs. كان الهدف من ذلك هو توليد ضوئي لأكسيد النيتريك بجرعات غير سامة ولكنها قادرة على نيترة ناقلات ال ABC على التيروزينات الحرجة لزيادة نشاطها، مما يقلل من تدفق الدوكسوروبيسين خارج خلايا السرطان. ولتحقيق هذا الهدف، تم استخدام خلايا سرطان الجلد M14 البشرية والتي تستطيع بطريقة جوهريّة أن تنتج ناقلات ABC متعددة. مع الطول الموجي الصحيح والقوة والإشعاع ، تطلق ال PNODOXOs أكسيد النيتريك الذي بدوره يقوم بنيترة البي جليكوبروتين وناقلات ال ABC الأخرى ، مما يزيد من السمية الخلوية للدوكسوروبيسين. هذه النتائج قد تمهد الطريق إلى المستقبل باستخدام مانحات ضوئية لأكسيد النيتريك تتميز بتنشيط واسع المجال لناقلات ال ABC. قد تؤدي هذه الميزة إلى زيادة احتباس وتسمم الخلايا بالعديد من الأدوية العلاجية الأخرى إلى جانب الدوكسوروبيسين. علاوة على ذلك ، تعتمد هذه الاستراتيجية على إطلاق مستحث للضوء لأكسيد النيتريك من خلال الوصول إلى إطلاق محكم لأكسيد النيتريك نستطيع التحكم به داخل الخلايا السرطانية، فتزيد هذه الاستراتيجية من الفائدة ضد الأورام المشععة المقاومة للأدوية، وتحد من الآثار الجانبية على الأنسجة الغير مسرطنة.

في الجزئين الثاني والثالث من الرسالة، تم التركيز على ارجاع الخلايا عن مقاومتها للدوكسوروبيسين بواسطة تنشيط البي جليكوبروتين في خلايا سرطان الثدي ثلاثي السلبية، حيث يعد الدوكسوروبيسين الخيار العلاجي الأول لهذه الخلايا ولكن تضعف فاعليته بسبب وجود البي جليكوبروتين. تم استخدام نوع من الخلايا البشرية لسرطان الثدي ثلاثي السلبية وهو (MDA-MB-231) والتي لديها نسبة قليلة من البي جليكوبروتين. أيضاً تم استخدام خلايا سرطان الثدي ثلاثي السلبية (MDA-MB-231/DX) والتي لديها القدرة على إنتاج البي جليكوبروتين والتي قمت

بإنتاجها بواسطة جرعات تدريجية من الدكسوروبيسين في وسط غذائي. كما تم استخدام خلايا من الفئران (JC) لديها نسبة عالية من البي جليكوبروتينين.

أولاً، تم اختبار اثني عشر مركباً طبيعياً نقياً تم اختيارهم وفقاً لأنشطتهم البيولوجية المختلفة. ولقد وجدت أن الجلابراتيفرين، وهو فلافونويد مستخلص من *Tephrosia purpurea*، تسبب في تسمم الخلايا الانتقائي والتفضيلي ضد الخلايا السرطانية المنتجة للبي جليكوبروتين عند معالجتها بالدكسوروبيسين. استطاع الجلابراتيفرين أن يعكس مقاومة الدكسوروبيسين في خطوط الخلايا السرطانية خارج الجسم الحي وفي أورام ال JC في الجسم الحي، دون أي سمية على باقي الخلايا الطبيعية. ميكانيكياً استطاعت مادة الجلابراتيفرين أن تثبط نشاط إنزيم ATPase الحفزي للبي جليكوبروتينين، والحد من الحد الأقصى لسرعة معدل الأيض والحد من تدفق الدكسوروبيسين خارج الخلايا. وقد نتج ذلك بسبب التفاعل المباشر بين الجلابراتيفرين و البي جليكوبروتينين. سمحت التجارب مع البي جليكوبروتين المحور بتحديد المجال المتمركز حول Glycine 185 كموقع الربط المقترض للجلابراتيفرين. في الواقع، فقد المركب فعاليته في ال Glycine-> Valine 185 للبي جليكوبروتين المحور. إن عكس مقاومة الدكسوروبيسين في حالة المعالجة المزودة مع الجلابراتيفرين تستطيع أن تقلل الجرعة اللازمة من الدكسوروبيسين للقضاء على خلايا السرطان المقاومة، وبالتالي تقليل سمية الدواء على باقي خلايا الجسم.

ثالثاً، تمت دراسة تأثير الكركمين كأحد بالمنتجات الطبيعية التي لديها القدرة على عكس مقاومة الخلايا للأدوية المتعددة، وهو مثبط معروف للبي جليكوبروتينين ولكنه يتأثر بانخفاض الاستقرار والذوبان والتوافر الحيوي. وللتغلب على هذه القيود، قمت بالتحقق من فعالية الكركمين الذي تم تحميله في جزيئات نانوية دهنية صلبة متوافقة حيويًا، مع أو بدون تغليفها بالشيتوزان، والتي لها القدرة على زيادة الاستقرار، والمحببة للماء والتي تزيد من قدرة الخلايا على امتصاص الكركمين. تم إثبات أن كل من الجزيئات النانوية المحملة بالكركمين أكثر فاعلية من خمسة إلى عشرة أضعاف عن استخدام الكركمين بمفرده وظهر ذلك في زيادة احتباس وسمية الدكسوروبيسين في خلايا سرطان الثدي الثلاثي السلبية MDA-MB-231 والتي لديها نسبة من البي جليكوبروتينين وخلايا ال JC التي تحتوي على نسبة عالية من البي جليكوبروتينين. كانت آثار التحسس الكيميائي ناتجة عن انخفاض أنواع الأكسجين التفاعلي داخل الخلايا وما ينتج عن ذلك من تثبيط محور Akt / IKK $\alpha$ - $\beta$  / NF-kB.

على وجه الخصوص اختزلت الجزيئات النانوية الدهنية الصلبة المحملة بالكركمين الربط من P65 / P50 إلى NF-kB المسؤول عن جين البي جليكوبروتينين. انخفض النشاط النسخي وبالتالي نقص mRNA والبروتين الخاص بالبي جليكوبروتينين. كما أنقذت الجزيئات النانوية الدهنية الصلبة المحملة بالكركمين بشكل فعال حساسية الدكسوروبيسين ضد أورام ال JC المقاومة للأدوية، دون وجود علامات على السمية في الخلايا الطبيعية الغير مسرطنة.

بشكل عام، استخدمت الدراسة العديد من الأساليب المبتكرة بناءً على مزيج من الفيزياء والكيمياء الطبية وتكنولوجيا النانو والكيمياء الحيوية وعلم الصيدلة. قد تمثل هذه التخصصات المتعددة تقدماً ملحوظاً في التغلب على مقاومة الخلايا السرطانية للأدوية المتعددة والمتعلقة بنواقل ال ABC.

المستخلص العربي

## 16. ARABIC ABSTRACT

تُعرف مقاومة الخلايا السرطانية لمجموعة واسعة من الأدوية المضادة للسرطان باسم مقاومة الأدوية المتعددة، والتي تشكل عائقاً قوياً أمام نجاح العلاج الكيميائي في التغلب على السرطان مما يؤدي إلى تطور الورم. و تكون هذه المقاومة في المرضى الذين يعانون من الأورام المختلفة وذلك بعد معالجتهم لفترات طويلة بالعلاج الكيميائي. ويعد المسؤول الرئيسي عن تلك المقاومة هو الناقلات (ATP Binding Cassette) (ABC)، وهي ناقلات مرتبطة بأغشية البلازما والتي تدفق الأدوية المتعددة خارج الخلايا، مما يحد من تراكم هذه الأدوية بداخلها وبالتالي يحد من تأثيرها السام على الخلايا. يعتبر الناقل الرئيسي ABC المتعلق بمقاومة الأدوية المتعددة هو ال بي جليكوبروتين. حتى الآن، تم اختبار جزيئات صغيرة مختلفة مثبطة للبي جليكوبروتين، على الرغم من أنها فعالة في خطوط الخلايا السرطانية خارج الكائن الحي، إلا أنها فشلت في النماذج قبل السريرية نظراً لسميتها العالية وافتقارها للتخصصية.

في هذه الدراسة تم بحث ثلاثة طرق بديلة لتنشيط البي جليكوبروتين بطريقة فعالة وآمنة:

أولاً: استخدام الجزيئات الديناميكية الضوئية، وهي جزيئات قادرة على إطلاق دواء الدوكسوروبيسين كعلاج كيميائي وأكسيد النيتريك كمنشط للبي جليكوبروتين وذلك فقط إذا تم تشعيه بأطوال موجية مناسبة داخل الخلايا السرطانية. ثانياً: استخدام المنتجات الطبيعية ضعيفة السمية على الخلايا الطبيعية الغير مسرطنة وفي نفس الوقت لها انتقائية عالية للخلايا السرطانية التي لديها نسبة عالية من البي جليكوبروتين. ثالثاً: استخدام طرق نانو تكنولوجية، مبنية على المشاركة بين الدوكسوروبيسين ومنتج طبيعي مثير للحساسية الكيميائية وهو الكركمين والذي تم تحميله في جسيمات نانوية دهنية صلبة متوافقة حيويًا.

في الجزء الأول من الرسالة، قمت باختبار صنف جديد من أكسيد النيتريك المثار ضوئياً والمطلق للدوكسوروبيسين PNODOXOs على خلايا سرطان الجلد M14 البشرية والتي تستطيع أن تنتج ناقلات ABC متعددة. تم إثبات أن التوليد الضوئي لأكسيد النيتريك بجرعات غير سامة كان له القدرة على نيترة البي جليكوبروتين وناقلات ال ABC الأخرى مما قلل من تدفق الدوكسوروبيسين خارج خلايا السرطان وبالتالي زاد من سميته الخلوية. في الجزئين الثاني والثالث من الرسالة، تم التركيز على ارجاع الخلايا عن مقاومتها للدوكسوروبيسين بواسطة تنشيط البي جليكوبروتين في خلايا سرطان الثدي ثلاثي السلبية، حيث يعد الدوكسوروبيسين الخيار العلاجي الأول لهذه الخلايا ولكن تضعف فاعليته بسبب وجود البي جليكوبروتين. تم استخدام نوع من الخلايا البشرية لسرطان الثدي ثلاثي السلبية وهو (MDA-MB-231) والتي لديها نسبة قليلة من البي جليكوبروتين. أيضاً تم استخدام خلايا سرطان الثدي ثلاثي السلبية (MDA-MB-231/DX) والتي لديها القدرة على إنتاج البي جليكوبروتين والتي قمت بإنتاجها بواسطة جرعات تدرجية من الدوكسوروبيسين في وسط غذائي. كما تم استخدام خلايا من الفئران (JC) لديها نسبة عالية من البي جليكوبروتين.

أولاً، تم اختبار اثني عشر مركباً طبيعياً نقياً تم اختيارهم وفقاً لأنشطتهم البيولوجية المختلفة. ولقد وجدت أن الجلبراتييفرين، وهو فلافونويد مستخلص من *Tephrosia purpurea*، تسبب في تسمم الخلايا الانتقائي والتفضيلي ضد الخلايا السرطانية المنتجة للبي جليكوبروتين عند معالجتها بالدوكسوروبيسين. استطاع الجلبراتييفرين أن يعكس مقاومة الدوكسوروبيسين في خطوط الخلايا السرطانية خارج الجسم الحي وفي أورام ال JC في الجسم الحي، دون أي سمية على باقي الخلايا الطبيعية. تم إثبات أن عكس مقاومة الدوكسوروبيسين في حالة المعالجة المزدوجة مع



الجلابراتيفرين تستطيع أن تقلل الجرعة اللازمة من الدوكسوروبيسين للقضاء على خلايا السرطان المقاومة، وبالتالي تقليل سمية الدواء على باقي خلايا الجسم.

ثالثاً، تمت دراسة تأثير الكركمين كأحد بالمنتجات الطبيعية التي لديها القدرة على عكس مقاومة الخلايا للأدوية المتعددة، وهو مثبت معروف للبي جليكوبروتين ولكنه يتأثر بانخفاض الاستقرار والذوبان والتوافر الحيوي. وللتغلب على هذه القيود، قمت بالتحقق من فعالية الكركمين الذي تم تحميله في جزيئات نانوية دهنية صلبة متوافقة حيويًا، مع أو بدون تغليفها بالشيتوزان، والتي لها القدرة على زيادة الاستقرار، والمحببة للماء والتي تزيد من قدرة الخلايا على امتصاص الكركمين. تم إثبات أن كل من الجزيئات النانوية المحملة بالكركمين أكثر فاعلية من خمسة إلى عشرة أضعاف عن استخدام الكركمين بمفرده وظهر ذلك في زيادة احتباس وسمية الدوكسوروبيسين في خلايا سرطان الثدي الثلاثي السلبية MDA-MB-231 والتي لديها نسبة من البي جليكوبروتين وخلايا ال JC التي تحتوي على نسبة عالية من البي جليكوبروتين. كما رفعت تلك الجزيئات بشكل فعال من حساسية الدوكسوروبيسين ضد أورام ال JC المقاومة للأدوية، دون وجود أي تأثير سام على الخلايا الطبيعية الغير مسرطنة.

بشكل عام، استخدمت الدراسة العديد من الأساليب المبتكرة بناءً على مزيج من الفيزياء والكيمياء الطبية وتكنولوجيا النانو والكيمياء الحيوية وعلم الصيدلة. قد تمثل هذه التخصصات المتعددة تقدماً ملحوظاً في التغلب على مقاومة الخلايا السرطانية للأدوية المتعددة والمتعلقة بنواقل ال ABC.